2013

Synthesis, Characterization And Application Of Pt Complexes With Pincer Ccc-Bis(Nhc) Ligands

Xiaofei Zhang
University of Mississippi

Synthesis, Characterization and Application of Pt Complexes with Pincer CCC-bis(NHC) Ligands

A Dissertation
presented in partial fulfillment of requirements
for the degree of Doctor of Philosophy
in the Department of Chemistry and Biochemistry
The University of Mississippi

by

XIAOFEI ZHANG

Advisor: Professor. T. Keith Hollis

May 2013

ABSTRACT

The unique metallation/transmetallation route for the synthesis of CCC-bis(NHC) pincer ligand supported transition metal complexes was extended to Pt. Several platinum complexes: 2-(1,3-bis(N-butylimidazol-2-ylidene) phenylene) (chloro) Pt(II), **1**; 2-(1,3-bis (N-butylimidazol-2-ylidene) phenylene) (bromo) Pt(II), **2**; 2-(1,3-bis(N-trimethylsilyl methyl-imidazol-2ylidene)phenylene)(chloro) Pt(II), **4**; trifluoroacetato-1κO:2κO';2κO: 3κO';3κO:4κO'-bis[2-(1,3-bis(N-trimethylsilylmethyl-imidazol-2-ylidene) phenylene)]-3κ^3C;4κ^3C-disilverdiplatinum (Ag-Ag) (2Ag-Pt) (Ag-Pt), **5**; 2-(1,3-bis(N-trimethylsilyl methyl-imidazol-2ylidene) phenylene) (trifluoroacetato) Pt(II), **6**; and 2-(1,3-bis(N-butylimidazol-2-ylidene) phenylene) (carbonyl) Pt(II) trifluoromethanesulfonate, **7** were synthesized and fully characterized. Their structures were confirmed with X-ray crystallography. Complexes **1**, **2**, **4**, **6**, and **7** exhibited distorted square planar configurations around the platinum metal center. Pt_2Ag_2 multimetal cluster **5** contains the first unsymmetrically-substituted example of a $PtAg_2$ metallocyclopropane. A distorted octahedral configuration was also found in the coordination sphere of one of the silver atoms. Multiple weak hydrogen bonds (WHB) including C–H…O, C–H…F and C–F…π interactions were identified in the lattice of cluster **5**. All the platinum complexes emitted in the visible light region. The blue emission of complexes **1** and **2** in solid state was found to be stable in ambient atmosphere (O_2 and H_2O). The emission of the MeOH solution of Pt_2Ag_2 multimetal cluster **5** was concentration dependent. These complexes are believed to be congeners of materials for organic light emitting diodes (OLEDs).

LIST OF ABREVIATIONS AND SYMBOLS

NHC	N-Heterocyclic Carbene(s)
COD	1,5-Cyclooctyldiene
DCM	Dichloromethane
DMF	Dimethylformamide
DMSO	Dimethyl Sulfoxide
THF	Tetrahydrofuran
TFA	Trifluoroacetic acid
Tf	Triflate
HPLC	High Performance Liquid Chromatography
IR	Infrared spectroscopy
MS	Mass Spectrum
NMR	Nuclear Magnetic Resonance
δ	Chemical Shift (ppm, NMR)
J	Coupling Constant (Hz, NMR)
Φ	Quantum Efficiency
UV	Ultraviolet Spectroscopy
DSC	Differential Scanning Calorimetry
TGA	Thermal Gravimetric Analysis
EA	Elemental Analysis

ACKNOWLEDGEMENTS

I would like to thank my committee, Prof. Daniel L. Mattern, Prof. Jason E. Ritchie, Prof. Gregory S. Tschumper, Prof. Nathan I. Hammer, and Prof. John M. Rimoldi for their extreme patience in the process. I would like to thank the Department of Chemistry and Graduate School for supporting me through my program. I would like to thank Prof. David H. Magers and Prof. Edward J. Valente for great suggestions regarding my studies. I would like to thank all my friends and coworkers for helping me through tough times and sharing the good ones. I want to express my deepest gratitude to my advisor, Prof. T. Keith Hollis, for his excellent guidance in every aspects and stages of my graduate studies.

Meanwhile I would like to give my special thanks my beloved wife, Bei, and daughter, Meiya.

TABLE OF CONTENTS

LIST OF TABLES

LIST OF FIGURES

CHAPTER 1

INTRODUCTION TO THE CCC-NHC LIGANDS

1.1 The history of carbene

The pioneering work of carbene species was carried out between the late 19th and early 20th centuries, by Eduard Buchner and co-workers.[1] Carbenes are defined as the electrically neutral species H_2C: and its derivatives, in which the carbon is covalently bonded to two monovalent groups of any kind or a divalent group and possesses two nonbonded electrons.[2] There are two known geometries for the carbenes: linear and bent. Linear carbenes are sp hybridized and their two nonbonding (p_x and p_y) orbitals are orthogonal to each other and the bonding axis. In the linear carbenes, the energy difference between the two nonbonding p orbitals is usually smaller than the electron pairing energy due to the symmetry. Therefore, the two nonbonded electrons trend to adopt parallel spins and occupy different p orbitals (triplet state).

Figure 1.1.1 The Electronic Representation of Singlet and Triplet Carbenes.

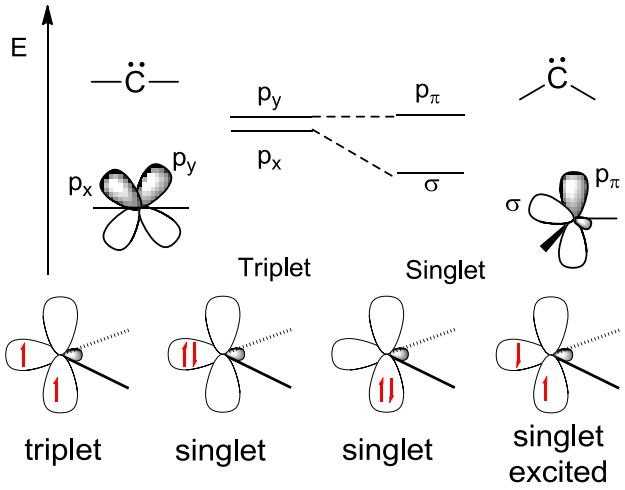

Most previously reported carbenes are bent. The bent carbenes are sp^2 hybridized with their p_y orbital remaining almost unchanged (usually assigned as p_π). The nonbonding sp^2 orbital (usually assigned as σ) can be considered as the p_x orbital of a linear carbene adopting some s character from its sp bonding orbitals. As the σ orbital is stabilized by gaining s character through hybridization, the energy gap between σ and p_π is usually larger than the electron pairing energy. Thus, the two nonbonded electrons are prone to occupy and share the σ orbital (singlet state).[3]

For a long time, carbenes were considered as highly reactive species. One of the earliest and most representative examples of carbene reactions is their addition to double bonds.[4] Although both singlet and triplet carbenes exhibited reactivity in these reactions,[5] the reaction mechanism are not the same. Singlet carbenes are believed to react in a concerted pathway, where their vacant p orbital acts as electrophile while their non-

bonding electron pair acts as nucleophile. The triplet carbene follows a radical pathway, where the non-bonding electrons of the carbene form bonds stepwise.[4a] The concerted mechanism leads to stereospecific products while the stepwise mechanism affords two diastereomers (Scheme 1.1.1).

Scheme 1.1.1 The Addition to Double bonds of Singlet and Triplet Carbenes.

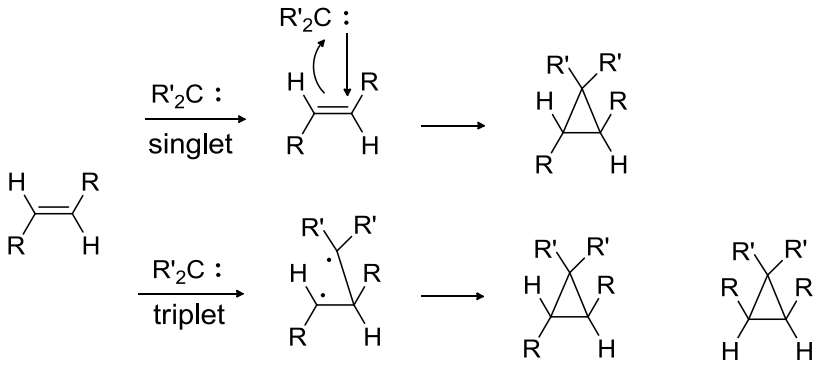

1.2 The N-heterocyclic carbenes (NHCs)

N-Heterocyclic carbenes (NHCs) were first reported by Öfele[6] and Wanzlick[7] in 1968 independently. At that time, they along with other carbenes were still considered as very reactive transient species. Almost 20 years later, following the first example of a stable singlet push-pull carbene,[8] Arduengo et al. isolated this type of ligand in the free state and determined their molecular structures by X-ray crystallography.[9] The bulkiness of the substitution groups on the nitrogen atoms was believed to be crucial to the enhanced stability of the carbene until the "unprotected" NHC species was isolated (Figure 1.2.1).[10]

Figure 1.2.1 Development of N-Heterocyclic Carbenes.

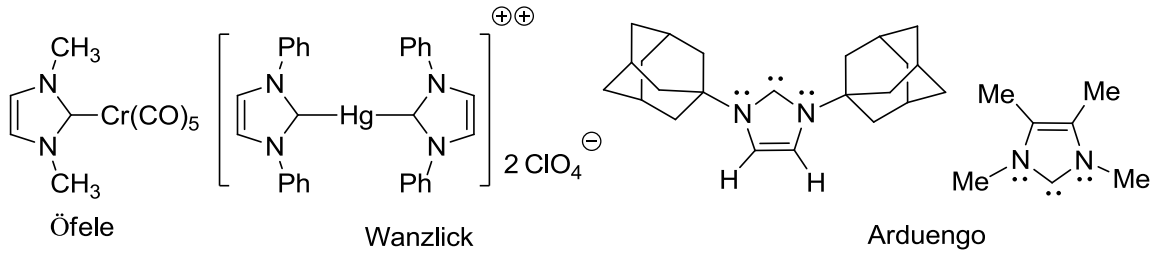

It is well accepted that the stability of the NHCs stems from their unique electronic configuration. In the NHCs, the σ orbital on the carbene carbon is stabilized through the electron withdrawing effect from the adjacent nitrogen atoms. Meanwhile, the p_π orbital aligns almost perfectly with the p orbitals of the nitrogen atoms. The electron lone pairs on the nitrogen atoms can easily delocalize among the NCN skeleton, which causes an increase of orbital energy by decreasing the electrophilicity of the p_π orbital. As a result, the NHCs gain extra stability in comparison with other singlet carbenes.

Figure 1.2.2 The Electronic Representation of N-Heterocyclic Carbenes.

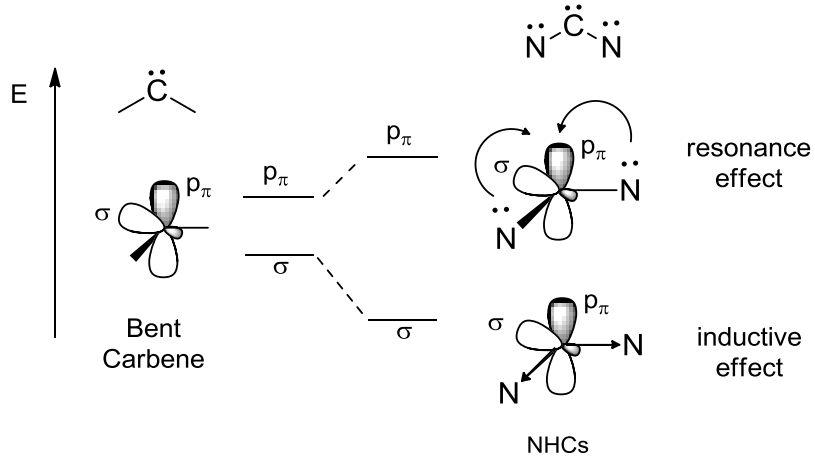

Various derivatives of NHCs have been developed in the recent several decades. Along with many substituted imidazol-2-ylidene systems **1**, the saturated version **2**,[11] and acyclic version **3**[12] singlet carbenes have been developed. Another class of singlet

carbenes, which was known as "abnormal" NHCs, including the imidazol-4-ylidene **4**,[13] 1,2,3-triazolylidene **5**,[14] and pyrazoliylidene **6**[15] systems, are now called "mesoionic carbenes (MICs)". The resonance structure of this class of carbenes cannot be drawn without adding additional charges.[16]

Figure 1.2.3 Derivatives of N-Heterocyclic Carbenes.

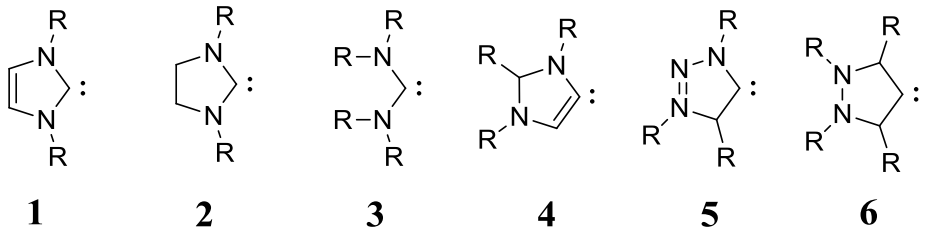

Although NHCs were initially regarded as alternatives to the well studied phosphine ligands for organometallic systems, they've exhibited unprecedented advantages under many conditions.[17] In comparison to the phosphine ligands, NHCs are stronger σ donor with very little π-backbonding character. This property allows less delocalization of the electrons on the coordinating transition metal, which facilitates an easier oxidative addition of reactant onto the metal.[18] Due to their intrinsically more sophisticated structures, NHCs have the advantages on both electronic and steric fine tunings. Many NHCs and their analogues have been applied as strong ligands for transition metals.[3,19] Those metal-NHC complexes exhibited high thermal stability as well as significant tolerance to the presence of air and moisture. Numerous applications of NHC-transition metal complexes to catalytic organic transformations have been demonstrated including olefin metathesis,[20] Pd cross-coupling reactions such as the Heck,[17b] Suzuki-Miyaura,[21] and etc.[22]

Figure 1.2.4 Grubs Catalysts.

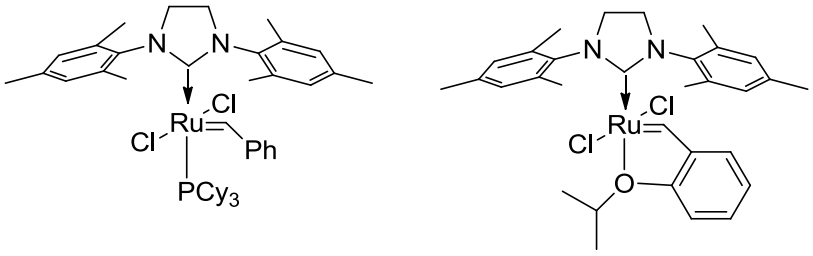

1.3 Pincer ligands

The first example of pincer ligand was reported by Shaw et al. in 1976,[23] and then formally named by van Koten in 1989.[24] Before the introduction of stable NHCs in 1991,[9] several pincer ligand systems were developed, e.g. PCP,[25] PNN,[26] PNP[27] and NCN[28] architectures. It is now defined as 'a tridentate ligand which is connected to the metal via at least one metal-carbon σ bond' by more recent review articles.[29] Transition metal pincer complexes usually exhibit a high degree of thermal stability due to the chelating effect. The electronic properties of pincer complexes are correlated to the donor atoms and their substituents, which allow fine tuning of the reactivity of the complexes. At the same time, stereochemical information can be introduced through the ligand architecture.

Figure 1.3.1 Typical Pincer Ligand Architectures.

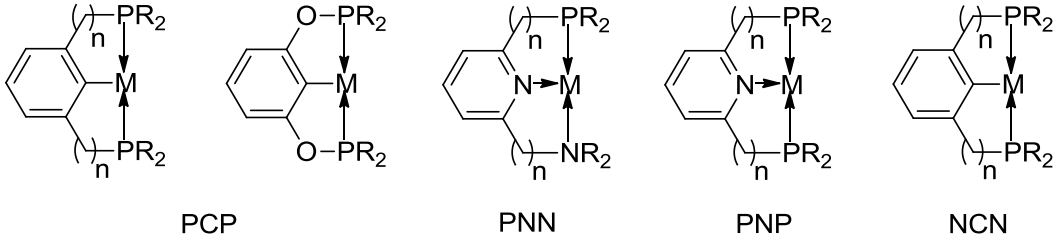

The application of the pincer complexes was developed many years behind their synthesis. They are used as catalysis,[29a,30] light emitters,[31] crystalline switches,[28b,32] chemical sensors,[33] and metal-organic framework (MOF) units.[32a,34]

In catalysis, the pincer transition metal complexes have demonstrated outstanding activities and robustness, which offered high turnover frequencies (TOF) and turnover numbers (TON). For instance, Shibasaki et al.[35] reported a modified PCP palladium pincer complex for the catalysis of iodobenzene and n-butyl acrylate coupling in 1999 (Scheme 1.3.1) This palladium pincer catalyst provided an unprecedented TON (8,900,000) for Heck reactions.

Scheme 1.3.1 PCP palladium pincer complex catalyzed Heck coupling reaction with high turnover number.

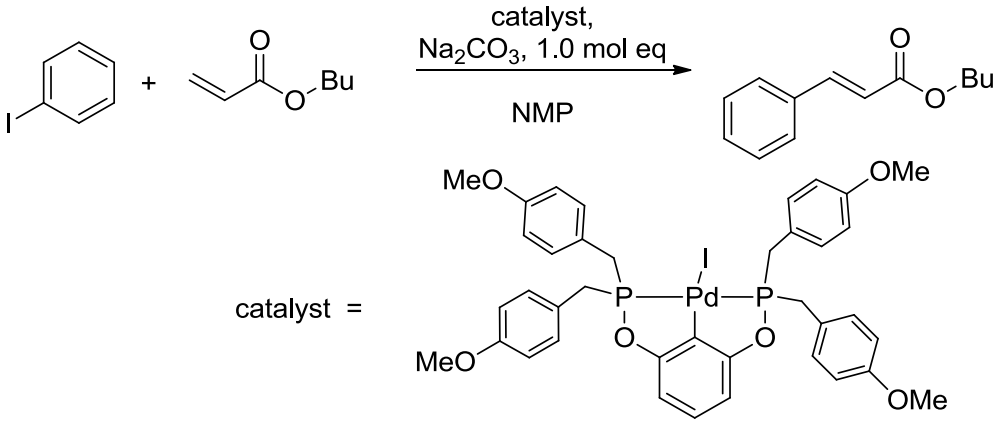

Other well known pincer catalysts include palladium-based complexes for Heck[36] and Suzuki[37] couplings, iridium and rhodium based complexes for hydroaminations[38] and dehydrogenations[39], nickel based complexes for Kharasch additions,[40] and Michael additions[41] (Scheme 1.3.2).

Scheme 1.3.2 Catalysis of pincer transition metal complexes.

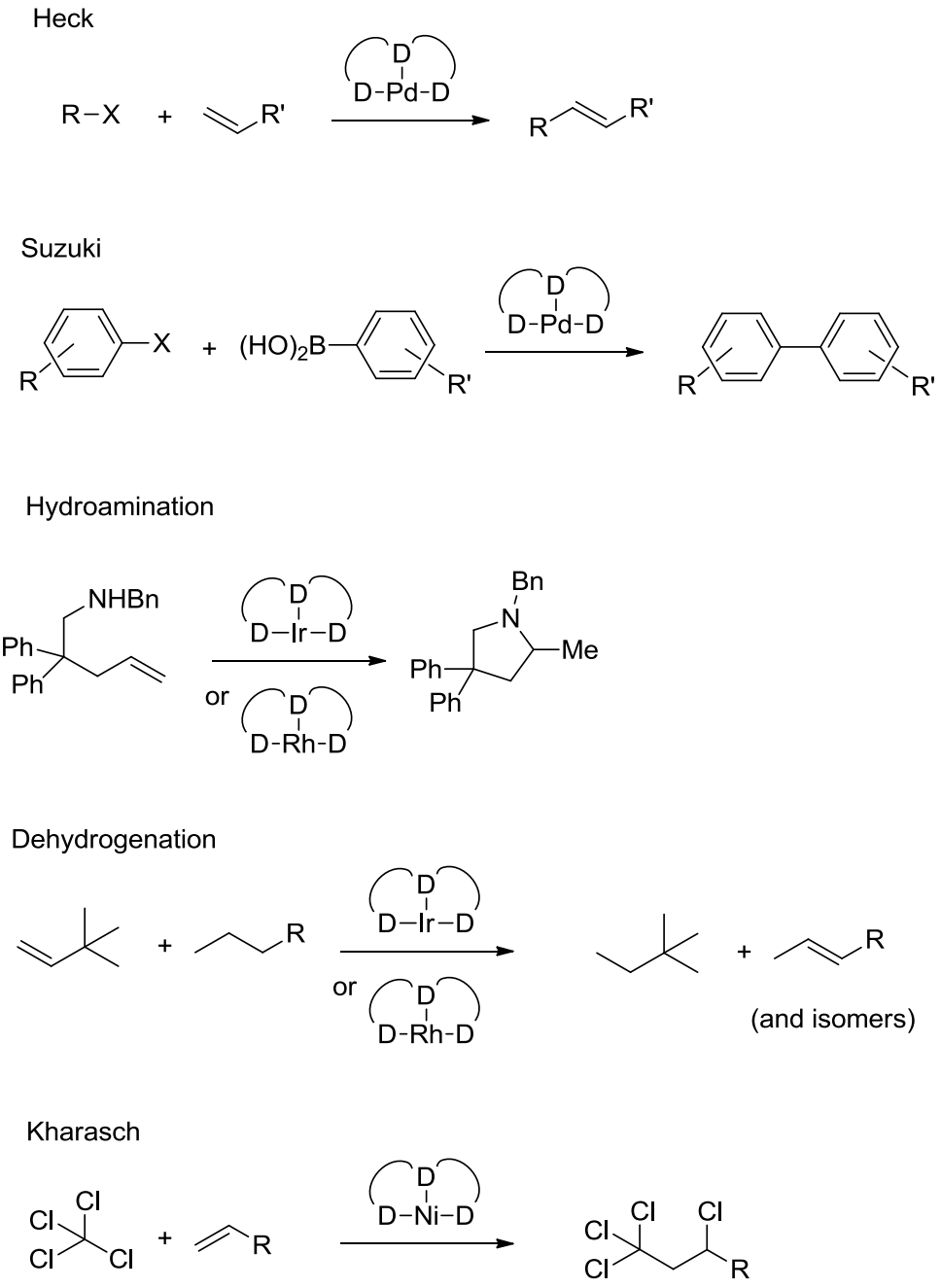

The studies of organic light-emitting devices (OLEDs) have grown rapidly after the proposal of the electroluminescence mechanism by Pope et al. in the 1960s.[42] Organometallic complexes were introduced into this field about 15 years ago due to the pioneering efforts of Thompson and coworkers[43] in improving the light-emitting

efficiency from the emitting mechanism. Emissive pincer transition metal complexes have only been reported in the very recent years.[31]

The essential difference between pure organic emitters and organo-transition metal emitters lies in the achievable light emitting efficiency. During the electroluminescence process, the emitter molecules are first stimulated into their excited states and become excitons. Statistically there will be 25% singlet and 75% triplet excitons.[44] In purely organic materials, the singlet excitons are allowed to spontaneously decay into the ground state, leading to fluorescence, while the triplet excitons will not decay emissively. In organometallic emitters, the spin-orbital coupling (SOC) caused by the transition metal may allow fast intersystem crossing (ISC), where all the excitons can decay first into the lowest triplet excited state and then to the ground state (Figure 1.3.2).[45] It is also possible for organo-transition metal emitters with very small energy gap between their first singlet and triplet excited states to thermally promote the triplet excitons to the singlet states and emit.[46] Therefore, the organometallic emitters possess a theoretic efficiency three times higher than the purely organic emitters.

Figure 1.3.2 Singlet and Triplet Emitters.
*Adapted from Reference 45c

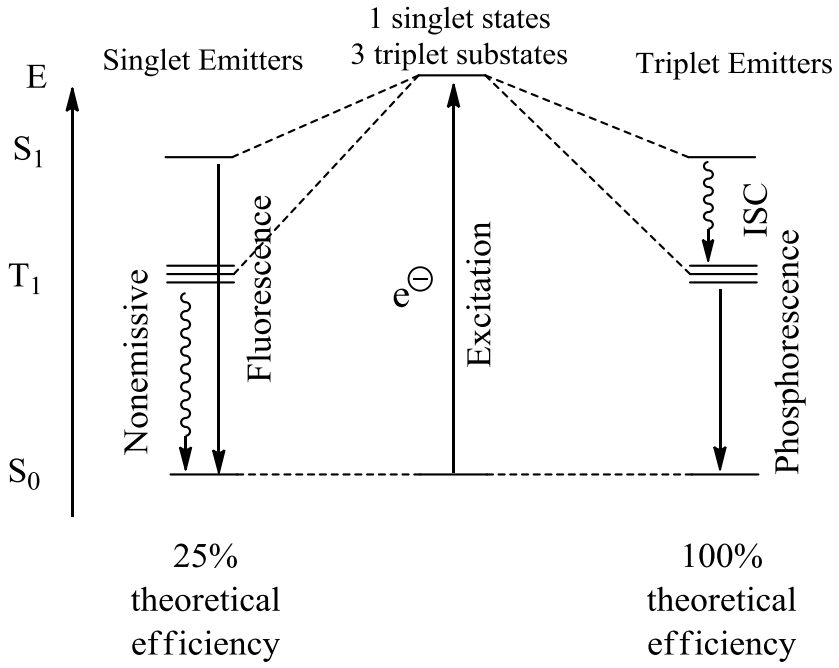

Due to the emission mechanism, the organometallic emitters are sometimes also called phosphorescent or triplet emitters.[47] As all other emitters, organometallic materials suffer from quenching and photo-bleaching processes. Quenching refers to the non-photon-induced decrease of emission.[48] It can occur via several different mechanisms. However, the process generally involves perturbation of the excited or ground electronic states of the emitter, which changes the emissive decay pathway. Photo-bleaching describes the loss of emission caused by photochemical destruction of the emitter.[49] Triplet emitters are commonly more susceptible to these processes since they have longer lifetime of their emissive excited states.

1.4 The CCC-NHC ligand system

Taking advantages from both NHCs and pincer structure, pincer NHC ligands have exhibited high stability and many applications in recent years. The aryl-bridged bis(NHC)-pincer ligands are of two major classes depending on the atoms making the bonds to the metal: CCC-bis(NHC) pincer complexes (xylylenyl-bridged[50] and phenylenyl-bridged systems[38,51]) and CNC-bis(NHC) pincer complexes (2,6-lutidenyl-bridged[52] and pyridylenyl-bridged systems[53]). Although the architectures are similar to each other structurally, their geometry and syntheses are significantly different. Moreover, metallation of some ligand architectures turned out to be far more difficult than others.

Figure 1.4.1 Pincer NHC Ligand Systems.

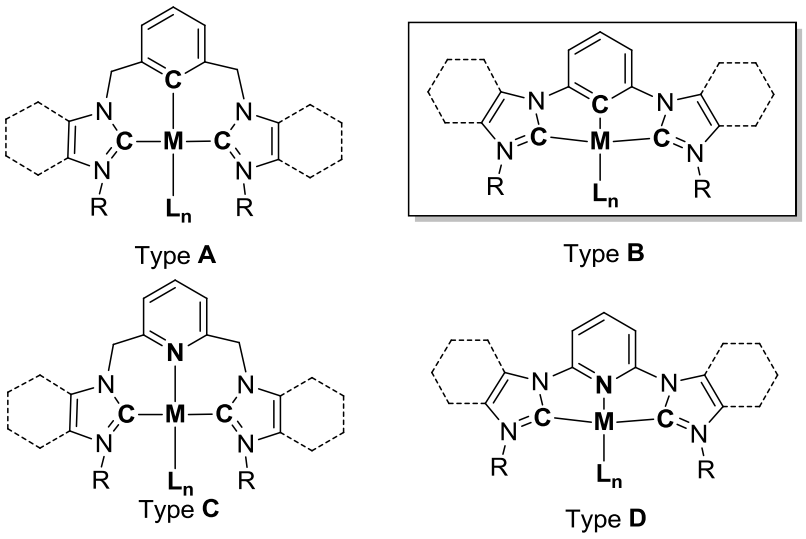

Type A C^C^C-NHC ligands (the ^ stands for the CH_2 linker between ligand fragments): The synthesis of this type of ligand precursor was first reported by Faller and Crabtree and coworkers[36d] as an one-step S_N2 reaction between 2-bromo-1,3-(bromomethyl)benzene and an N-substituted imidazole. The bromo substitution at the 2

position proved to be critical for the following metallation step, where the ligand precursor was treated with a strong base and then a transition metal source at elevated temperature. The aromatic conjugation in this type of structure is discontinued by the two CH_2 linkers. Metal complexes of this type are often reported as a mixture of atropisomers at room temperature (Figure 1.4.2) Palladium complexes of this type have demonstrated reactivity for Heck couplings.[23]

Figure 1.4.2 Synthesis of Type A C^C^C-NHC architecture.

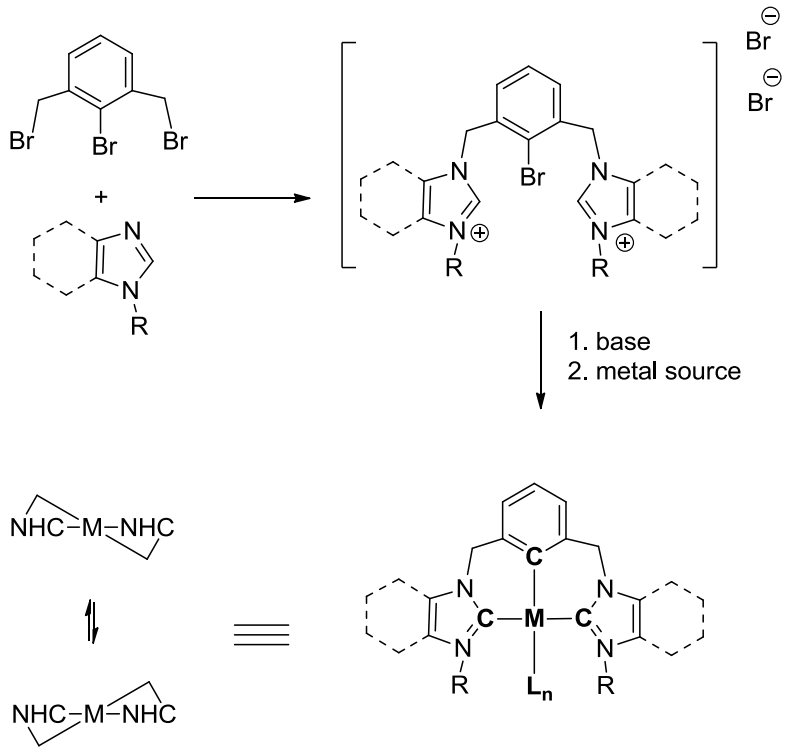

Type C C^C^C-NHC ligands: The synthesis is quite similar to the type A ligands. Instead of 2-bromo-1,3-bis(bromomethyl)benzene, 2,6-bis(bromomethyl)pyridine was used as the bridging fragment. As a decent donor, the nitrogen on the pyridine coordinates relatively easily to transition metals during metallation. Type C complexes are structurally similar to type A architectures and were also reported as a mixture of

atropisomers along the N_{py}-metal axis at room temperature. This type of ligands has been metallated with palladium,[52] ruthenium,[54] silver (not a pincer),[55] mercury,[56] etc.

Type D CNC-NHC ligands: This type of ligand precursor was first synthesis by Chen and Lin[57] through a nucleophilic substitution of N-substituted imidazole on 2,6-dibromopyridine. Treating the ligand precursor with a strong base and then a metal source usually would lead to metallation with moderate to high yields.[58] In contrast to type A and type C complexes, the fragments of the CNC backbones of type D architectures were often reported to be in the same plane.[59]

Our group has introduced the class of phenylenyl-bridged CCC-bis(NHC) pincer ligand systems.[60] The pincer CCC-bis(NHC) ligand architectures have been successfully incorporated to many transition metals.[38,51] The metal pincer complexes have demonstrated applications in catalysis, light emitting devices (LED) and crystal designing.

Work of the author has been focused mainly on the syntheses, characterization and application of platinum pincer CCC-bis(NHC) complexes.

CHAPTER 2

SYSTHESIS AND CHARACTERIZATION OF CCC-NHC-PLATINUM COMPLEXES

2.1 Research Background

The impact of inorganic and organometallic compounds in photonic applications has been growing rapidly. Recent reports have illustrated their importance in developments for artificial photosynthesis,[61] photocatalytic splitting of water,[62] solar cell applications,[63] organic light-emitting diodes (OLEDs),[64] and photoluminescence.[65] A recent paper detailed the pyridylene CNC-bis(NHC) pincer ligand Pt system and its photoluminescence.[66] This chapter reports the synthesis of CCC-bis(NHC) pincer ligand supported transition metal complexes 2-(1,3-bis(N-butylimidazol-2-ylidene)phenylene)(chloro)Pt(II), **1**, and its bromo analog, **2**, using the metallation/transmetallation methodology. X-ray crystal structure determinations revealed complexes **1** and **2** to have distorted square planar configurations around the metal. Photophysical and thermal properties of these complexes are reported, and their extended photo-stability in air is discussed and contrasted.

2.2 Result and Discussion

2.2.1 Synthesis and Characterization

The CCC-NHC pincer ligand precursors were synthesized using the methodology developed in our group.[38,51,60,67] Simultaneous activation of the three C-H bonds of the tridentate ligand was achieved through the well-established basicity and electrophilicity of $Zr(NMe_2)_4$.[38,51,67-68] A Pt(II) source was added to the *in situ* prepared Zr reagent to achieve transmetallation (Scheme 2.2.1.1). All reactions were carried out at room temperature under an inert atmosphere. When transmetallation was complete, water was added, and excess Zr reagent was decomposed and precipitated. The identity of each complex was established by ^{1}H and ^{13}C NMR spectroscopy, ESI-MS, and elemental analysis (see 2.4 Experimental Section). Two of the primary observations in the ^{1}H NMR spectra were the disappearance of the imidazolium protons (11.27 ppm, 2H) and an aryl H (8.96 ppm). The ^{1}H NMR data of chloro complex **1** and bromo complex **2** also indicated characteristic long range ^{195}Pt-^{1}H coupling. The NHC carbon signal of chloro complex **1** was observed at 171.7 ppm with $^{1}J_{Pt\text{-}C}$ = 1168 Hz. The Pt bound aryl carbon signal was observed at 133.8 ppm with $^{1}J_{Pt\text{-}C}$ = 937 Hz. The NHC carbon signal of bromo complex **2** was observed at 170.5 ppm with $^{1}J_{Pt\text{-}C}$ = 1166 Hz. The Pt bound aryl carbon signal of **2** was observed at 134.0 ppm with $^{1}J_{Pt\text{-}C}$ = 953 Hz. All chemical shifts and coupling constants were similar to those previously reported for Pt-NHC complexes.[66,69] ESI-MS of Pt-Cl **1** revealed the molecular ion plus Na (575 Da). The molecular ion was observed for the Pt-Br complex **2** (595 Da). The experimental values for the CHN analyses of both complexes were within acceptable range.

Scheme 2.2.1.1 Synthesis of CCC^{Bu}-NHC-Pt(II)-X complexes **1** and **2**.

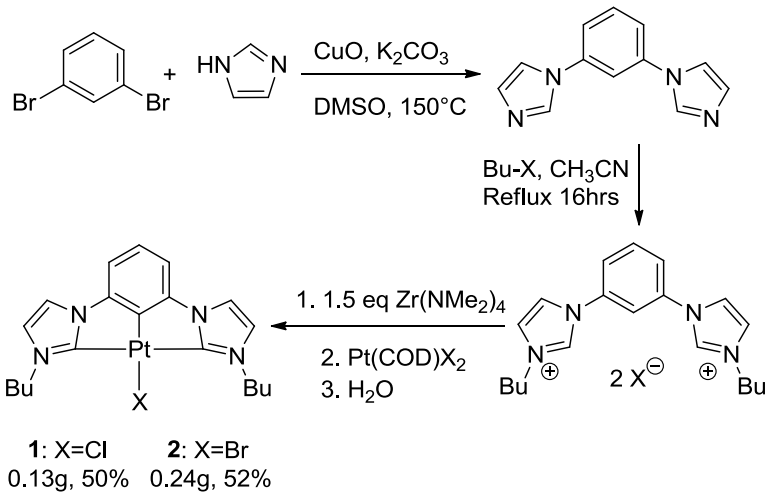

X-ray quality crystals of chloro complex **1** were obtained by slow diffusion of Et_2O into a CH_2Cl_2 solution. X-ray quality crystals of bromo complex **2** were observed after transmetallation and were collected from the reaction mixture. ORTEP® representations of the molecular structures of **1** and **2** are depicted in Figure 2.2.1.1.[70] Selected bond distances and angles for complexes **1** and **2** have been listed in Table 2.1.1.1 and were consistent with previously reported Pt(II) metal complexes.[66,69a,71] The structural data for the pyridylene-bridged CNC analog has been listed for comparison.[66] The structure of complexes **1** and **2** were similar. The Pt-$C_{carbene}$ bond distances in chloro complex **1** (2.030(3) Å and 2.035(3) Å) and in bromo complex **2** (2.037(6) Å and 2.036(6) Å) fell into the range observed for neutral and cationic Pt(II) pincer complexes.[66,69a,71] Both complexes displayed distorted square planar configurations at the metal center, which has been commonly seen for four-coordinate Pt(II) complexes.[69a,71] The C7-Pt(II)-X atoms were linear (**1**: 179.40(8) º and **2**: 178.66(18) º). However, the C2-Pt(II)-C13 angles were bent (**1**: 157.44(11) º and **2**: 157.3(2) º) due to ligand constraints.

It was possible to compare the metric data for Pt-Cl complex **1** to its pyridylene bridged CNC analog. The Pt-C_{aryl} bond length of complex **1** (1.941(3) Å) was slightly shorter (~0.025 Å) than the Pt-N bond length of the pyridylene-bridged CNC complex, while the Pt-C_{NHC} bonds of complex **1** were about 0.06 Å longer.[66] In comparing the Pt-Cl bond distances, a greater trans-influence of the C_{aryl} anionic ligand was notable in the longer bond length (2.3997(7) Å vs. 2.278(2) Å, Table 2.2.1.1). Other metric data for the two compounds were very similar.

Figure 2.2.1.1 ORTEP® diagram (50% thermal ellipsoids) of CCC^{Bu}-NHC- Pt(II)-Cl **1** and CCC^{Bu}-NHC- Pt(II)-Br **2**. Hydrogen atoms omitted for clarity.

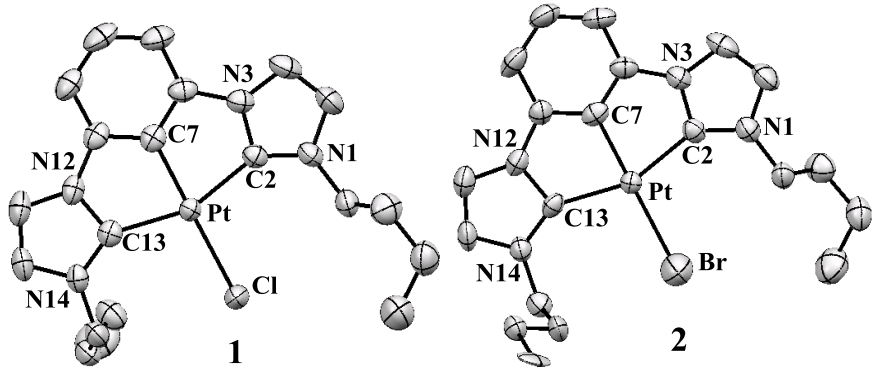

Table 2.2.1.1 Selected bond lengths and angles data of CCC^{Bu}-NHC-Pt(II)-X complexes **1** and **2**, and the CNC^{Bu}-NHC-Pt(II)-Cl complex.

	Selected Bond Length (Å)				Selected Bond Angle (°)		
	Pt-C2	Pt-C7	Pt-C13	Pt-X	C7-Pt-X	C2-Pt-C13	C7-Pt-C2
1	2.030(3)	1.941(3)	2.035(3)	2.3997(7)	179.40(8)	157.44(11)	78.58(11)
2	2.037(6)	1.955(6)	2.036(6)	2.5028(8)	178.67(18)	157.3(2)	78.9(3)
		Pt-N			N-Pt-Cl		
CNC[a]	1.972(8)	1.968(5)	1.978(9)	2.278(2)	178.79(18)	158.1(3)	79.1(3)

[a] Pyridylene-bridged CNC analog with X = Cl. Data from reference 6.

2.2.2 Photophysical Studies

Complexes **1** and **2** were found to emit blue light with UV stimulation. Their absorption and emission data in MeOH solution have been included in Table 2.2.2.1 and Figure 2.2.2.1a. In MeOH solution, the UV absorption spectra of complexes **1** and **2** were nearly identical. Both exhibited a major absorption peak around 265 nm and minor peaks near 323 and 355 nm which were ascribed as mixed metal to ligand charge transfer and ligand centered (MLCT-LC) transitions.[72] The d-d transitions that lead to absorption peaks above 400 nm with significant strength were consistent with a distorted square planar configuration of each complex.[73] The emission spectra of complexes **1** and **2** were very similar except the ratio of major peaks (Figure 2.2.2.1a). Observed solution quantum efficiencies were 1.3% for complex **1** and 1.5% for complex **2** (Table 2.2.2.1). Lifetimes of excited states in methanol solutions were 215 ns for complex **1** and 1.7 μs for complex **2** (Figure 2.2.2.3), which was comparable to organometallic complexes of related structures.[65b]

Table 2.2.2.1 Photophysical properties of CCC^{Bu}-NHC-Pt(II)-X complexes **1** and **2** in MeOH solution.

	λ_{abs}/nm ($\varepsilon \times 10^{-3}$ M^{-1} cm^{-1})	λ_{em}/nm (relative int.)	Φ_{obs}/%	τ/μs
1	265 (22.9), 323 (3.3), 355 (5.7), 416 (0.12), 441 (0.08)	449 (100), 474 (63) [a]	1.3 [b]	0.21
2	266 (24.0), 323 (3.5), 358 (6.2), 416 (0.13), 440 (0.08)	450 (100), 474 (77) [a]	1.5 [b]	1.7

[a] Irradiated with 360 nm. [b] Referenced to quinine sulfate.

In the solid state, the strong blue emission of complexes **1** and **2** varies only slightly (Figure 2.2.2.1b). While sharing λ_{max} at 472 nm, complex **2** had a more intense shoulder peak at 455 nm, which suggested a Pt to halogen interaction was involved in the emission process. The emission curves extended to about 600 nm, but the sharp drop after the peak at ~480 nm gave the complexes a pure blue color. Compared to the pyridine bridged analog reported by Lee et al.,[66] complexes **1** and **2** gave relatively narrow emission peaks (half peak width of ~50 nm), and they were blue shifted 100-150 nm. Decay of the excited state of complexes **1** and **2** in the solid state exhibited a bi-exponential pattern (Figure 2.2.2.2). The lifetimes of excited states of **1** and **2** are comparable to other known organometallic complexes.[74] No difference in lifetime was observed between ambient and vacuum (10^{-5} torr) conditions for the solid state.

Figure 2.2.2.1 Emission and absorption data of CCC^{Bu}-NHC-Pt(II)-X complexes **1** and **2** in a) MeOH solution; Insertion: d-d transitions, and b) solid state at 298K (irradiated at 355 nm).

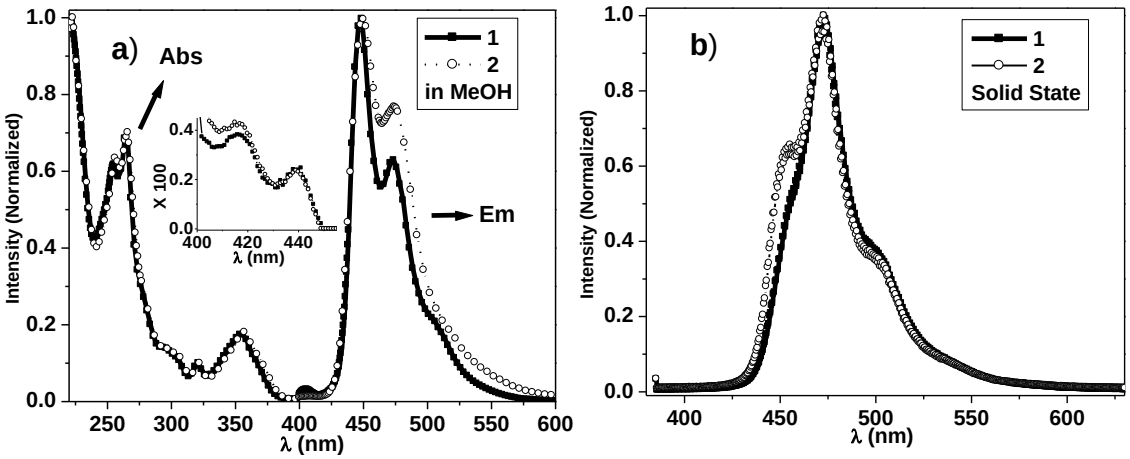

Figure 2.2.2.2. Lifetime decay curves of **1** and **2** in solid state.

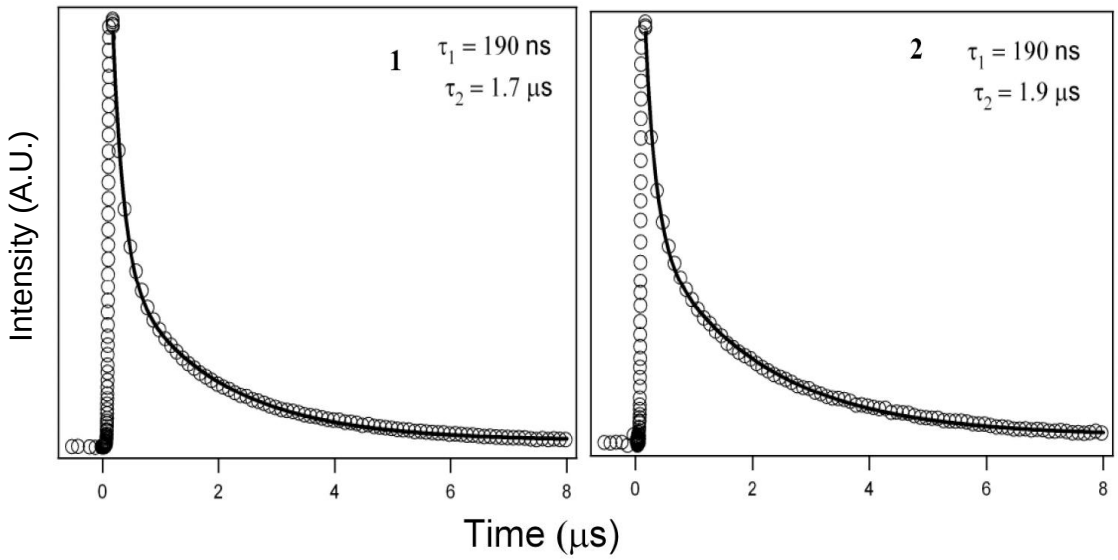

Figure 2.2.2.3. Lifetime decay curves of **1** and **2** in MeOH solution.

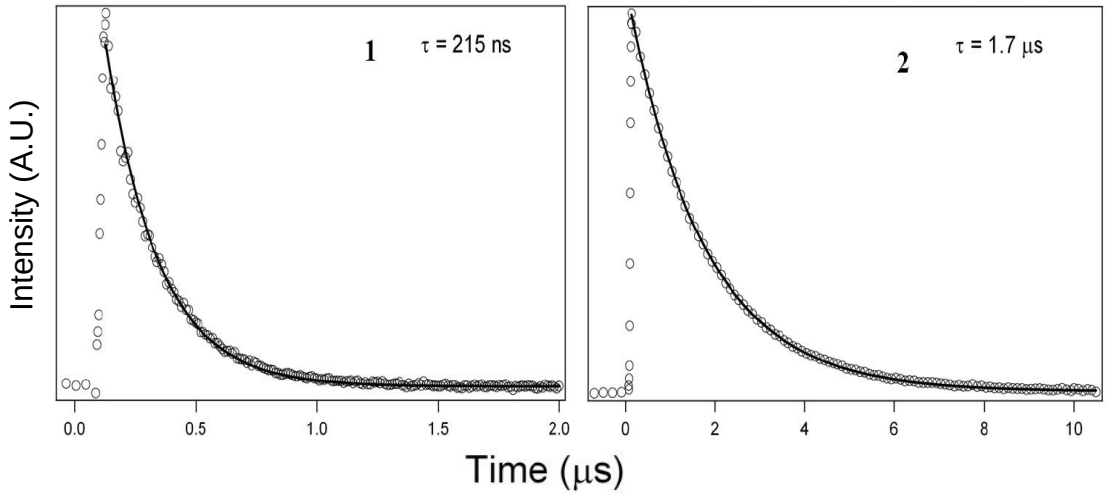

2.2.3 Thermophysical Studies

Thermostability is crucial to OLED emitter candidates. The thermal properties of complexes **1** and **2** were investigated by TGA and DSC. It was found that the compounds melted at approximately 280 ℃ and remained as super-cooled liquids over a large

temperature range (Figure 2.2.3.1). The 10% weight loss temperatures ($T_{\Delta 10\%}$) were about 380 ℃ (Figure 2.2.3.2). Notably, complexes **1** and **2** evaporated and deposited on the glass wall of the furnace. Spectroscopic analysis of the residues (fluorescent, NMR, and ESI-MS) indicated the compounds remained unchanged.

Figure 2.2.3.1 DSC thermograms of **1** and **2**. Programmed from 25 ℃ to 300 ℃ to 30 ℃.

* Nitrogen flow is at 20 ml/min and temperature gradient is 20 ℃/min.

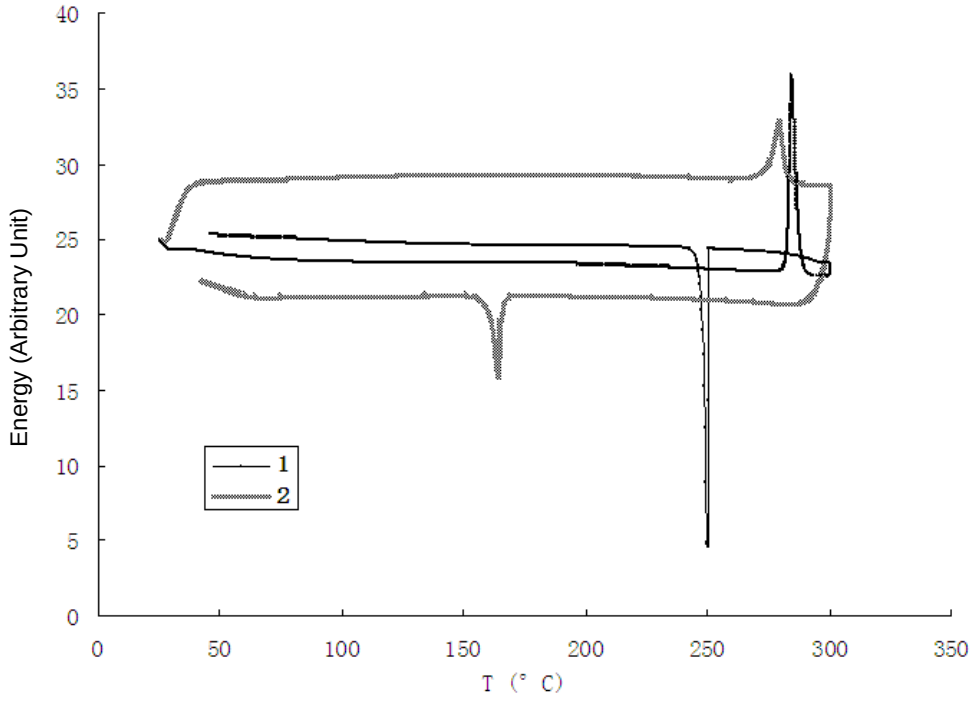

Figure 2.2.3.2 TGA spectra of **1** and **2**.

* Nitrogen flow is at 20 ml/min and temperature gradient is 20 ℃/min.

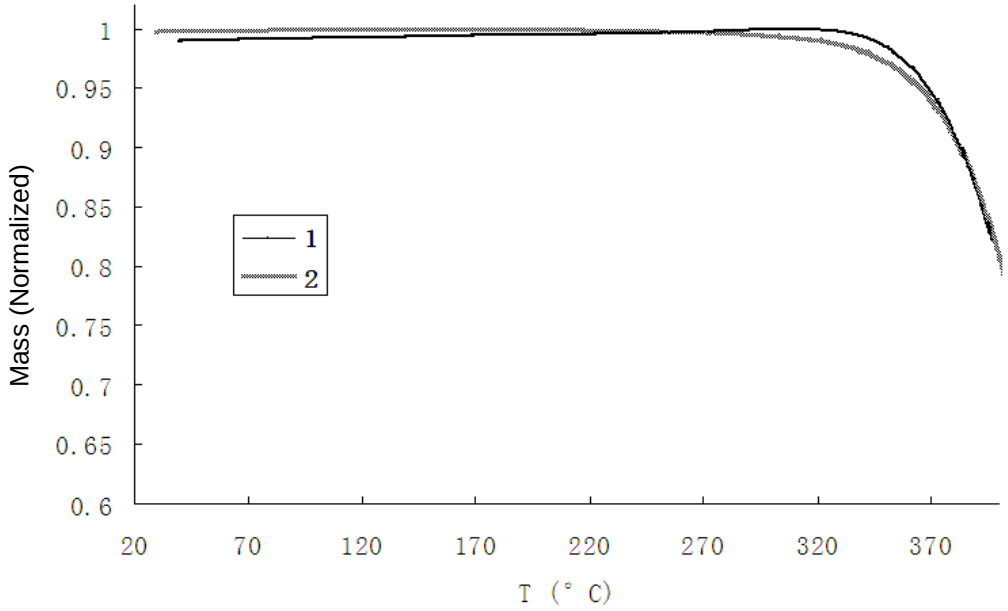

2.2.4 Photostability in Air

Previous studies of Pt NHC complexes suggested that their emissions could be stable under inert atmosphere over an extended period of time.[74c,75] Interestingly, the emissions of complexes **1** and **2** were found to be stable even in ambient atmosphere (room temperature and 30~50% humidity). Time resolved emission spectra of **1** and **2** was presented in Figure 2.2.4.1. The authentic blue λ_{max} (472 nm) of complexes **1** and **2** retained >97% intensity over 6 hrs continuous irradiation. The shape of the spectra remained unvaried during the measurements (Figure 2.2.4.1 and Table 2.2.4.1). These data indicated that complexes **1** and **2** did not photobleach in air with UV irradiation.

Figure 2.2.4.1 Time dependence of emission of solid state **1** and **2** in air over 6 hrs. Irradiated at 355 nm.

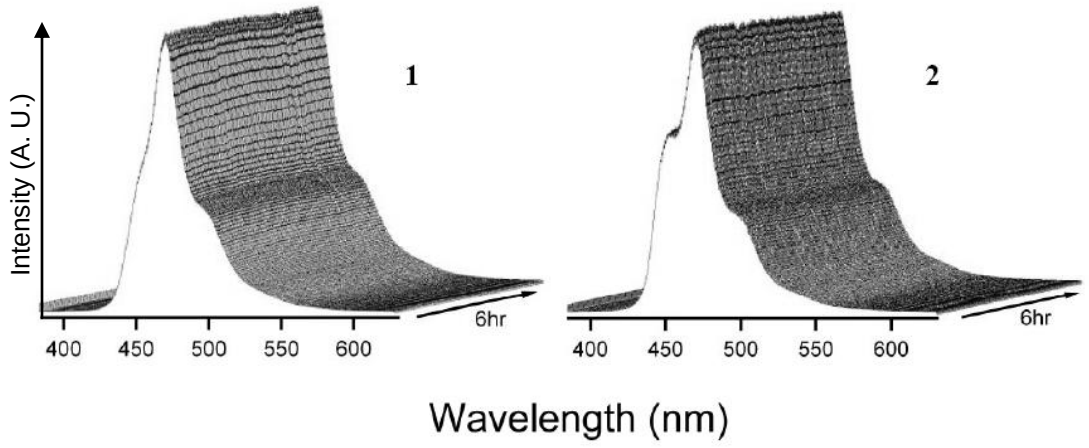

The photostability test under N_2 and ambient atmosphere was also carried out on four commercially-available emitters: tris-(8-hydroxyquinoline)aluminum (**Alq_3**),[64a,76] tris[2-(4,6-difluorophenyl) pyridinato-C^2,N]iridium(III) (**$Ir(dfppy)_3$**),[77] 8-hydroxyquinolinezinc (**Znq_2**)[78] and lithium tetra(2-methyl-8-hydroxyquinolinato)boron (**LBMQ**)[79] (Scheme 2.2.4.1). Three of the emitters, **Alq_3**, **Znq_2**, and **LBMQ** were found to be stable to photo excitation under nitrogen (no significant loss of emission intensity after 6 h). **$Ir(dfppy)_3$** showed significant loss of intensity of $_{max}$ (29%) after 6 h of photo excitation under the same conditions. When these commercially-available complexes were irradiated under ambient atmosphere, moderate to severe photo-bleaching was observed. **$Ir(dfppy)_3$** exhibited a loss of more than half of its initial emission strength and a visible darkening on the irradiated surface after only one hour (Table 2.2.4.1). When significant photo-bleaching (>10%) was observed in any condition, a control experiment was carried out to calibrate the contribution to decomposition from other pathways. In the control experiment, an initial emission spectrum **A** was collected and the analyte was then kept under the same conditions with the radiation beam blocked. After an hour the irradiation

was resumed and another emission spectrum **B** was taken. The loss of emission intensity between spectra **A** and **B** was ascribed to the sum of decompositions through all other pathways. Since each spectrum took ~2 min to accumulate, a significant measurement-induced photo-bleaching was observed for the less photo-stable analytes (Figure 2.2.4.2-5). An exponential fitting based on the decay curve was applied to retrieve the photo-bleaching during the initial 2min irradiation. During the one hour in the dark all compounds were found to undergo <1% decomposition, which confirms a direct correlation between photo-bleaching and loss of emission strength. In comparing the pincer Pt(II) complexes **1** and **2** and the four commercially-available emitters, these observations indicated that the Pt complexes were much more photo-stable in ambient atmosphere.

Scheme 2.2.4.1 Four commercially-available emitters.

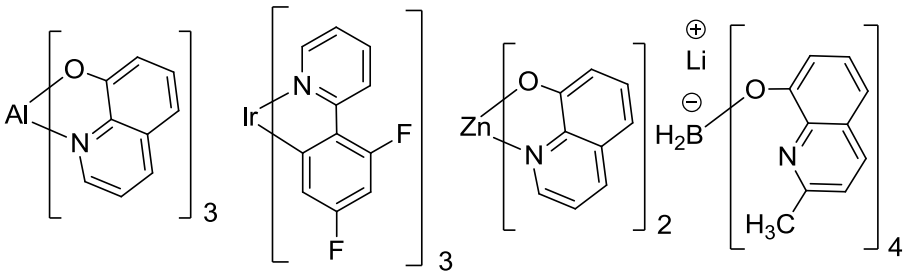

Alq_3 **$Ir(dfppy)_3$** **Znq_2** **LBMQ**

Table 2.2.4.1 Solid state emission and lifetime data of CCC^{Bu}-NHC-Pt(II)-X complexes **1**, **2**, and four commercially-available emitters.

	λ_{em}/nm (relative int. %) [a]	% remaining intensity [b]		τ_{obs}/μs	
		In N_2	In air	In air	In vac
1	445 (39), 472 (100), 502 (42)	--	99(0.4)	0.19/1.7	0.19/1.7
2	455 (66), 472 (100), 502 (33)	--	97(0.3)	0.19/1.9	0.19/1.9
Alq_3	506 (100)	99(0.2)	51(3.8)	0.016[c]	
$Ir(dfppy)_3$	499 (100)	71(4.6)	46(3.0) [d]	--	
Znq_2	536 (100)	99(1.8)	78(1.8)	0.025[e]	
LBMQ	463 (100)	99(0.3)	84(5.6)	--	

[a] Irradiated at 355 nm [1.67mW/cm^2]. [b] $_{max}$ after 6h of continuous excitation. Data presented are an average of 3 measurements, (standard deviation) values are included in parentheses. [c] See reference 18, data collected under nitrogen. [d] After 1h. [e] See reference 43, data collected under nitrogen.

Figure 2.2.4.2. Time dependent fluorescent of Alq_3 in N_2 (left) and in air (right)*.

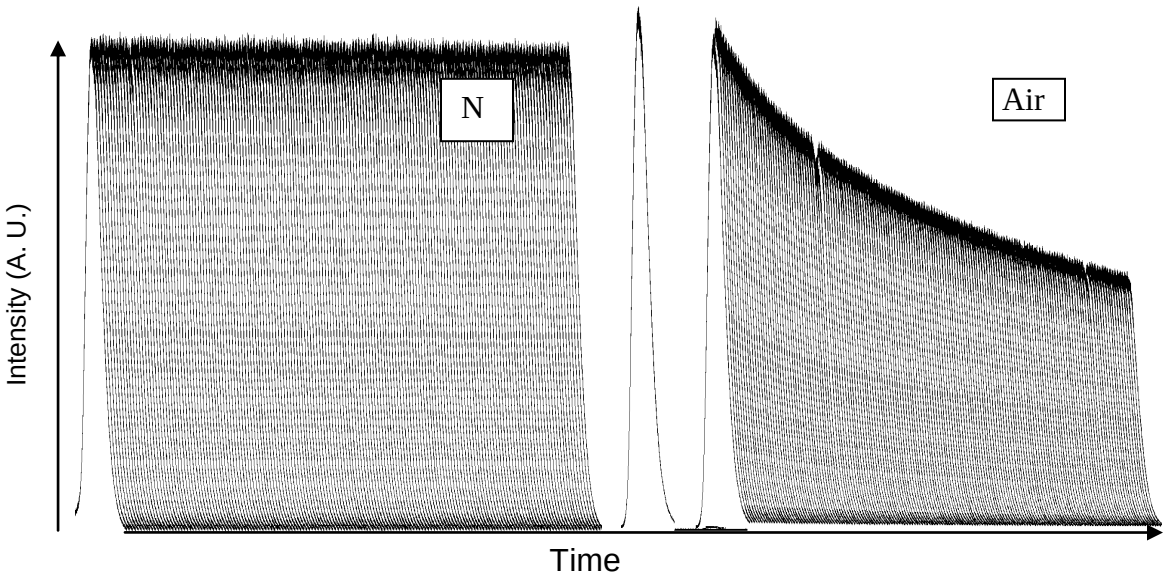

* Sample was set in dark for 1 hr (gap) before 6hrs continuous irradiation.

Figure 2.2.4.3 Time dependent fluorescent of $Ir(dfppy)_3$ in N_2 (left)* and in air (right)**.

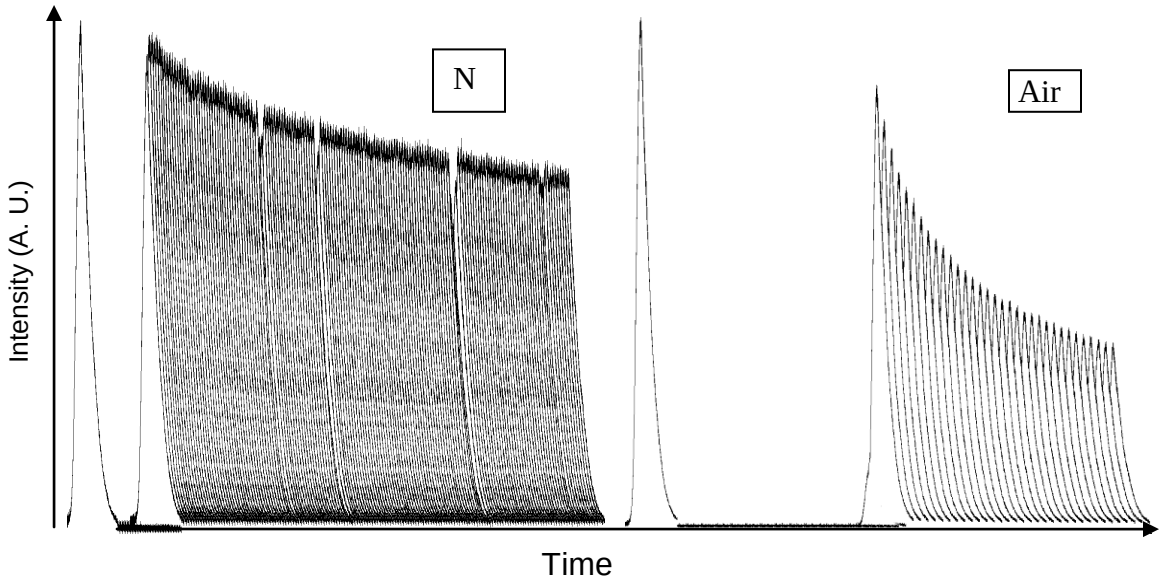

* Sample was set in dark for 1 hr (gap) before 6hrs continuous irradiation.

** Sample was set in dark for 1 hr (gap) before 1hrs continuous irradiation.

Figure 2.2.4.4 Time dependent fluorescent of Znq_2 in N_2 (left) and in air (right)*.

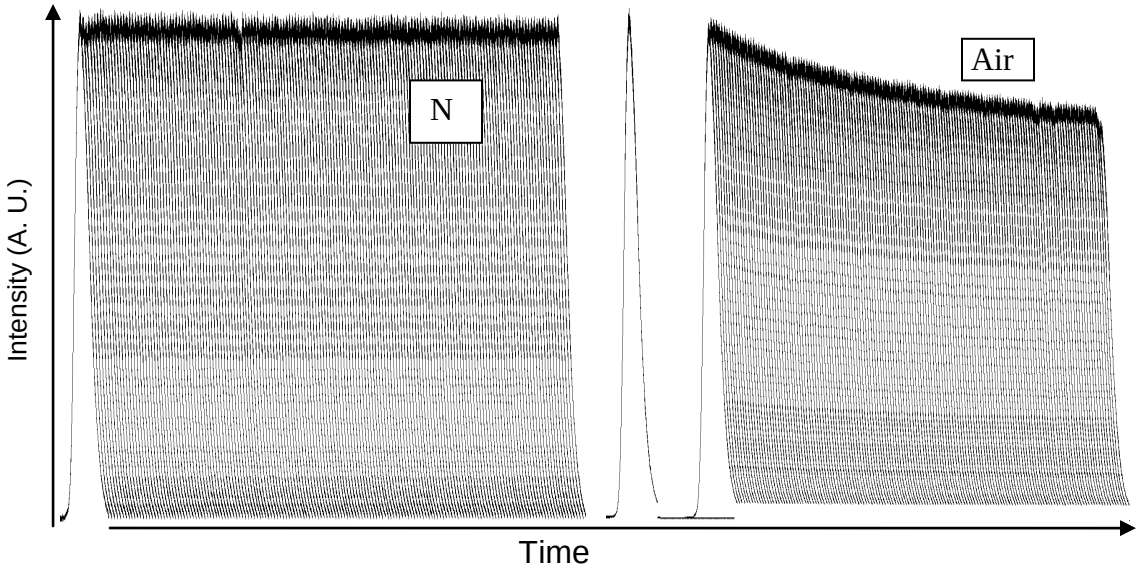

* Sample was set in dark for 1 hr (gap) before 6hrs continuous irradiation.

Figure 2.2.4.5 Time dependent fluorescent of LBMQ in N_2 (left) and in air (right)*.

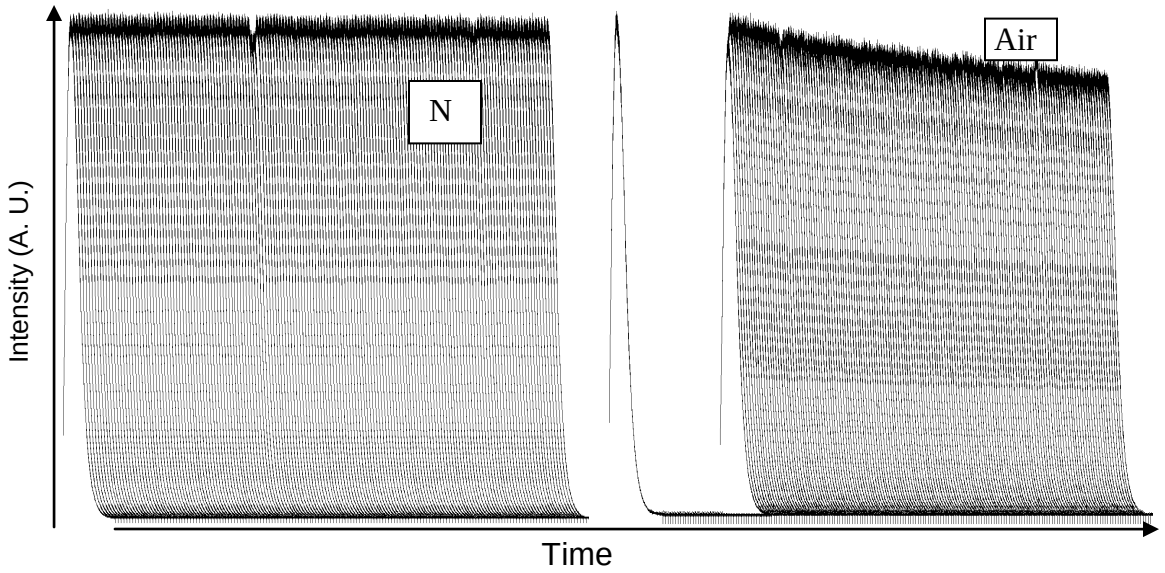

* Sample was set in dark for 1 hr (gap) before 6hrs continuous irradiation.

2.3 Conclusions

The synthesis and characterization of two novel CCC-NHC pincer Pt(II) complexes **1** and **2** have been reported. They displayed distorted square planar configurations as expected for d^8 four coordinated transition metal compounds. Complexes **1** and **2** were found to emit bright blue light in the solid state under UV irradiation with emissions that were stable in ambient atmosphere (O_2 and H_2O) for extended periods. At the same time, they were found to be thermo-stable under N_2 atmosphere upon evaporation, which suggested that they would be suitable for thermo-deposition processing.

2.4 Experimental Section

General Procedures: All starting materials were purchased from Sigma-Aldrich®, Fisher Scientific® or Strem®. The reagents used as received unless otherwise mentioned. All solvents were dried and were degassed by passing through a basic alumina column under Ar protection.[80] All reactions involving organometallic reagents were carried out under N_2 or Ar atmosphere using standard glovebox and Schlenk line techniques. NMR spectra were collected using Bruker Avance 300 or 500 spectrometers and were referenced to the residual solvent peak (δ in ppm, J in Hz). Electro-spray ionization mass spectra were collected using a Waters Micromass ZQ mass spectrometer. Elemental analyses were carried out by Columbia Analytical Service or on a PerkinElmer 2400 Series II CHNS/O analyzer. UV-visible absorption spectra were collected using a HP 8453 UV-Visible system. Emission spectra were collected using a PerkinElmer LS 55 fluorescence spectrometer. Photo-stability studies were carried out by exposing the solid

sample to 355 nm radiation. The light source was a Xenon lamp, and the detector was a photodiode array placed behind a filter next to the sample chamber. Lifetime measurements were carried out using 10Hz pulsed 355 nm Nd:YAG laser output as the pumping source and a photomultiplier tube as detector. TGA/DSC data were collected on PerkinElmer Pyris 1 TGA/DSC 4000, with nitrogen flow at 20 mL/min and temperature gradient set at 20 ℃/min.

2-(1,3-Bis(N-butylimidazol-2-ylidene)phenylene)(chloro) Pt(II), (1). 1,3-Bis(1-butylimidazolium-3-yl)benzene dichloride (0.20 g, 0.50 mmol), tetrakis(dimethylamino)zirconium (0.17 g, 0.63 mmol) and CH_2Cl_2 (~4.0 mL) were combined. The mixture was stirred for 1 hr at room temperature to afford a red solution. [Pt(COD)Cl_2] (0.19 g, 0.50 mmol) was added and was stirred vigorously at room temperature for 6 hrs. The reaction mixture was transferred to a round bottom flask that contained 1 mL of distilled water, and the precipitate was removed by filtration. The filtrate was concentrated under vacuum to afford a yellow solid. The solid was washed with water (2 1 mL), cold CH_2Cl_2 (2 1 mL), and Et_2O (3 3 mL), and was dried under vacuum yielding a yellow crystalline solid (0.13 g, 50 %). X-ray quality crystals were grown by slow diffusion of diethyl ether vapor into a CH_2Cl_2 solution of **1**. ^{1}H NMR (CD_2Cl_2; 300.132 MHz): δ 7.40 (dd, 2H, J = 2.0 Hz, J = 9.0 Hz, imid), 7.01 (dd, 2H, J = 2.0 Hz, J = 9.0 Hz, imid), 7.16 (t, 1H, J = 7.8 Hz, p-Ph), 6.93 (dd, 2H, J = 8.0 Hz, J^4 Pt-H = 16.1 Hz, m-Ph), 4.69 (t, 4H, J = 7.3 Hz, NCH_2), 1.86 (quintet, 4H, J = 7.5 Hz), 1.45 (sextet, 4H, J = 7.7 Hz), 0.97 (t, 6H, J = 7.4 Hz); ^{13}C NMR (d-DMSO; 75.476 MHz, 350K): δ 171.7 (J^1 Pt-C = 1068 Hz), 144.1, 133.8 (J^1 Pt-C = 937 Hz), 123.3, 121.1, 115.7, 107.6, 47.7, 32.7, 18.8, 13.2; ESI-MS: Calculated for $C_{20}H_{25}ClN_4PtNa$ [M+Na] (m/z):

575 (100%), 574 (93%), 573 (74%), 576 (45%), 577 (42%) Found: 575 (100%), 574 (96%), 573 (78%), 576 (46%), 577 (43%); Elemental Analysis: Calculated: C, 43.52; H, 4.57; N, 10.15; Found: C, 43.19; H, 4.09; N, 9.90.

2-(1,3-Bis(N-butylimidazol-2-ylidene)phenylene)(bromo) Pt(II), (2). 1,3-Bis (1-butylimidazolium-3-yl)benzene dibromide (0.48 g, 1.0 mmol), tetrakis(dimethylamino)zirconium (0.32 g, 1.2 mmol), and THF (10 mL) were stirred for 1 hr at room temperature yielding a cloudy suspension. [Pt(COD)Br_2] (0.463 g, 1.0 mmol) was added and the reaction mixture was stirred at room temperature for 8 hrs yielding a cloudy yellow suspension. After standing for 10 min, a yellow precipitate was observed with a clear reddish supernatant liquid. The precipitate was collected and washed with toluene (3 3 mL), yielding an analytically pure yellow solid (0.242 g, 52%). Some of the solid was directly used for X-ray crystallography. ^{1}H NMR (CD_2Cl_2; 300.132 MHz): δ 7.40 (dd, 2H, J = 2.0 Hz, J = 9.0 Hz, imid), 7.01 (dd, 2H, J = 2.0 Hz, J = 9.0 Hz, imid), 7.18 (t, 1H, J = 7.8 Hz, p-Ph), 6.93 (dd, 2H, J = 8.0 Hz, J^4Pt-H = 17.8 Hz, m-Ph), 4.76 (t, 4H, J = 7.3 Hz, NCH_2), 1.87 (quintet, 4H, J = 7.5 Hz), 1.45 (sextet, 4H, J = 7.7 Hz), 0.97 (t, 6H, J = 7.4 Hz); ^{13}C NMR (d-DMSO; 75.476 MHz, 350K): δ 170.5 (J^1 Pt-C = 1166 Hz), 143.8, 134.0 (J^1 Pt-C = 953 Hz), 122.8, 121.3, 115.4, 107.5, 48.3, 32.8, 18.6, 13.1; ESI-MS: Calculated for $C_{20}H_{25}BrN_4Pt$ [M+] (m/z): 595.1 Found: 595.0; Elemental Analysis: Calculated: C, 40.28; H, 4.22; N, 9.39; Found: C, 40.10; H, 3.94; N, 9.30.

X-Ray Crystallography. X-ray quality crystals of **1** and **2** were mounted atop fine glass fibers. Diffraction experiments were performed on an Oxford Diffraction Systems

Gemini S diffractometer with MoKα radiation (λ = 0.71073 Å) at 298K. The structures were solved and refined using SHELX suite programs.

CHAPTER 3

SYNTHESIS, CHARACTERIZATION, PHOTOLUMINESCENCE, AND SIMULATIONS OF A CCC-NHC SUPPORTED Pt_2Ag_2 MIXED-METAL CLUSTER CONTAINING A $PtAg_2$ METALLO-CYCLOPROPANE

3.1 Research Background

Multi-metal organometallic systems, especially those containing metal-metal interactions, are of increasing interest due to their unique chemical and physical properties,[81] their versatile practical applications, and their challenges to theoretical understanding.[82] They have been found to be useful for catalysis,[83] crystal engineering[84] and light-emitting materials design.[85] Several examples of multi-metal systems taking advantage of the closed-shell d^{10}-d^{10} or d^8-d^{10} interactions have been reported.[86] The formation and character of these metal-metal interactions, also called "metallophilic bonds",[81c] are still not fully understood.[87] The Pt-Ag interaction is one of the most common d^8-d^{10} interactions.[88] The syntheses of multi-metal complexes containing Pt-Ag dative bonds were often achieved through the reaction of a four coordinated platinum(II) precursor with a silver(I) salt, resulting in Pt-Ag bonds[81c,88b] or Pt-Ag-Ag metallocyclopropanes.[89]

The discovery of stable carbenes,[8] especially the unique stability of N-heterocyclic carbenes (NHCs),[9-12] has stimulated many applications. NHCs have been widely established as ligands

for transition metals.[3,19] NHC-containing organometallic complexes have shown significant activity in catalytic organic transformations including hydroformylation,[90] hydrosilylation,[91] hydrogenation,[92] olefin metathesis,[20] polymerization,[93] Pd cross-coupling reactions,[17b,18b,21,94] and more.[22,95] In addition, they have been demonstrated to catalyze C-heteroatom bond forming reactions to make C-N,[94b,96] C-Si,[91,97] and C-O bonds.[98] Furthermore, they have exhibited useful photophysical properties for material applications.[65b,65d,74c,99] Pincer ligands, due to their robustness and variety, have become widely investigated and applied architectures in modern organometallic chemistry.[29b,100] The combination of NHCs and pincer ligand chemistry has attracted considerable attention in recent years.[36c,36e,57,100b,101]

In this chapter, the synthesis of the platinum(II) pincer CCC-bis(NHC) complex **4** and its reaction with silver(I) trifluoroacetate and silver(I) acetate are described. An unprecedented mixed metal atom cluster **5** and a ligand exchange product **6** were obtained depending on the reaction stoichiometry. However, when reacted with excess or stoichiometric amount of silver(I) acetate, only the simple ligand exchange product **6** was obtained. The structural and photophysical properties of these metal complexes were investigated. A large emission wavelength shift (~150 nm) was found for the solution of complex **5** depending on the concentration, which provides a gateway for further understanding the character of metallophilic bonds and for new approaches toward white-light emission.[102] To the best of our knowledge, the structure of cluster **5** is different from all previously reported Pt_2Ag_2 complexes, which are symmetrical with respect to the central Ag-Ag bond.

3.2 Result and Discussion

3.2.1 Synthesis and Characterization

Synthesis and Characterization of CCC-bis(NHC)-Pt^{II}-Cl complex (4).

The ligand precursor **3** was synthesized using a modified literature procedure.[60] The Pt(II) pincer CCC-bis(NHC) complex **4** was obtained from a one-pot, two-step metallation/transmetallation process (Scheme 3.2.1.1) analogous to our previously reported methodology.[38,51,67] First, by applying $Zr(NMe_2)_4$, the two imidazolium rings were deprotonated and the C-H bond of the phenyl ring was activated yielding a CCC-bis(NHC)-Zr species.[51b] Dichloro(1,5-cyclooctadiene)platinum(II) was added to the in situ generated Zr reagent, and transmetallation to Pt occured. Both steps led to quantitative conversion as monitored by ^{1}H NMR spectra.

In CCC-bis(NHC)-Pt^{II}-Cl complex **4**, the carbons directly bonded to the Pt metal exhibited the characteristic Pt-C coupling pattern with large coupling constants (J^1 Pt-C_{aryl} = 944 Hz; J^1 Pt-C_{NHC} = 1174 Hz) in the ^{13}C NMR spectrum. The NHC carbene signal (δ = 172.8 ppm) was in the downfield region as expected.[66,69] ESI-MS revealed the $[M\text{-}Cl]^+$ fragment at m/z = 576 Da. Mass spectroscopy with milder ionization technique, MALDI, did not capture the parent molecular ion. The experimental values of elemental analysis (C, H, N) were within acceptable range.

Scheme 3.2.1.1 Synthesis of CCC- bis(NHC)-Pt^{II}-Cl Complexes **4**

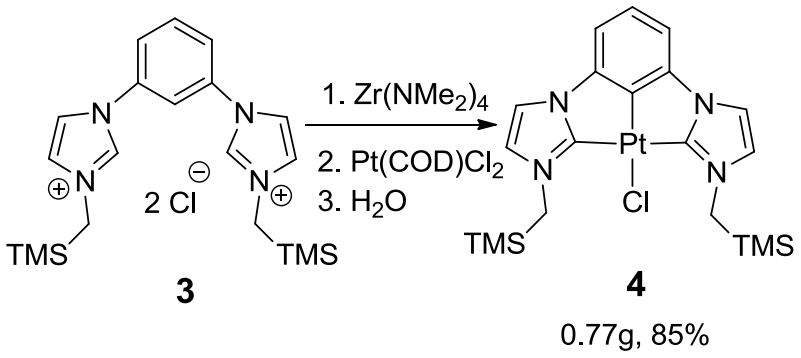

The structure of complex **4** was confirmed by X-ray crystallography (Figure 3.2.1.1 and Table 3.2.1.1). In the solid state complex **4** adopted C_2 symmetry along the C_{aryl}-Pt-Cl axis and was close packed in the C_2/c space group. The Pt-C_{NHC} bond distance in **4**, 2.024(3) Å, falls in the range observed for neutral and cationic Pt(II) NHC complexes.[66,69a,71b,103] The Pt-C_{aryl} bond length, 1.929(3) Å, was ~0.15 Å shorter than the Pt-C_{aryl} bond lengths in mono-dentate complexes.[104] The coordination sphere of Pt(II) in complex **4** was a distorted square planar configuration, which is commonly seen for four-coordinated Pt(II) complexes.[69a,71b] The C7-Pt-Cl atoms were linear (180 º). However, the C1-Pt-C1' angle was bent (157.39(13) º). The acute angle was attributed to ligand constraints.

Figure 3.2.1.1 ORTEP diagram (50% thermal ellipsoids) of CCC-bis(NHC)-Pt^{II}-Cl complex **4**. Hydrogen atoms omitted for clarity. Selected metric data presented in Table 3.2.1.1.

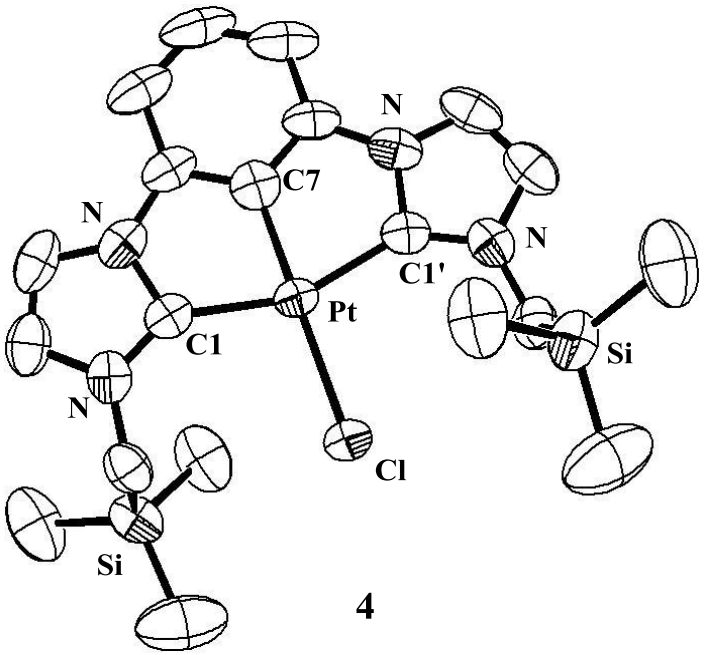

4

Table 3.2.1.1 Selected Bond Length and Angle Data of CCC-bis(NHC)-Pt^{II}-Cl Complex **4**, Pt_2Ag_2 Cluster **5** and CCC-bis(NHC)-Pt^{II}-O_2CCF_3 Complex **6**

Selected Bond Lengths (Å)

	4	**5**		**6**
		Pt1	Pt2	
Pt-C7 [a]	1.929(3)	1.932(3)	1.931(5)	1.937(4)
Pt-C1 [a]	2.024(3)	2.024(4)	2.021(3)	2.035(5)
Pt-C1' [a]	2.024(3)	2.046(3)	2.023(3)	2.030(5)
Pt-X [b]	2.4053(8)	2.137(3)	2.135(3)	2.163(6)

Selected Bond Angles (°)

	4	**5**		**6**
		Pt1	Pt2	
C7-Pt-X [a,b]	180.0(1)	175.9(1)	176.7(1)	167.1(2)
C1-Pt-C7 [a]	78.7(1)	78.6(1)	79.2(2)	79.1(2)
C1'-Pt-C7 [a]	78.7(1)	78.8(1)	79.3(2)	78.3(2)
C1-Pt-X [a,b]	101.30(7)	98.2(1)	104.1(1)	98.7(2)

[a] Numbering are different for cluster **5** and complex **6**

[b] For complex **4**, X = Cl, for cluster **5** and complex **6**, X = ***O***$COCF_3$

Ligand metathesis of CCC-bis(NHC)-Pt^{II}-Cl complex (4)

Ligand exchange on transition metal complexes with silver salts is a common procedure. Considering the general poor solubility of Ag salts, initial experiments of ligand metathesis of complex **4** were conducted with excess (≥2.0 equiv) of AgO_2CCF_3 (Scheme 3.2.1.2). When the ^1H NMR spectra of the reaction indicated complete conversion of the starting material, the solution portion was decanted and an orange product was isolated. Although the ^1H and ^{13}C NMR spectra had the anticipated changes for a simple ligand metathesis reaction, the ^{19}F NMR spectrum exhibited two broad peaks at 73.81 ppm ($w_{1/2}$ = ~150 Hz) and 72.98 ppm ($w_{1/2}$ = ~210 Hz). This observation was consistent with more than one type of coordinating trifluoroacetato ligand and indicated that exchange was occurring on the NMR time scale in solution. Exact Mass ESI-TOF-MS revealed three major fragments at masses much greater than the simple ligand exchange product. The peak at 1708.0896 Da was ascribed to the composition of $[C_{46}H_{58}Ag_2F_9N_8O_6Pt_2Si_4]^+$. On the basis of X-ray crystal structure determination (*vide infra*) this formula was assigned as $[M\text{-}(O_2CCF_3)]^+$, $[[(C_{20}H_{29}N_4Si_2)Pt(O_2CCF_3)]_2[Ag_2(O_2CCF_3)]]^+$. The base peak at 1486.1912 Da equaled to a fragment of $[C_{44}H_{58}AgF_6N_8O_4Pt_2Si_4]^+$, which was $[M\text{-}Ag(O_2CCF_3)_2]^+$. Also observed was a peak at 1265.2849 Da indicating a fragment of $[C_{42}H_{58}F_3N_8O_2Pt_2Si_4]^+$, which was $[M\text{-}Ag_2(O_2CCF_3)_3]^+$. All peaks exhibited high agreement with the calculated isotope patterns. These data were consistent with a multi-metal cluster with the

composition of $[CCC\text{-}Pt^{II}\text{-}O_2CCF_3]_2[AgO_2CCF_3]_2$. Recrystallization of the product yielded no change in the spectral data. The synthesis was reproducible.

Scheme 3.2.1.2 Ligand Metathesis of CCC-bis(NHC)-Pt^{II}-Cl Complex **4** with Silver Trifluoroacetate; Insertions: isolated solids under UV excitation

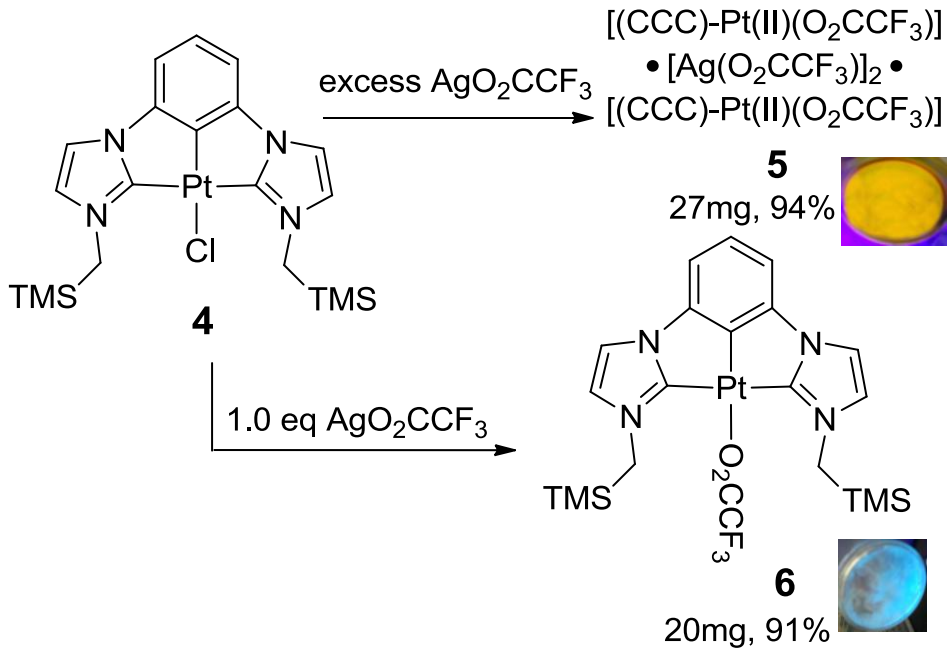

X-ray quality crystals of **5** were grown by slow diffusion of hexanes vapor into a CH_2Cl_2 solution. Diffraction analysis revealed a unique structure with bridging trifluoroacetato ligands and Pt-Ag and Ag-Ag interactions. ORTEP representations of the molecular structure are depicted in Figure 3.2.1.2, and the numerical data of selected bond lengths and angles are listed in Table 3.2.1.1 and Table 3.2.1.2. An unsymmetric Pt_2Ag_2 core was found in the crystal structure, containing a scalene Pt-Ag-Ag triangle (Ag1-Ag2 = 2.8430(4) Å, Pt1-Ag1 = 3.1413(4) Å and Pt1-Ag2 = 2.9335(3) Å) and a second Pt-Ag interaction (Pt2-Ag2 = 2.9104(3) Å) supported by trifluoroacetato ligands. The known Pt-Ag-Pt sandwich-like structures have the two Pt ligand spheres oriented in 'head to head' (∠ L-Pt1-Pt2-L = ~0 °)[85b,86a,86b,89] or 'head to tail' (∠ L-Pt1-Pt2-L = ~180 °)

configurations (Scheme 3.2.1.3).[81c,105] In cluster **5**, the two Pt ligand spheres are oriented in a configuration that is approaching perpendicular with a C_{aryl}-Pt-Pt-C_{aryl} dihedral angle of 57 °.

Scheme 3.2.1.3 Ligand Spheres of Pt-Ag-Pt Sandwich-Like Structures

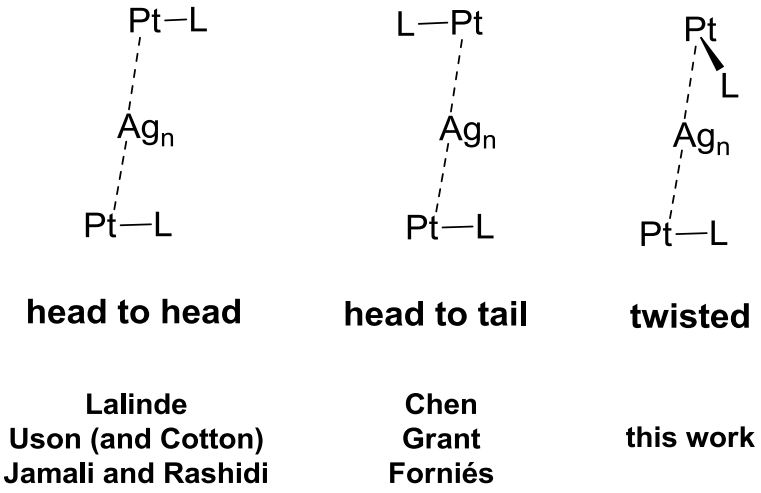

Another interesting feature of the structure was that the coordination sphere of atom Ag2 displayed a distorted octahedral configuration. The three Ag-O bonds in Ag2 coordination sphere (Ag2-O29 = 2.403(3) Å, Ag2-O43 = 2.308(3) Å, and Ag2-O48 = 2.416(3) Å) are largely ionic ($Ag^+ + O^{2-}$ = 1.29 + 1.26[106] = 2.55 Å). While the Ag-O bonds in Ag1 coordination sphere (Ag1-O34 = 2.180(3) Å, and Ag1-O41 =2.177(3) Å) are majorly covalent (Ag + O = 1.45 + 0.68[107] = 2.13 Å) (Table 3.2.1.2). The Pt atoms in cluster **5** are 6-coordinated, Pt1, and 5-coordinated, Pt2, which is uncommon for Pt of +2 formal oxidation state.[108] The bulky TMS groups adopted meso instead of a trans conformation in cluster **5** (Figure 3.2.1.2a). Comparing the metric data of the Pt coordination sphere for the monomeric precursor **4**, CCC-bis(NHC)-Pt^{II}-Cl, and Pt-

O_2CCF_3 complex **6** (*vide infra*) to that of the cluster **5** in Table 3.2.1.1 revealed essentially no change ($\Delta \leq 0.03$ Å for same type of bonds).

Weak hydrogen bonds (WHB) C–H…O, C–H…F and C–F…π interactions were also identified within the crystal structure of cluster **5**. In spite of being more frequently reported, only one intermolecular C–H…O bond was found with a C…O distance of 3.098 Å. On the other hand, many C–H…F bonds were found in cluster **5**. Asensio et al. summarized the reported C_F–H…F interactions to have a H…F distance range of 2.5–2.9 Å and a C_F–H…F angle range of 110–170 °,[109] where C_F stands for partially fluorinated carbon. Others have suggested the same range for non-fluorinated carbon systems.[110] As depicted in Figure 3.2.1.3a, b, and c, there are three well-defined intramolecular C–H…F bonds and two pairs of intermolecular C–H…F bonds, where the position of the H atom can be deduced with high certainty. Moreover, there are four intramolecular C_{methyl}…F distances within the range generally considered C–H…F bonds (Figure 3.2.1.3d). Two C–F…π interactions are also demonstrated in Figure 3.2.1.3e. Although these interactions have been considered to be very weak individually ($<$ 5 kcal/mol),[111] the number present here suggests that they may play a significant role in the formation of the unique configuration of cluster **5**.

Figure 3.2.1.2 ORTEP diagram (50% thermal ellipsoids) of Pt_2Ag_2 cluster **5**. a) all heavy atoms presented; b) hydrogen atoms, trifuoromethyl groups and trimethylsilyl groups omitted for clarity.

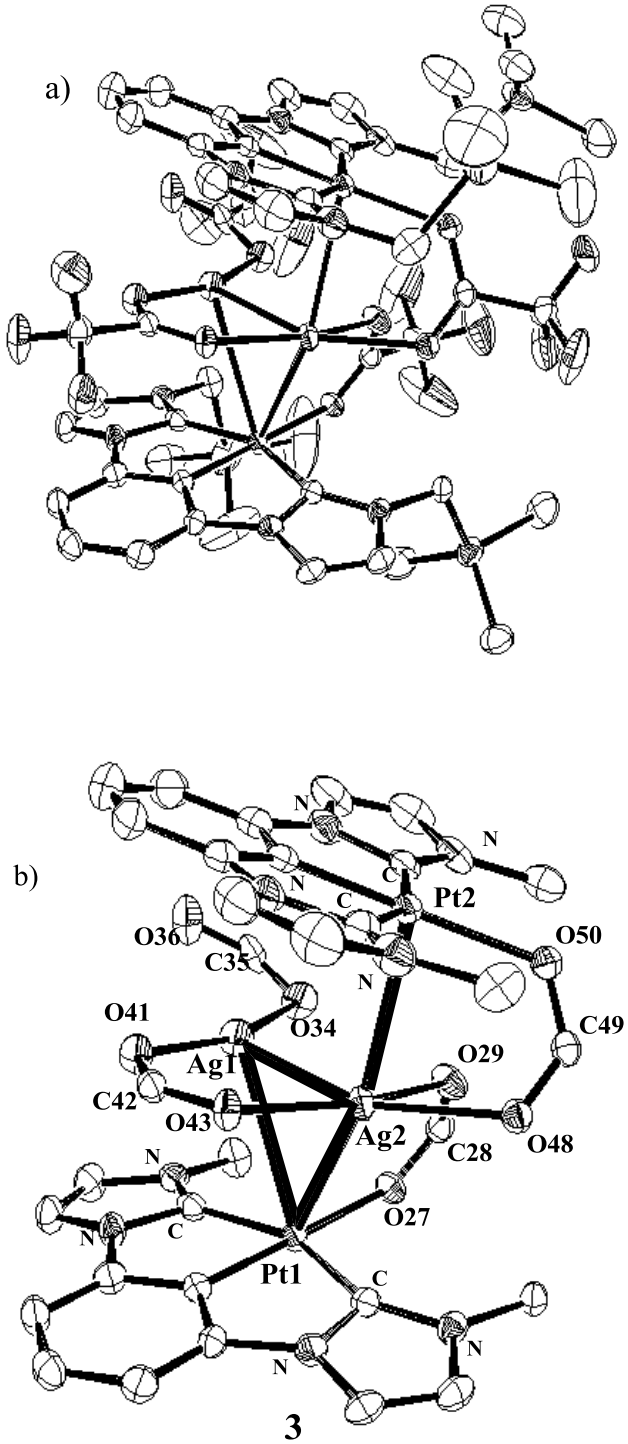

Table 3.2.1.2 Selected Bond Length and Angle Data of Pt_2Ag_2 Cluster **5**.

Selected Bond Length (Å)				Selected Bond Angle ( )	
Pt1-Ag1	3.1413(4)	Ag1-Ag2	2.8430(4)	Ag1-Pt1-Ag2	55.68(1)
Pt1-Ag2	2.9335(3)	Ag1-O34	2.180(3)	Pt1-Ag1-Ag2	58.45(1)
Pt1-O27	2.137(3)	Ag1-O41	2.177(3)	Pt1-Ag2-Ag1	65.86(1)
Pt2--Ag1	3.973(4)	Ag2-O29	2.403(3)	Ag1-Ag2-Pt2	87.33(1)
Pt2-Ag2	2.9104(3)	Ag2-O43	2.308(3)	Ag1-Pt2-Ag2	45.63(1)
Pt2-O50	2.135(3)	Ag2-O48	2.416(3)	Ag2-Ag1-Pt2	47.04(1)
C28-O29	1.235(4)	C28-O27	1.252(4)	Pt1-Ag2-Pt2	149.94(1)
C35-O36	1.219(6)	C35-O34	1.245(4)	Ag1-Pt1-O27	83.16(1)
C42-O43	1.236(5)	C42-O43	1.245(3)	Ag2-Pt1-O27	86.72(1)
C49-O48	1.228(3)	C49-O50	1.260(4)	O27-Pt1-Pt2-O50	56.11

Figure 3.2.1.3 C–H…F bonds and C–F…π interactions of Pt_2Ag_2 cluster **5**. a, b, c and d) intra- and inter- molecular C–H…F bonds; e) C–F…π interactions.

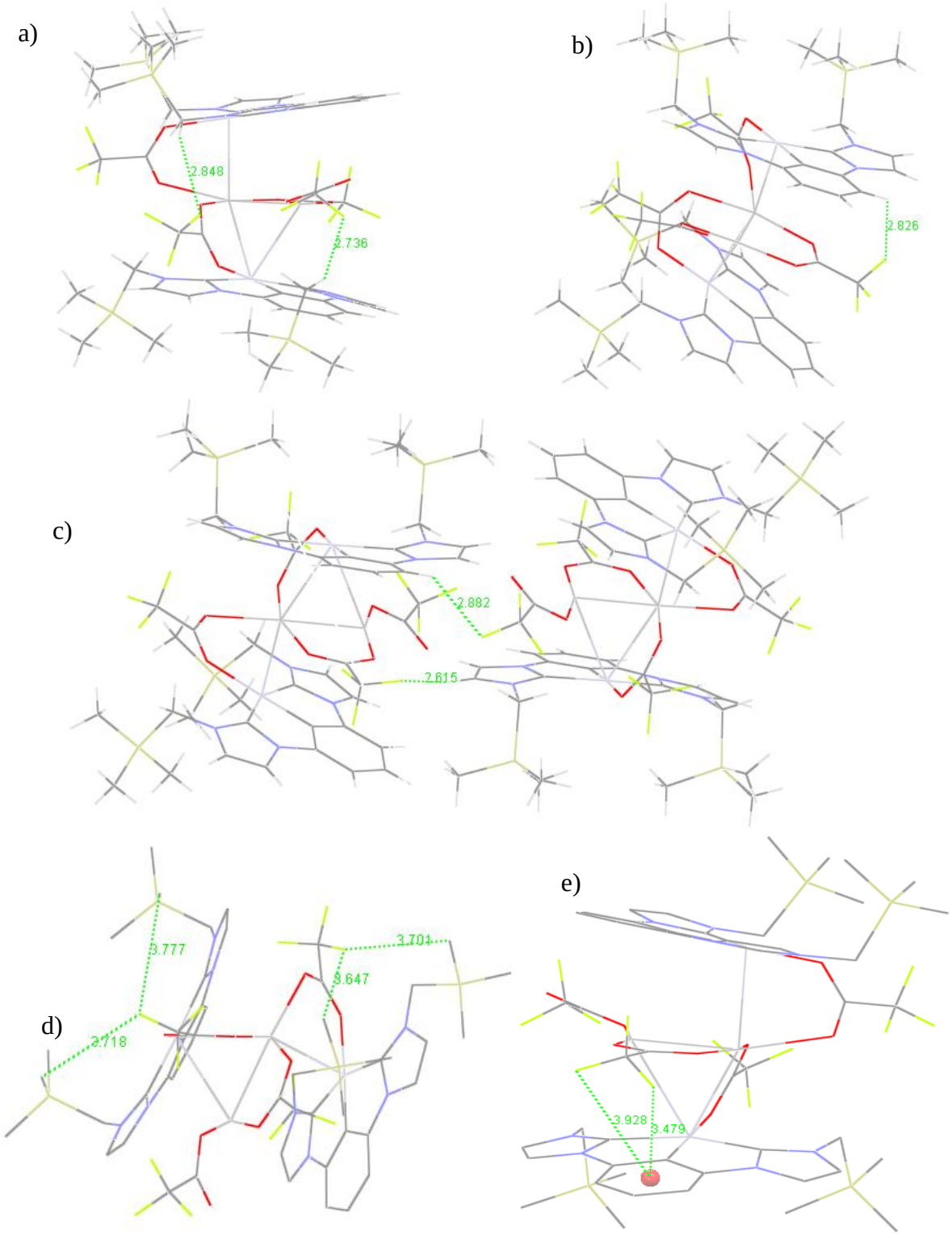

When 1.0 equivalent of silver(I) trifluoroacetate was used in the reaction with complex **4**, the simple metathesis product **6** was obtained (Scheme 3.2.1.2). This product had an upfield shift of the -NCH_2- signal in the ^{1}H NMR spectrum from δ 4.49 to δ 3.81 instead of δ 3.65 ppm as found in the spectrum of cluster **5**. The ^{13}C NMR spectrum of complex **6** revealed the -CF_3 group at δ = 117.8 with C-F coupling J^1 = 245 Hz and the carbonyl group at 161.6 ppm with C-F coupling J^2 = 35 Hz. The ^{19}F NMR spectrum of complex **6** indicated a sharp singlet peak at 74.32 ppm. The formation of complex **6** was further confirmed with an elemental analysis within the acceptable range (see 3.4 Experimental Section).

X-ray quality crystals of complex **6** were obtained by defusing hexanes vapor into a CH_2Cl_2 solution. An ORTEP presentation of complex **6** is depicted in Figure 4. Selected bond length and bond angle data are listed in Table 3.2.1.1 and are all within normal range. In close comparison of the Pt coordination spheres in cluster **5** and complex **6**, the bond lengths are almost identical except the Pt-O bond in complex **5** is slightly elongated (2.163(6) Å *vs* 2.137(3) and 2.135(3) Å, Table 3.2.1.1). The bond also bend a little out of the Pt coordination plane in complex **6** ($\angle$ C_{aryl}-Pt-O = 167.1(2)° *vs* 175.9(1) and 176.7(1)°, Table 3.2.1.1).

Figure 3.2.1.4 ORTEP diagram (50% thermal ellipsoids) of CCC-bis(NHC)-Pt^{II}-O_2CCF_3 complex **6**. Hydrogen atoms omitted for clarity. Selected metric data presented in Table 3.2.1.1.

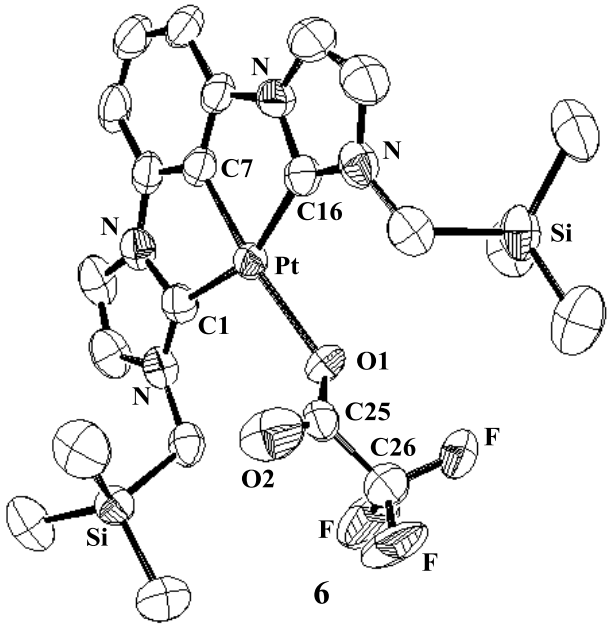

3.2.2 Computational Studies

To investigate the unusual 'twisted' configuration of cluster **5**, computational simulation was carried out. It is a challenge to simulate large organometallic systems which contain various metal-metal, and/or π-π stacking, and/or hydrogen bond, and/or other interactions. The structures of complex **6** and cluster **5** were optimized using several density functional theory (DFT)[112] functionals, including TPSSTPSS[113], PBEPBE[114], B3LYP[115] and M06[116]. The LANL2DZ[117] basis set was adopted for Pt, Ag, and Si atoms, and 6-31G(d')[118] basis set was used for other atoms. Table 3.2.2.1 shows that the selected bond length and

variance obtained by TPSSTPSS, PBEPBE, B3LYP and M06 compared to the X-ray crystal diffraction data. The results show that the TPSSTPSS functional is more suitable for the calculation of this Pt_2Ag_2 organometallic system. A hard fit of computational optimized geometry over the structure of cluster **5** is presented in Figure 3.2.2.1.

Table 3.2.2.1 Comparison of Computational Results and Experimental (X-ray) for Different Methods

Selected Bond Length (Å)/Variance[a] (%)

	Complex **6**			
	TPSSTPSS	PBEPBE	B3LYP	M06
Pt-C7	1.95/0.6	1.94/0.4	1.95/0.6	1.95/0.6
Pt-C1	2.04/0.1	2.03/0.2	2.05/0.6	2.05/0.5
Pt-C16	2.06/1.2	2.05/0.9	2.07/1.8	2.06/1.3
Pt-O	2.17/0.4	2.19/1.2	2.19/1.1	2.18/0.9
	Cluster **5**			
	TPSSTPSS	PBEPBE	B3LYP	M06
Pt1-C7	1.96/1.1	1.95/1.0	1.95/0.9	1.95/1.0
Pt1-C1	2.07/2.1	2.05/1.1	2.06/1.8	2.05/1.5
Pt1-C13	2.05/0.2	2.07/0.9	2.07/1.2	2.08/1.8
Pt1-O27	2.20/3.0	2.20/3.0	2.20/3.1	2.19/2.6
Pt2-C61	1.98/1.3	1.95/0.9	1.95/1.0	1.95/1.0
Pt2-C55	2.07/2.3	2.05/1.2	2.06/1.7	2.06/1.7
Pt2-C67	2.05/1.5	2.06/1.8	2.07/2.5	2.08/2.8

Pt2-O50	2.19/2.4	2.22/3.8	2.21/3.7	2.22/3.8
Pt1-Ag1	3.13/0.3	3.29/4.9	3.76/19.7	3.58/14.0
Pt1-Ag2	3.13/6.6	3.09/5.2	3.23/10.1	2.95/0.7
Ag1-Ag2	2.86/0.5	2.88/1.3	3.03/6.7	2.92/2.6
Pt2-Ag2	2.99/2.7	2.98/2.4	3.05/4.9	2.91/0.0

[a] Variance is calculated as $Var = \frac{|calc. - exp.|}{exp.} \times 100\%$

Figure 3.2.2.1 Hard-fit of computational (red) structure versus the experimental (black) structure of cluster **5**.

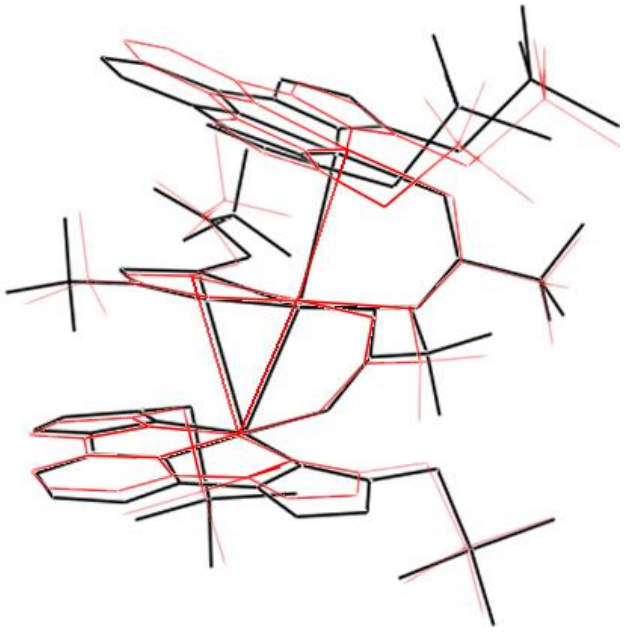

The hypothetical ‘head to head’ and ‘head to tail’ configurations of the cluster were also modeled using the parameters obtained from the simulated cluster **5** structure. Optimization of these configurations applying the same method (TPSSTPSS) and basis sets led to local energy mimima of them (Figure 3.2.2.2). In comparison with the ‘twisted’ configuration, the ‘head to head’ and ‘head to tail’ conformations are less stable.

Figure 3.2.2.2 a) Optimized geometry and relative stabilization energy of hypothetical 'head to head' and 'head to tail' configurations of Pt_2Ag_2 cluster **5**.

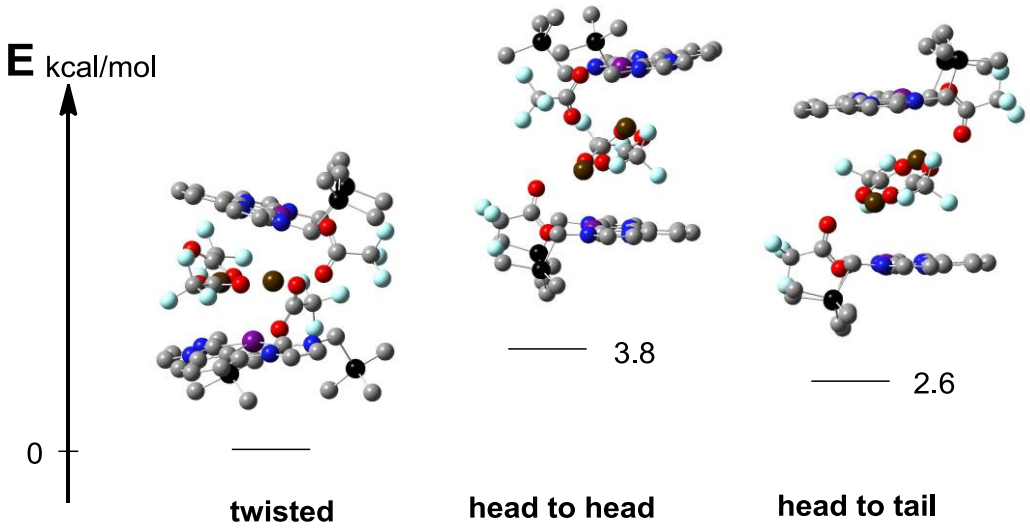

3.2.3 Photophysical Studies

The dilute solution (~10^{-4} M) absorption and emission spectra of complexes **4**, **5** and **6** are presented in Figure 3.2.3.1. The absorption spectra of complexes **4** and **6** both exhibited peaks at 230, 269, 323 and 355 nm (Figure 3.2.3.1a). Cluster **5** shared those absorptions and contained shoulders at 280, 307 and 385 nm as well (Figure 3.2.3.1a). Since the majority of the absorption spectra could be ascribed to metal-to-ligand charge-transfer alone (MLCT) or its admixture of ligand-centered (MLCT-LC) transitions, the change in the spectra implied there were weak Pt-Ag interactions even in the very dilute solution. This observation agreed with the results of ESI-TOF-MS measurements. Emission spectra indicated a similar trend as the absorptions; the solution of cluster **5** gave rise to a low-energy shoulder from 490 to 570 nm (Figure 3.2.3.1b).

Figure 3.2.3.1 Solution phase photophysical properties of complexes **4**, **5** and **6**. a) UV-Vis absorption; b) emission (excited with 350 nm radiation).

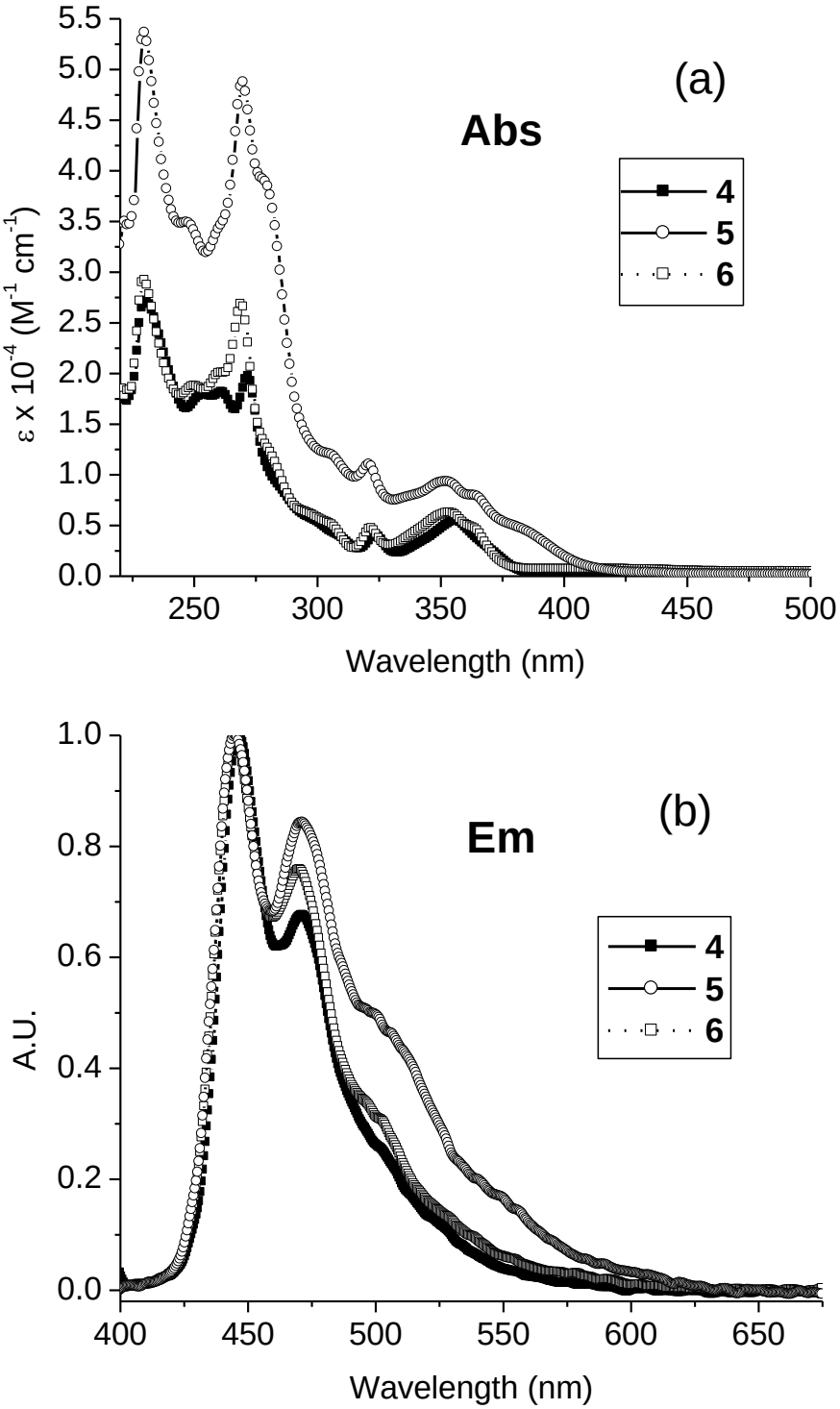

Excitation spectra of complex **4**, **5**, and **6** all indicated efficient stimulation around 350 nm (Figure 3.2.3.2). Solid state emission of complexes **4** and **6** fell in the same region (440—520 nm) as their solution phase, while a significant red-shift and broadening were observed in the solid state emission of cluster **5** compared to its solution phase emission (Figure 3.2.3.3). To investigate the source of these changes, a series of emission spectra were taken on the cluster **5** solutions at different concentrations. Solutions of high concentration gave emission spectra resembling the solid state emission, while the dilute solutions exhibited more complex emission spectra (Figure 3.2.3.4 vs. Figure 3.2.3.1b, **5**). A possible explanation of this phenomenon is that some cluster **5** molecules are dissociating their [CCC-Pt-(O_2CCF_3)] part in the solution phase. This dissociation is reversible, and the equilibrium between dissociating and non-dissociating molecules is depended on the concentration. As the concentration decreases, the equilibrium is shifted to favor dissociation and the solution exhibits photophysical properties more like the CCC-bis(NHC)-Pt^{II}-O_2CCF_3 complex **6**.

Figure 3.2.3.2 Excitation spectra of complexes **4**, **5**, and **6** (detected at 450 nm)

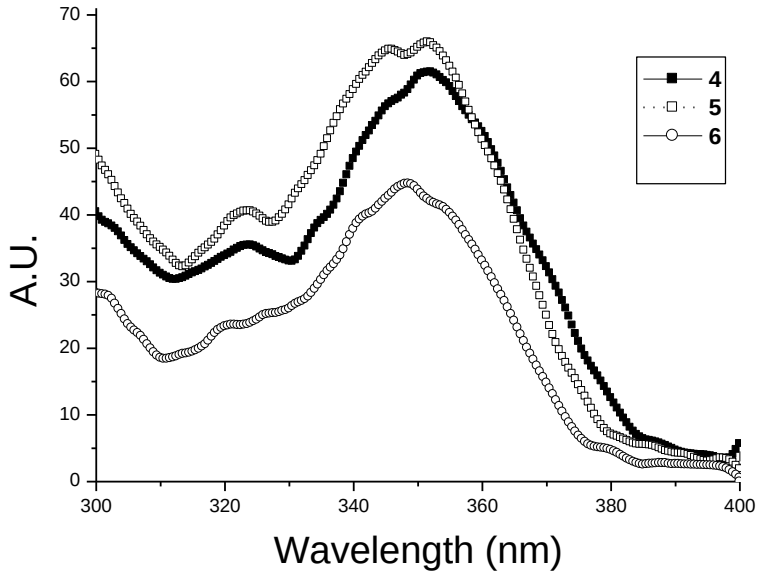

Figure 3.2.3.3 Solid state emission of complexes **4**, **5** and **6** (excited with 350 nm radiation).

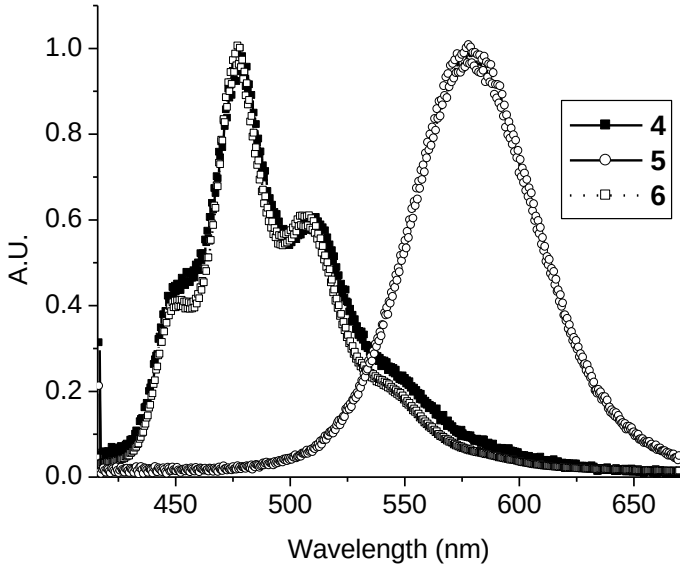

Figure 3.2.3.4 Normalized concentration dependent emission of cluster **5** solutions (excited with 350 nm radiation).

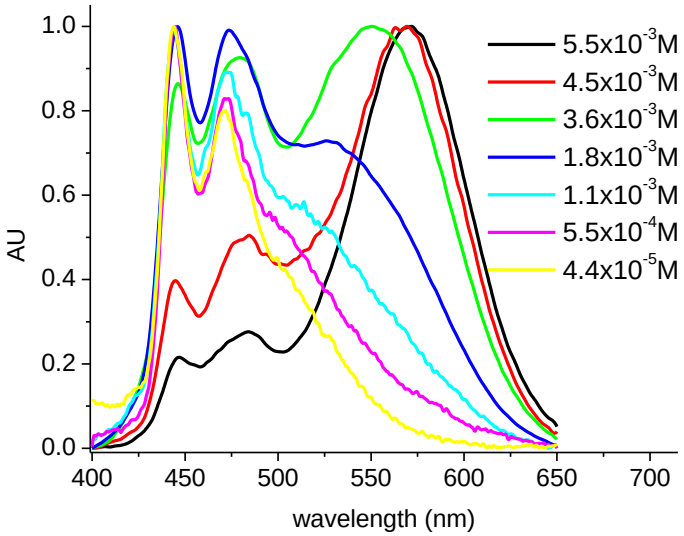

3.3 Conclusions

Pincer CCC-bis(NHC)-Pt^{II}-Cl complex **4**, multinuclear [Pt_2Ag_2] cluster **5**, and CCC-bis(NHC)-Pt^{II}-O_2CCF_3 **6** were synthesized and characterized. Cluster **5** was found to adopt an unprecedented 'twisted' (∠ L-Pt1-Pt2-L = 57 °) configuration consisting of an unsymmetrical multi-transition metal core in the solid state. Multiple weak interactions including inter- and intra-molecular C–H…O, C–H…F and C–F…π interactions were identified in the structure of cluster **5**. The unusual configuration of cluster **5** in the solid state was investigated with experimental and theoretical methods. Results of computational studies indicated that the previously reported 'head to head' and 'head to tail' configurations are less stable than the 'twisted' configuration in this system. Solution phase emission spectra of the complexes revealed an interesting concentration dependence of the photophysical properties of cluster **5**.

3.4 Experimental Section

General Procedures: All starting materials were purchased from Sigma-Aldrich, Fisher Scientific or Strem and were used as received unless otherwise noted. All solvents used in reactions were dried and degassed by passage through a basic alumina column under Ar.[80] All reactions involving organometallic reagents were carried out under N_2 or Ar atmosphere using standard glovebox or Schlenk line techniques. NMR spectra were collected using Bruker Avance 300 or 500 MHz spectrometers and referenced to the residual solvent peak. Electro-spray-ionization-mass spectra were collected using a Synapt HDMS (Waters UK Ltd., Manchester, UK). MALDI-TOF mass spectra were obtained using a Bruker Autoflex mass spectrometer equipped with a nitrogen laser at

near threshold laser intensity. Trans-2-[3-(4-tert-butylphenyl)-2-methyl-2-propenylidene]malononitrile (DCTB) was used as the matrix with a 1:1000 analyte/matrix ratio. A volume of 2 μL of the analyte-matrix mixture was applied to the target and air-dried. Elemental analysis was carried out on a PerkinElmer 2400 Series II CHNS/O Analyzer. UV-visible absorption spectra were collected using an HP 8453 UV-Visible system. Emission spectra were collected using a PerkinElmer LS 55 fluorescence spectrometer.

2-(1,3-Bis(N-trimethylsilylmethylimidazol-2-ylidene)phenylene)(chloro) platinum (II), (4). 1,3-Bis (1-trimethylsilylmethylimidazolium-3-yl)benzene dichloride was obtained using a modified literature procedure[60] (0.67 g, 1.5 mmol) freshly sublimed $Zr(NMe_2)_4$ (0.42 g, 1.6 mmol) and CH_2Cl_2 (~8 mL) were combined in an air tight vial. The mixture was stirred for 1 hr at room temperature to afford a dark red homogenous solution. 2-(1,3-Bis(N-trimethylsilylmethylimidazol-2-ylidene)phenylene)bis(chloro)(dimethylamido) zirconium (IV). ^{1}H NMR (CD_2Cl_2; 300 MHz): δ 7.45 (d, 2H, J = 1.8 Hz), 7.27 (t, 1H, J = 7.8 Hz), 7.07 (s, 1H), 7.04 (t, 1H, J = 7.8 Hz), 6.98 (d, 2H, J = 1.8 Hz), 4.08 (br, 4H), 2.88 (s, 6H), 0.15 (s, 18H). $[Pt(COD)Cl_2]$ (0.55 g, 1.5 mmol) was added and stirring continued vigorously at room temperature for another 6 hrs. The reaction mixture was transferred to a round bottom flask that contained 0.5 mL of distilled water. The precipitate was removed by filtration. The filtrate was concentrated under vacuum to afford a yellow solid. The solid was washed with water (2 × 1 mL), cold CH_2Cl_2 (2 × 1 mL), Et_2O (2 × 2 mL), and was dried under vacuum yielding a yellow crystalline solid (0.77 g, 85 %). X-ray quality crystals were grown by slow diffusion of hexanes vapor into a concentrated CH_2Cl_2 solution of **4**.

^{1}H NMR (CD_2Cl_2; 300 MHz): δ 7.39 (d, 2H, J = 2.0 Hz), 7.15 (t, 1H, J = 8.0 Hz), 6.93-6.86 (m, 4H), 4.49 (s, 4H), 0.15 (s, 18H); ^{13}C NMR (CD_2Cl_2; 75 MHz): δ 172.8 (J^1 Pt-C = 1174 Hz), 145.5 (J = 24 Hz), 135.1 (J^1 Pt-C = 944 Hz), 123.6, 121.8 (J = 27 Hz), 115.4 (J = 42 Hz), 107.6 (J = 32 Hz), 41.5, -2.3; MALDI-TOF (m/z): 576.190 $[M\text{-}Cl]^+$ ($C_{20}H_{28}N_4PtSi_2$); Elemental Analysis: Calcd for $C_{20}H_{28}N_4PtSi_2Cl$: C, 39.24; H, 4.77; N, 9.15; Found: C, 39.36; H, 4.71; N, 9.04.

Trifluoroacetato-1κO-tris-μ-trifluoroacetato-1κO:2κO';2κO:3κO';3κO:4κO'-bis[2-(1,3-bis(N-trimethylsilylmethyl-imidazol-2-ylidene)phenylene)]-3κ^{3}C;4κ^{3}C-disilverdiplatinum(Ag—Ag)(2Ag—Pt)(Ag—Pt), (5). 2-(1,3-Bis(N-trimethylsilylmethyl-imidazol-2-ylidene)phenylene)(chloro) platinum (II), (**4**) (20 mg, 0.033 mmol), silver trifluoroacetate (15 mg, 0.066 mmol), and CH_2Cl_2 (~3 mL) were combined and stirred for 1 hr at room temperature yielding a red supernatant and a white precipitate. The crude mixture was filtered through Celite, concentrated, redissolved in CH_2Cl_2 (~3 mL), and filtered through Celite. The solvent was removed under reduced pressure yielding an orange solid (27 mg, 94%). X-ray quality crystals were grown by slow diffusion of hexanes into a saturated CH_2Cl_2 solution of **5**. ^{1}H NMR (CD_2Cl_2; 300 MHz): δ 7.42 (d, 2H, J = 2.0 Hz), 7.12 (t, 2H, J = 7.8 Hz), 6.92-6.83 (m, 4H), 3.65 (s, 4H), 0.10 (s, 18H); ^{13}C NMR (CD_2Cl_2; 75 MHz, 350K): δ 172.2 (J^1 Pt-C = 1156 Hz), 162.4-161.0 (m), 145.7 (J = 25 Hz), 125.9, 125.6 (J = 944 Hz), 122.2 (J = 27 Hz), 116.8 (J = 42 Hz), 108.4 (J = 32 Hz), 41.4, -2.7; ^{19}F NMR (CD_2Cl_2; 470 MHz): δ 72.98 (br), 73.81 (br); ESI-MS Exact Mass (m/z): calculated for $[M\text{-}(O_2CCF_3^-)]^+$ ($C_{46}H_{58}Ag_2F_9N_8O_6Pt_2Si_4$): 1708.0871 , found: 1708.0896; Elemental Analysis: Calcd for

5 $\cdot$½(C_6H_{14}), $C_{51}H_{65}Ag_2F_{12}N_8O_8Pt_2Si_4$: C, 32.86; H, 3.51; N, 6.01; Found: C, 32.78; H, 3.20; N, 6.32.

2-(1,3-Bis(N-trimethylsilylmethylimidazol-2-ylidene)phenylene)(trifluoroacetato) platinum (II), (6). 2-(1,3-Bis(N-trimethylsilylmethylimidazol-2-ylidene)phenylene)(chloro) platinum (II), (**4**) (20 mg, 0.033 mmol), silver trifluoroacetate (7.2 mg, 0.033 mmol) and CH_2Cl_2 (~3 mL) were combined in a reaction vial. The mixture was stirred for 1 hr at room temperature yielding a yellow supernatant and a white precipitate. The crude mixture was filtered through Celite, concentrated, redissolved in CH_2Cl_2 (~3 mL), and filtered through Celite. The solvent was removed under reduced pressure yielding a yellow solid (20 mg, 91%). X-ray quality crystals were grown by slow diffusion of hexanes into a saturated CH_2Cl_2 solution of **6**. ^{1}H NMR (CD_2Cl_2; 300 MHz): δ 7.40 (d, 2H, J = 2.0 Hz), 7.12 (t, 1H, J = 7.5 Hz), 6.92-6.82 (m, 4H), 3.81 (s, 4H), 0.12 (s, 18H); ^{13}C NMR (CD_2Cl_2; 75.476 MHz, 350K): δ 173.9 (J^1 Pt-C = 1205 Hz), 162.4-161.0 (m), 145.7 (J = 25 Hz), 129.1 (J = 972 Hz), 124.2, 121.6 (J = 28 Hz), 115.9 (J = 44 Hz), 107.8 (J = 33 Hz), 41.4, -2.7; ^{19}F NMR δ (CD_2Cl_2; 470 MHz): 74.32; Elemental Analysis: Calcd for $C_{20}H_{29}ClN_4PtSi_2$: C, 38.31; H, 4.24; N, 8.12; Found: C, 37.92; H, 4.09; N, 8.04.

X-Ray Crystallography. X-ray quality crystals of **4** and **5** were mounted atop fine glass fibers. Diffraction experiments were performed on an Oxford Diffraction Systems Gemini S diffractometer with MoK radiation (λ = 0.71073 Å) at 298K. The structures were solved and refined using the SHELX suite. The structure of complex **6** was resolved on a recently commercialized Rigaku *XtaLAB mini* small molecule diffraction system.

Computational Details. Theoretical calculations were carried out using the Gaussian09[119] implementation of TPSSTPSS[113] (the Tao, Perdew, Staroverov, and Scuseri exchange functional and the τ-dependent gradient-corrected functional of Tao, Perdew, Staroverov, and Scuseria), PBEPBE[114] (the 1996 functional of Perdew, Burke and Ernzerhof exchange functional and the 1996 gradient-corrected Perdew, Burke and Ernzerhof correlation functional), B3LYP[115] (Becke's three-parameter functional and the Lee-Yang-Parr functional) and M06[116] (the hybrid functional of Truhlar and Zhao) density functional theory (DFT)[112]. All calculations were conducted with the same basis set combination. The basis set for platinum was the Hay and Wadt basis set and effective core potential (ECP) combination (LanL2DZ)[117] as modified by Couty and Hall, where the two outermost p functions have been replaced by a (41) split of the optimized platinum 6p functions and silver 5p functions.[120] The 6-31G(d') basis set[118] was used for all other atoms. Spherical harmonic d functions were used throughout, i.e. there were five angular basis functions per d function. All structures were fully optimized and frequency calculations (analytical for DFT) were performed on all ground-state structures to ensure a zeroth-order saddle point (a local minimum) was achieved.

CHAPTER 4

INVESTIGATION OF ELECTRONIC PROPERTIES OF A CCC-NHC PINCER Pt-CO COMPLEX

4.1 Research Background

Although often called "phosphine mimics",[17c,121] N-heterocyclic carbenes (NHCs) are perhaps better described as phosphine complements. They commonly make more robust metal complexes, which was ascribed to the relatively high activation energy of cleavage of a metal-carbene bond to form a free carbene species.[95,122] Moreover, there is increasing experimental evidence that NHCs provide catalytic activity and scope that surpasses phosphine ligands.[123] A number of experimental and theoretical efforts investigating the electronic properties of NHCs have been reported.[3,124] Overwhelmingly, the NHC is generally recognized as a strong σ donating ligand (carbene lone pair) and weak π donating ligand (nitrogen lone pairs).[125] However, the true nature of NHCs remains largely veiled.

Pincer (tridentate-*mer*) bisNHC ligands have drawn much interest in recent years, due to their entropically enhanced stability and versatility which allows fine tuning of ligand steric hinderance, electron donating strength, bite angles, and chirality.[95] Among reported pincer bis-NHC architectures, phenyl bridged bis-N-heterocyclic carbene (CCC-NHC)[38,51,67] ligands have demonstrated several unique properties in comparison with their xylylene bridged C^C^C-

NHC,[50,126] pyridylene bridged CNC-NHC,[36c,36e,53-54,58a,59,127] and 2,6-lutidinyl bridged C^N^C-NHC[36e,52,126a,128] pinceranalogues. For instance, only the CCC-NHC ligands have been reported to form mixed normal-abnormal carbene complexes.[129] Moreover, regardless their synthetic pathways, ligands with CH_2 spacers (C^C^C-NHC and C^N^C-NHC) were "tilted", and the N-pyridinyl fragment was found dissociable under certain circumstances.[101c,130]

In this chapter, the synthesis of a pincer CCC-NHC platinum(II) carbonyl complex **7** was prepared and characterized with various spectroscopic techniques. Its photophysical behavior is reported. Its CO stretching frequency was compared to published analogues.

4.2 Result and Discussion

4.2.1 Synthesis and Characterization

Synthesis and Characterization of CCC-NHC-Pt^{II}-CO complex (7). CCC-NHC-Pt^{II}-Cl complex **1** was synthesized using the previously reported procedure.[60] A cationic intermediate was obtained from **1** by abstraction of the chloride with stoichiometric silver triflate in CH_2Cl_2 at room temperature under an inert atmosphere. This reaction mixture was treated with carbon monoxide to yield the carbonyl complex **7** (Scheme 4.2.1.1). The one-pot, two-step reaction led to a shift of the N-CH_2- signal from δ 4.69 to 4.16, indicating a quantitative conversion. The large shift (0.53 ppm) indicated a significant increase of electron density on the Pt center when switching chloride to carbonyl ligand. Moreover, sterically direct shielding of those protons by the CO electron cloud could also contribute. The ^{13}C NMR spectrum of complex **7** contained the CO carbon at δ 184.8

and the Pt-C_{NHC} carbon at δ 166.5, which were very close to the data previously reported for other pincer Pt-CO complexes (δ Pt-CO = 183.87[131]; δ Pt-C_{NHC} =167.3[132]).Trace CH_2Cl_2 composition was identified in the NMR spectroscopic data, which was also reflected in the elemental analysis result. Complex **7** exhibited a characteristic CO stretching at 2079 cm^{-1} in the IR spectrum.

Scheme 4.2.1.1 Synthesis of CCC-NHC-Pt^{II}-Cl Complexes **7**

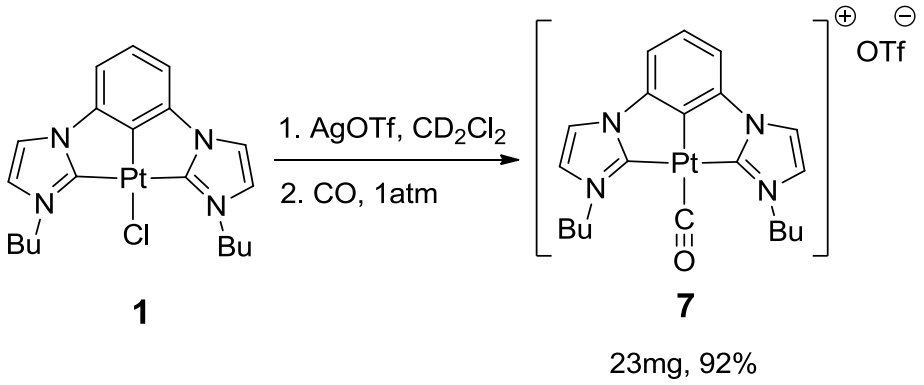

The structure of complex **7** was confirmed by X-ray crystallography (Figure 4.2.1.1). The imidazole and phenyl rings of complex **7** were almost coplanar, along with which the carbonyl group formed a distorted square-planar geometry around the platinum metal center. Ligand constrains were observed due to the shortened Pt-C_{phenyl} bond (~0.15 Å shorter than the Pt-C_{aryl} bond lengths in mono-dentate complexes)[104] and bent C_{NHC}-Pt-C_{NHC} angle (155.4). All the metric data fell in the range observed for neutral and cationic Pt(II) NHC complexes.[66,69a,71b,103] The structure of complex **7** was very similar to the previously reported pyridinyl bridging analogue.[132]

Figure 4.2.1.1 ORTEP diagram (30% thermal ellipsoids) of CCC-NHC-Pt^{II}-CO complex **7**. Hydrogen atoms omitted for clarity. Selected bond lengths (Å) and angles (deg): Pt—C1 = 2.048(10), Pt—C5 = 1.963(10), Pt—C10 = 2.038(10), Pt—C21 = 1.902(16), C21-O1 = 1.130(14); C1-Pt-C5 = 78.2(4), C1-Pt-C10 = 155.4(4), C5-Pt-C21 = 174.9(5), Pt-C21-O1 = 175.7(13).

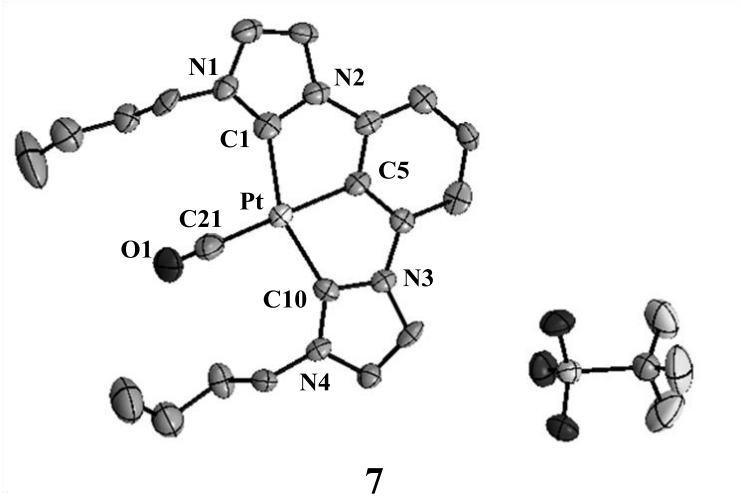

7

Photophysical studies of CCC-NHC-Pt^{II}-CO complex (7). Complex **7** was found to emit yellow light with UV stimulation. Its absorption and emission data in MeOH solution is demonstrated in Figure 4.2.1.2. In MeOH solution, the UV absorption spectra of complex **7** exhibited a major absorption peak around 265 nm and minor peaks near 290, 323 and 355 nm which were ascribed as mixed metal to ligand charge transfer and ligand centered (MLCT-LC) transitions.[72] The emission of complex **7** fell between 530 to 600 nm, which agrees with the observed green-yellow emitting color.

Figure 4.2.1.2. Emission and absorption data of CCC^{Bu}-NHC-Pt(II)-CO/OTf complex **7** in MeOH solution at 298K (irradiated at 355 nm).

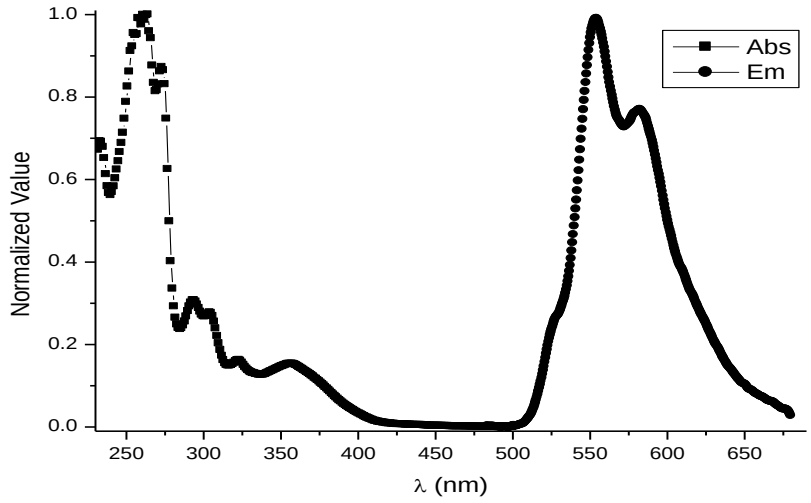

The lifetime of the excited state was measured with a pulsed laser simulation and a bi-exponential pattern was observed (Figure 4.2.1.3). The scale of lifetime suggests a mix of triplet and singlet emission.

Figure 4.2.1.3. Emission decay data of CCC^{Bu}-NHC-Pt(II)-CO/OTf complex **7** in MeOH solution at 298K (irradiated at 355 nm).

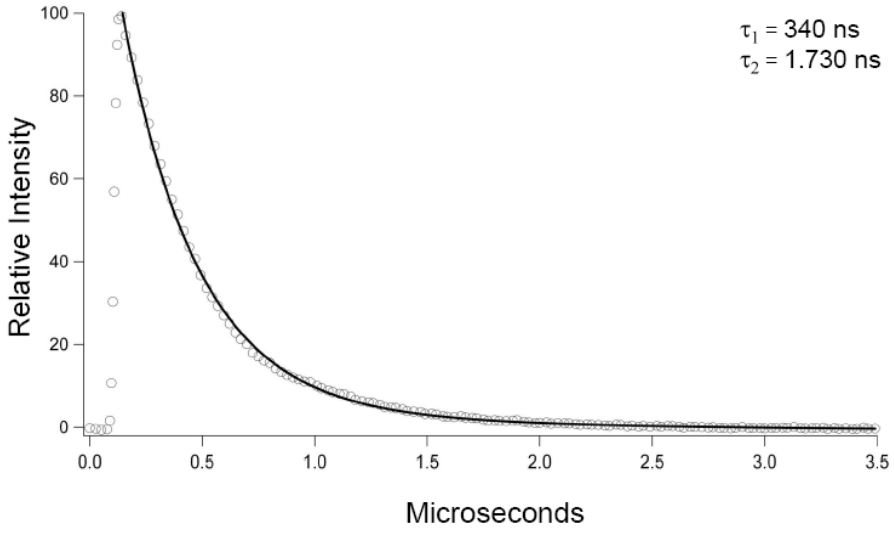

Photostability of complex **7** was also investigated. Complex **7** was photobleached 17% over 6h (Figure 4.2.1.4).

Figure 4.2.1.4. Photostability data of CCC^{Bu}-NHC-Pt(II)-CO/OTf complex **7** at 298K (irradiated at 355 nm).

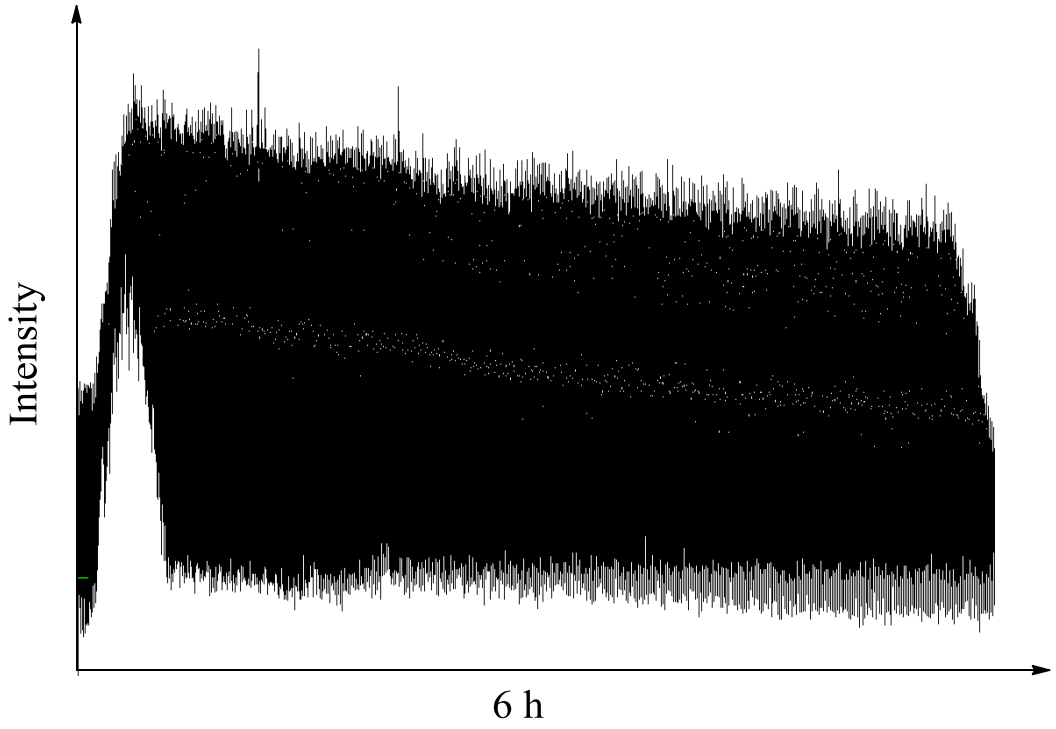

Tolman model and its variations have been one of the most well established standards of measuring the electron donicity of metal complexes. The CO stretching frequency value of CCC-NHC-Pt-CO/OTf complex **7** was compared to other known monometallic pincer Pt-CO complexes (Scheme 4.2.1.2).[131-133] Notably the CO stretching frequencies are largely dependent on the *trans* fragments of the complexes and are quite insensitive to the *cis* fragments. Therefore, it is not a very good indicator of the electron donicity of the tridentate ligand architecture systems.

Scheme 4.2.1.2 Monometallic Pincer Pt-CO Complexes and Their CO Stretching Frequency.

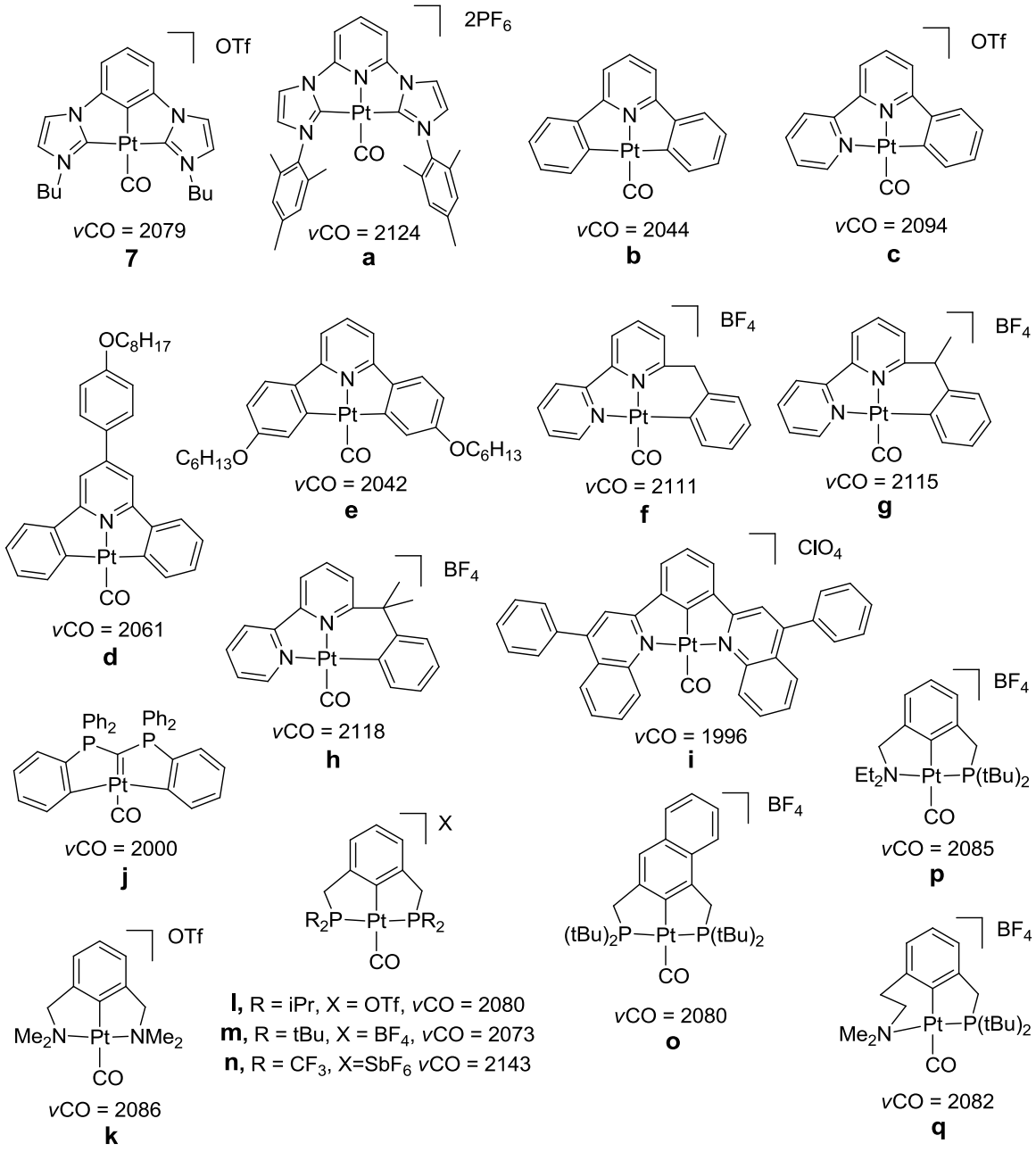

The only case when a carbene is trans to the carbonyl group was reported by Petz and Neumuller in 2011 (**j**, Scheme 4.2.1.2),[133f] where a non-cyclic PCP carbene was used to

bridge two phenyl groups in the ligand backbone. Comparing structure **j** with **b**, the PCP carbene has very similar electron donating abilities to phenyl fragment on the trans position.

4.3 Conclusions

In summary, a pincer CCC-NHC-Pt^{II}-CO/OTf complex **7** was prepared and characterized. The complex adopted distorted square planar geometry with the CO trans to the bridging phenyl group. The IR CO stretching frequency was found to be an insensitive indicator for the tridentate ligand architechtures.

4.4 Experimental Section

General Procedures: All starting materials were purchased from Sigma-Aldrich, Fisher Scientific or Strem and were used as received unless otherwise noted. All solvents used in reactions were dried and degassed by passage through a basic alumina column under Ar.[80] All reactions involving organometallic reagents were carried out under N_2 or Ar atmosphere using standard glovebox or Schlenk line techniques. NMR spectra were collected using Bruker Avance 300 or 500 MHz spectrometers and referenced to the residual solvent peak. Electro-spray-ionization-mass spectra were collected using a Synapt HDMS (Waters UK Ltd., Manchester, UK). MALDI-TOF mass spectra were obtained using a Bruker Autoflex mass spectrometer equipped with a nitrogen laser at near threshold laser intensity. Trans-2-[3-(4-tert-butylphenyl)-2-methyl-2-propenylidene]malononitrile (DCTB) was used as the matrix with a 1:1000 analyte/matrix ratio. A volume of 2 μL of the analyte-matrix mixture was applied to the

target and air-dried. Elemental analysis was carried out on a PerkinElmer 2400 Series II CHNS/O Analyzer. UV-visible absorption spectra were collected using an HP 8453 UV-Visible system. Emission spectra were collected using a PerkinElmer LS 55 fluorescence spectrometer.

2-(1,3-Bis(N-butylimidazol-2-ylidene)phenylene)(carbonyl) platinum (II), (7). 2-(1,3-Bis(N-butylimidazol-2-ylidene)phenylene)(carbonyl) platinum (II), (**1**), which was obtained using a literature procedure[60] (20 mg, 0.036 mmol), was combined with AgOTf (9.3 mg, 0.036 mmol) in an air-tight screw-capped NMR tube. Pre-dried CD_2Cl_2 (ca. 0.6 mL) was added to the NMR tube, which was then sealed and ultra-sounded for 15 min. A steady flow of CO gas was directed into the reaction solution for 5 min. The NMR tube was re-sealed and ultra-sounded for another 15 min, yielding quantitative conversion according to NMR spectroscopic data. The reaction mixture was filtered through Celite, concentrated, redissolved in CH_2Cl_2 (~1 mL), and filtered through Celite again. The solvent was removed under reduced pressure, the remaining solid was washed with cold CH_2Cl_2 (2 × 0.5 mL) and Et_2O (2 × 0.5 mL), and was dried under vacuum yielding a yellow solid (23 mg, 92%). X-ray quality crystals were grown by slow evaporation of solvent from a CH_2Cl_2 solution of **7**. ^{1}H NMR (CD_2Cl_2; 300 MHz): δ 7.60 (d, 2H, J = 2.0 Hz), 7.34 (t, 1H, J = 8.0 Hz), 7.26 (d, 2H, J = 2.0 Hz), 7.15 (dd, 2H, J_{H-H} = 8.0 Hz, J_{Pt-H} = 12.0 Hz), 4.16 (t, 4H, J = 7.5 Hz), 1.91 (pentet, 4H, J = 7.5 Hz), 1.46 (sextet, 4H, J = 7.5 Hz), 1.00 (t, 6H, J = 7.5 Hz); ^{13}C NMR (CD_2Cl_2; 125 MHz): δ 184.8 (Pt-CO), 166.5 (Pt-C_{NHC}), 147.5, 142.1, 131.2, 122.8, 118.0, 110.4, 52.8, 34.3, 20.3, 13.9; IR (KBr pellet): (Pt-*CO*) 2079; ESI-MS (m/z): 516 $[M-CO]^+$ ($C_{20}H_{25}N_4Pt$); Elemental Analysis: Calcd for

$C_{22}H_{25}F_3N_4O_4PtS \cdot 1/6(CH_2Cl_2)$: C, 37.62; H, 3.61; N, 7.92; Found: C, 37.44; H, 3.32; N, 7.90.

X-Ray Crystallography. X-ray quality crystal of **7** was mounted atop fine glass fibers. Diffraction experiments were performed on an Oxford Diffraction Systems Gemini S diffractometer with MoK radiation (λ = 0.71073 Å) at 298K. The structures were solved and refined using the SHELX suite.

BIBLIOGRAAPHY

(1) (a) Buchner, E.; Curtius, T. *Berichte der deutschen chemischen Gesellschaft* **1885**, *18*, 2377-2379; (b) Buchner, E.; Feldmann, L. *Berichte der deutschen chemischen Gesellschaft* **1903**, *36*, 3509-3517.
(2) McNaught, A. D.; Wilkinson, A.; Blackwell Scientific Publications: Oxford, 1997.
(3) Bourissou, D.; Guerret, O.; Gabbai, F. P.; Bertrand, G. *Chem. Rev.* **2000**, *100*, 39-91.
(4) (a) Skell, P. S.; Woodworth, R. C. *J. Am. Chem. Soc.* **1956**, *78*, 4496-4497; (b) Beckwith, A. L. J.; Redmond, J. W. *J. Am. Chem. Soc.* **1968**, *90*, 1351-1353; (c) Strausz, O. P.; Thap, D. M.; Font, J. *J. Am. Chem. Soc.* **1968**, *90*, 1930-1931; (d) Creary, X. *J. Am. Chem. Soc.* **1980**, *102*, 1611-1618.
(5) (a) Skell, P. S.; Woodworth, R. C. *J. Am. Chem. Soc.* **1959**, *81*, 3383; (b) Wiberg, K. B.; Ciula, R. P. *J. Am. Chem. Soc.* **1959**, *81*, 5261; (c) Mahler, W. *J. Am. Chem. Soc.* **1962**, *84*, 4600; (d) Moore, W. R.; Moser, W. R.; LaPrade, J. E. *J. Org. Chem.* **1963**, *28*, 2200.
(6) Öfele, K. *J. Organomet. Chem.* **1968**, *12*, P42-P43.
(7) Wanzlick, H. W.; Schönherr, H. J. *Angew. Chem.* **1968**, *80*, 154-154.
(8) Igau, A.; Grutzmacher, H.; Baceiredo, A.; Bertrand, G. *J. Am. Chem. Soc.* **1988**, *110*, 6463-6466.
(9) Arduengo, A. J., III; Harlow, R. L.; Kline, M. *J. Am. Chem. Soc.* **1991**, *113*, 361-363.
(10) Arduengo, A. J.; Dias, H. V. R.; Harlow, R. L.; Kline, M. *J. Am. Chem. Soc.* **1992**, *114*, 5530-5534.
(11) Arduengo, A. J.; Goerlich, J. R.; Marshall, W. J. *J. Am. Chem. Soc.* **1995**, *117*, 11027-11028.
(12) Alder, R. W.; Allen, P. R.; Murray, M.; Orpen, A. G. *Angew. Chem. Int. Ed. Engl.* **1996**, *35*, 1121-1123.
(13) Grundemann, S.; Kovacevic, A.; Albrecht, M.; Faller Robert, J. W.; Crabtree, H. *Chem. Commun.* **2001**, *0*, 2274-2275.
(14) Mathew, P.; Neels, A.; Albrecht, M. *J. Am. Chem. Soc.* **2008**, *130*, 13534-13535.
(15) Han, Y.; Huynh, H. V.; Tan, G. K. *Organometallics* **2007**, *26*, 6581-6585.
(16) Guisado-Barrios, G.; Bouffard, J.; Donnadieu, B.; Bertrand, G. *Angew. Chem. Int. Ed.* **2010**, *49*, 4759-4762.
(17) (a) Enders, D.; Gielen, H.; Raabe, G.; Runsink, J.; Teles, J. H. *Chem. Ber.* **1996**, *129*, 1483-1488; (b) Herrmann, W. A.; Elison, M.; Fischer, J.; Kocher, C.; Artus, G. R. J. *Angew. Chem. Int. Ed. Engl.* **1995**, *34*, 2371-2374; (c) Herrmann, W. A.; Köcher, C. *Angew. Chem. Int. Ed. Engl.* **1997**, *36*, 2162-2187.
(18) (a) McGuinness, D. S.; Cavell, K. J.; Skelton, B. W.; White, A. H. *Organometallics* **1999**, *18*, 1596-1605; (b) McGuinness, D. S.; Cavell, K. J. *Organometallics* **2000**, *19*, 741-748.
(19) (a) Crudden, C. M.; Allen, D. P. *Coord. Chem. Rev.* **2004**, *248*, 2247-2273; (b) Cavallo, L.; Correa, A.; Costabile, C.; Jacobsen, H. *J. Organomet. Chem.* **2005**, *690*, 5407-5413; (c) Scott, N. M.; Nolan, S. P. *Eur. J. Inorg. Chem.* **2005**, 1815-1828; (d) Lee, H. M.; Lee, C. C.; Cheng, P. Y. *Curr. Org. Chem.* **2007**, *11*, 1491-1524; (e) Schuster, O.; Yang, L.; Raubenheimer, H. G.; Albrecht, M. *Chem. Rev.* **2009**, *109*, 3445-3478; (f) Hahn, F. E.; Jahnke, M. C. *Angew. Chem. Int. Ed.* **2008**, *47*, 3122-3172; (g) Gil, W.; Trzeciak, A. M.

Coord. Chem. Rev. **2011**, *255*, 473-483; (h) Jacobsen, H.; Correa, A.; Poater, A.; Costabile, C.; Cavallo, L. *Coord. Chem. Rev.* **2009**, *253*, 687-703.
(20) (a) McReynolds, M. D.; Dougherty, J. M.; Hanson, P. R. *Chem. Rev.* **2004**, *104*, 2239-2258; (b) Grubbs, R. H.; Miller, S. J.; Fu, G. C. *Acc. Chem. Res.* **1995**, *28*, 446-452; (c) Monfette, S.; Fogg, D. E. *Chem. Rev.* **2009**, *109*, 3783-3816; (d) Tallarico, J. A.; Randall, M. L.; Snapper, M. L. *Tetrahedron* **1997**, *53*, 16511-16520; (e) Buchmeiser, M. R. *Chem. Rev.* **2000**, *100*, 1565-1604; (f) Chatterjee, A. K.; Choi, T.-L.; Sanders, D. P.; Grubbs, R. H. *J. Am. Chem. Soc.* **2003**, *125*, 11360-11370; (g) Connon, S. J.; Blechert, S. *Angew. Chem. Int. Ed.* **2003**, *42*, 1900-1923; (h) Lozano-Vila, A. M.; Monsaert, S.; Bajek, A.; Verpoort, F. *Chem. Rev.* **2010**, *110*, 4865-4909.
(21) (a) Altenhoff, G.; Goddard, R.; Lehmann, C. W.; Glorius, F. *J. Am. Chem. Soc.* **2004**, *126*, 15195-15201; (b) Huynh, H. V.; Han, Y.; Ho, J. H. H.; Tan, G. K. *Organometallics* **2006**, *25*, 3267-3274; (c) Marion, N.; Navarro, O.; Mei, J.; Stevens, E. D.; Scott, N. M.; Nolan, S. P. *J. Am. Chem. Soc.* **2006**, *128*, 4101-4111.
(22) (a) Hillier, A. C.; Grasa, G. A.; Viciu, M. S.; Lee, H. M.; Yang, C. L.; Nolan, S. P. *J. Organomet. Chem.* **2002**, *653*, 69-82; (b) Samojłowicz, C.; Bieniek, M.; Grela, K. *Chem. Rev.* **2009**, *109*, 3708-3742; (c) Díez-González, S.; Marion, N.; Nolan, S. P. *Chem. Rev.* **2009**, *109*, 3612-3676; (d) Nair, V.; Vellalath, S.; Babu, B. P. *Chem. Soc. Rev.* **2008**, *37*, 2691-2698.
(23) Moulton, C. J.; Shaw, B. L. *J. Chem. Soc., Dalton Trans.* **1976**, 1020-1024.
(24) van Koten, G. *Pure Appl. Chem.* **1989**, *61*, 1681-1694.
(25) (a) Gupta, M.; Hagen, C.; Kaska, W. C.; Cramer, R. E.; Jensen, C. M. *J. Am. Chem. Soc.* **1997**, *119*, 840-841; (b) Xu, W.-w.; P. Rosini, G.; Krogh-Jespersen, K.; S. Goldman, A.; Gupta, M.; M. Jensen, C.; C. Kaska, W. *Chem. Commun.* **1997**, 2273-2274; (c) Wang, Z.; Sugiarti, S.; Morales, C. M.; Jensen, C. M.; Morales-Morales, D. *Inorg. Chim. Acta* **2006**, *359*, 1923-1928.
(26) Vuzman, D.; Poverenov, E.; Shimon, L. J. W.; Diskin-Posner, Y.; Milstein, D. *Organometallics* **2008**, *27*, 2627-2634.
(27) Fan, L.; Foxman, B. M.; Ozerov, O. V. *Organometallics* **2004**, *23*, 326-328.
(28) (a) Gossage, R. A.; van de Kuil, L. A.; van Koten, G. *Acc. Chem. Res.* **1998**, *31*, 423-431; (b) Albrecht, M.; van Koten, G. *Angew. Chem. Int. Ed.* **2001**, *40*, 3750-3781.
(29) (a) Singleton, J. T. *Tetrahedron* **2003**, *59*, 1837-1857; (b) van der Boom, M. E.; Milstein, D. *Chem. Rev.* **2003**, *103*, 1759-1792.
(30) (a) Kisała, J.; Ruman, T. *Curr. Org. Chem.* **2011**, *15*, 3486-3502; (b) Albrecht, M.; Lindner, M. M. *Dalton Trans.* **2011**, *40*, 8733-8744.
(31) (a) Cheng, G.; Chen, Y.; Yang, C.; Lu, W.; Che, C.-M. *Chemistry – An Asian Journal* **2013**, *8*, 1754-1759; (b) Batema, G. D.; Lutz, M.; Spek, A. L.; van Walree, C. A.; Donegá, C. d. M.; Meijerink, A.; Havenith, R. W. A.; Pérez-Moreno, J.; Clays, K.; Büchel, M.; Dijken, A. v.; Bryce, D. L.; van Klink, G. P. M.; Koten, G. v. *Organometallics* **2008**, *27*, 1690-1701.
(32) (a) Albrecht, M.; Lutz, M.; Spek, A. L.; van Koten, G. *Nature* **2000**, *406*, 970-974; (b) Albrecht, M.; Lutz, M.; Schreurs, A. M. M.; Lutz, E. T. H.; Spek, A. L.; van Koten, G. *J. Chem. Soc., Dalton Trans.* **2000**, *0*, 3797-3804.
(33) (a) Albrecht, M.; Gossage, R. A.; Lutz, M.; Spek, A. L.; van Koten, G. *Chemistry – A European Journal* **2000**, *6*, 1431-1445; (b) Albrecht, M.; Schlupp, M.; Bargon, J.; Koten, G. v. *Chem. Commun.* **2001**, *0*, 1874-1875.

(34) Kim, M. K.; Bae, K.-L.; Ok, K. M. *Crystal Growth & Design* **2011**, *11*, 930-932.
(35) Miyazaki, F.; Yamaguchi, K.; Shibasaki, M. *Tetrahedron Lett.* **1999**, *40*, 7379-7383.
(36) (a) Ohff, M.; Ohff, A.; Van der Boom, M. E.; Milstein, D. *J. Am. Chem. Soc.* **1997**, *119*, 11687-11688; (b) Morales-Morales, D.; Redon, R.; Yung, C.; Jensen, C. M. *Chem. Commun.* **2000**, 1619-1620; (c) Peris, E.; Loch, J. A.; Mata, J.; Crabtree, R. H. *Chem. Commun.* **2001**, 201-202; (d) Gründemann, S.; Albrecht, M.; Loch, J. A.; Faller, J. W.; Crabtree, R. H. *Organometallics* **2001**, *20*, 5485-5488; (e) Tulloch, A. A. D.; Danopoulos, A. A.; Tizzard, G. J.; Coles, S. J.; Hursthouse, M. B.; Hay-Motherwell, R. S.; Motherwell, W. B. *Chem. Commun.* **2001**, 1270-1271; (f) Bergbreiter, D. E.; Osburn, P. L.; Liu, Y. S. *J. Am. Chem. Soc.* **1999**, *121*, 9531-9538.
(37) (a) Suzuki, A. *J. Organomet. Chem.* **1999**, *576*, 147-168; (b) Miyaura, N.; Suzuki, A. *Chem. Rev.* **1995**, *95*, 2457-2483; (c) Bedford, R. B.; Draper, S. M.; Scully, P. N.; Welch, S. L. *New J. Chem.* **2000**, *24*, 745-747; (d) Zim, D.; Gruber, A. S.; Ebeling, G.; Dupont, J.; Monteiro, A. L. *Org. Lett.* **2000**, *2*, 2881-2884.
(38) Bauer, E. B.; Andavan, G. T. S.; Hollis, T. K.; Rubio, R. J.; Cho, J.; Kuchenbeiser, G. R.; Helgert, T. R.; Letko, C. S.; Tham, F. S. *Org. Lett.* **2008**, *10*, 1175-1178.
(39) (a) Crabtree, R. H.; Mihelcic, J. M.; Quirk, J. M. *J. Am. Chem. Soc.* **1979**, *101*, 7738-7740; (b) Crabtree, R. H.; Parnell, C. P.; Uriarte, R. J. *Organometallics* **1987**, *6*, 696-699; (c) Gupta, M.; Hagen, C.; Flesher, R. J.; Kaska, W. C.; Jensen, C. M. *Chem. Commun.* **1996**, 2083-2084; (d) Wang, K.; Goldman, M. E.; Emge, T. J.; Goldman, A. S. *J. Organomet. Chem.* **1996**, *518*, 55-68; (e) Liu, F.; Pak, E. B.; Singh, B.; Jensen, C. M.; Goldman, A. S. *J. Am. Chem. Soc.* **1999**, *121*, 4086-4087.
(40) (a) Van De Kuil, L. A.; Grove, D. M.; Gossage, R. A.; Zwikker, J. W.; Jenneskens, L. W.; Drenth, W.; Van Koten, G. *Organometallics* **1997**, *16*, 4985-4994; (b) Grove, D. M.; Verschuuren, A. H. M.; van Koten, G.; van Beek, J. A. M. *J. Organomet. Chem.* **1989**, *372*, C1-C6.
(41) (a) Stark, M. A.; Richards, C. J. *Tetrahedron Lett.* **1997**, *38*, 5881-5884; (b) Giménez, R.; Swager, T. M. *J. Mol. Catal. A: Chem.* **2001**, *166*, 265-273; (c) Stark, M. A.; Jones, G.; Richards, C. J. *Organometallics* **2000**, *19*, 1282-1291.
(42) (a) Pope, M.; Kallmann, H. P.; Magnante, P. *The Journal of Chemical Physics* **1963**, *38*, 2042-2043; (b) Sano, M.; Pope, M.; Kallmann, H. *The Journal of Chemical Physics* **1965**, *43*, 2920-2921.
(43) Baldo, M. A.; O'Brien, D. F.; You, Y.; Shoustikov, A.; Sibley, S.; Thompson, M. E.; Forrest, S. R. *Nature* **1998**, *395*, 151-154.
(44) (a) McGlynn, S. P.; Azumi, T. *Molecular spectroscopy of the triplet state*; Prentice-Hall, 1969; (b) Klessinger, M.; Michl, J. *Excited States and Photo-Chemistry of Organic Molecules*; Wiley, 1995.
(45) (a) Yersin, H. In *Transition Metal and Rare Earth Compounds*; Springer Berlin Heidelberg: 2004; Vol. 241, p 1-26; (b) Yersin, H. In *Organometallic triplet emitters for OLED applications: controlling emission properties by chemical variation*, 2004; pp 124-132; (c) Yersin, H. *Highly Efficient OLEDs with Phosphorescent Materials*; Wiley, 2008.
(46) Yersin, H. B. S.; Monkowius, U. B. a. A. L. WO, 2010; WO 2010/006681 A1.
(47) Shinar, J.; *Organic Light-Emitting Devices*; Springer: New York, **2004**.
(48) (a) Yu, J.; Hu, D.; Barbara, P. F. *Science* **2000**, *289*, 1327-1330; (b) Kersting, R.; Lemmer, U.; Deussen, M.; Bakker, H. J.; Mahrt, R. F.; Kurz, H.; Arkhipov, V. I.; Bässler,

H.; Göbel, E. O. *Phys. Rev. Lett.* **1994**, *73*, 1440-1443; (c) Gulbinas, V.; Zaushitsyn, Y.; Sundström, V.; Hertel, D.; Bässler, H.; Yartsev, A. *Phys. Rev. Lett.* **2002**, *89*, 107401; (d) Arkhipov, V. I.; Bässler, H. *physica status solidi (a)* **2004**, *201*, 1152-1187; (e) Bagnich, S. A.; Bassler, H.; Neher, D. *The Journal of Chemical Physics* **2004**, *121*, 9178-9183; (f) Yan, M.; Rothberg, L. J.; Papadimitrakopoulos, F.; Galvin, M. E.; Miller, T. M. *Phys. Rev. Lett.* **1994**, *73*, 744-747.

(49) (a) Kaminorz, Y.; Smela, E.; Inganäs, O.; Brehmer, L. *Adv. Mater.* **1998**, *10*, 765-769; (b) Scott, J. C.; Kaufman, J. H.; Brock, P. J.; DiPietro, R.; Salem, J.; Goitia, J. A. *J. Appl. Phys.* **1996**, *79*, 2745-2751; (c) Park, S.-J.; Gesquiere, A. J.; Yu, J.; Barbara, P. F. *J. Am. Chem. Soc.* **2004**, *126*, 4116-4117; (d) Bonfigli, F.; Brogioli, D.; Vincenti, M. A.; Montereali, R. M. *J. Opt. Technol.* **2011**, *78*, 419-423; (e) Gordon, M. P.; Ha, T.; Selvin, P. R. *Proc. Natl. Acad. Sci. U. S. A.* **2004**, *101*, 6462-6465; (f) Weiss, S. *Science* **1999**, *283*, 1676-1683.

(50) (a) Hahn, F. E.; Jahnke, M. C.; Pape, T. *Organometallics* **2007**, *26*, 150-154; (b) Danopoulos, A. A.; Tulloch, A. A. D.; Winston, S.; Eastham, G.; Hursthouse, M. B. *Dalton Trans.* **2003**, 1009-1015.

(51) (a) Cho, J.; Hollis, T. K.; Helgert, T. R.; Valente, E. J. *Chem. Commun.* **2008**, 5001-5003; (b) Rubio, R. J.; Andavan, G. T. S.; Bauer, E. B.; Hollis, T. K.; Cho, J.; Tham, F. S.; Donnadieu, B. *J. Organomet. Chem.* **2005**, *690*, 5353-5364.

(52) Hahn, F. E.; Jahnke, M. C.; Gomez-Benitez, V.; Morales-Morales, D.; Pape, T. *Organometallics* **2005**, *24*, 6458-6463.

(53) (a) Pugh, D.; Boyle, A.; Danopoulos, A. A. *Dalton Trans.* **2008**, 1087-1094; (b) Danopoulos, A. A.; Pugh, D.; Wright, J. A. *Angew. Chem. Int. Ed.* **2008**, *47*, 9765-9767.

(54) Poyatos, M.; Mata, J. A.; Falomir, E.; Crabtree, R. H.; Peris, E. *Organometallics* **2003**, *22*, 1110-1114.

(55) Simons, R. S.; Custer, P.; Tessier, C. A.; Youngs, W. J. *Organometallics* **2003**, *22*, 1979-1982.

(56) Haque, R. A.; Salman, A. W.; Guan, T. S.; Abdallah, H. H. *J. Organomet. Chem.* **2011**, *696*, 3507-3512.

(57) Chen, J. C. C.; Lin, I. J. B. *J. Chem. Soc., Dalton Trans.* **2000**, 839-840.

(58) (a) Danopoulos, A. A.; Wright, J. A.; Motherwell, W. B.; Ellwood, S. *Organometallics* **2004**, *23*, 4807-4810; (b) Danopoulos, A. A.; Winston, S.; Motherwell, W. B. *Chem. Commun.* **2002**, *0*, 1376-1377.

(59) Danopoulos, A. A.; Tsoureas, N.; Wright, J. A.; Light, M. E. *Organometallics* **2003**, *23*, 166-168.

(60) Vargas, V. C.; Rubio, R. J.; Hollis, T. K.; Salcido, M. E. *Org. Lett.* **2003**, *5*, 4847-4849.

(61) (a) Moore, T. A.; Gust, D.; Mathis, P.; Mialocq, J. C.; Chachaty, C.; Bensasson, R. V.; Land, E. J.; Doizi, D.; Liddell, P. A.; Lehman, W. R.; Nemeth, G. A.; Moore, A. L. *Nature* **1984**, *307*, 630-632; (b) Gust, D.; Moore, T. A.; Moore, A. L. *Acc. Chem. Res.* **2001**, *34*, 40-48; (c) Chakraborty, S.; Wadas, T. J.; Hester, H.; Schmehl, R.; Eisenberg, R. *Inorg. Chem.* **2005**, *44*, 6865-6878; (d) Wasielewski, M. R. *Chem. Rev.* **1992**, *92*, 435-461; (e) Hambourger, M.; Moore, G. F.; Kramer, D. M.; Gust, D.; Moore, A. L.; Moore, T. A. *Chem. Soc. Rev.* **2009**, *38*, 25-35.

(62) (a) Archer, M. D.; Bolton, J. R. *J. Phys. Chem.* **1990**, *94*, 8028-8036; (b) Borja, M.; Dutta, P. K. *Nature* **1993**, *362*, 43-45; (c) Bard, A. J.; Fox, M. A. *Acc. Chem. Res.* **1995**, *28*,

141-145; (d) Jarosz, P.; Du, P. W.; Schneider, J.; Lee, S. H.; McCamant, D.; Eisenberg, R. *Inorg. Chem.* **2009**, *48*, 9653-9663; (e) Navarro, R. M.; Alvarez-Galvan, M. C.; de la Mano, J. A. V.; Al-Zahrani, S. M.; Fierro, J. L. G. *Energy Environ. Sci.* **2010**, *3*, 1865-1882; (f) Walter, M. G.; Warren, E. L.; McKone, J. R.; Boettcher, S. W.; Mi, Q. X.; Santori, E. A.; Lewis, N. S. *Chem. Rev.* **2010**, *110*, 6446-6473.
(63) (a) Becquerel, A.-E. *C. R. Acad. Sci. Paris* **1839**, *9*, 561; (b) Mayo, E. I.; Kilsa, K.; Tirrell, T.; Djurovich, P. I.; Tamayo, A.; Thompson, M. E.; Lewis, N. S.; Gray, H. B. *Photochem. Photobiol. Sci.* **2006**, *5*, 871-873; (c) Helgesen, M.; Sondergaard, R.; Krebs, F. C. *J. Mater. Chem.* **2010**, *20*, 36-60.
(64) (a) Tang, C. W.; Vanslyke, S. A. *Appl. Phys. Lett.* **1987**, *51*, 913-915; (b) Burroughes, J. H.; Bradley, D. D. C.; Brown, A. R.; Marks, R. N.; Mackay, K.; Friend, R. H.; Burns, P. L.; Holmes, A. B. *Nature* **1990**, *347*, 539-541; (c) Bauer, R.; Finkenzeller, W. J.; Bogner, U.; Thompson, M. E.; Yersin, H. *Org. Electron.* **2008**, *9*, 641-648; (d) Finkenzeller, W. J.; Hofbeck, T.; Thompson, M. E.; Yersin, H. *Inorg. Chem.* **2007**, *46*, 5076-5083; (e) Finkenzeller, W. J.; Thompson, M. E.; Yersin, H. *Chem. Phys. Lett.* **2007**, *444*, 273-279; (f) Zhong, C. M.; Duan, C. H.; Huang, F.; Wu, H. B.; Cao, Y. *Chem. Mater.* **2011**, *23*, 326-340.
(65) (a) Moudam, O.; Rowan, B. C.; Alamiry, M.; Richardson, P.; Richards, B. S.; Jones, A. C.; Robertson, N. *Chem. Commun.* **2009**, 6649-6651; (b) Au, V. K. M.; Wong, K. M. C.; Zhu, N. Y.; Yam, V. W. W. *J. Am. Chem. Soc.* **2009**, *131*, 9076-9085; (c) Tam, A. Y.-Y.; Wong, K. M.-C.; Yam, V. W.-W. *J. Am. Chem. Soc.* **2009**, *131*, 6253 - 6260; (d) Chi, Y.; Chou, P. T. *Chem. Soc. Rev.* **2010**, *39*, 638-655.
(66) Lee, C. S.; Sabiah, S.; Wang, J. C.; Hwang, W. S.; Lin, I. J. B. *Organometallics* **2010**, *29*, 286-289.
(67) Cho, J.; Hollis, T. K.; Valente, E. J.; Trate, J. M. *J. Organomet. Chem.* **2011**, *696*, 373-377.
(68) Spencer, L. P.; Winston, S.; Fryzuk, M. D. *Organometallics* **2004**, *23*, 3372-3374.
(69) (a) Ahrens, S.; Strassner, T. *Inorg. Chim. Acta* **2006**, *359*, 4789-4796; (b) Berthon-Gelloz, G.; Buisine, O.; Briere, J. F.; Michaud, G.; Sterin, S.; Mignani, G.; Tinant, B.; Declercq, J. P.; Chapon, D.; Marko, I. E. *J. Organomet. Chem.* **2005**, *690*, 6156-6168.
(70) Farrugia, L. *J. Appl. Crystallogr.* **1997**, *30*, 565.
(71) (a) Vanderploeg, A.; Vankoten, G.; Vrieze, K.; Spek, A. L. *Inorg. Chem.* **1982**, *21*, 2014-2026; (b) Fantasia, S.; Petersen, J. L.; Jacobsen, H.; Cavallo, L.; Nolan, S. P. *Organometallics* **2007**, *26*, 5880-5889.
(72) Yersin, H.; Donges, D. In *Transition Metal and Rare Earth Compounds*; Yersin, H., Ed.; Springer Berlin / Heidelberg: 2001; Vol. 214, p 81-186.
(73) Drago, R. S. *Physical Methods in Chemistry*; Saunders, 1977.
(74) (a) Zhang, L. Y.; Li, B.; Shi, L. F.; Li, W. L. *Opt. Mater.* **2009**, *31*, 905-911; (b) Evans, R. C.; Douglas, P.; Winscom, C. J. *Coord. Chem. Rev.* **2006**, *250*, 2093-2126; (c) Unger, Y.; Zeller, A.; Ahrens, S.; Strassner, T. *Chem. Commun.* **2008**, 3263-3265; (d) Unger, Y.; Meyer, D.; Strassner, T. *Dalton Trans* **2010**, *39*, 4295-4301.
(75) Unger, Y.; Zeller, A.; Taige, M. A.; Strassner, T. *Dalton Trans.* **2009**, 4786-4794.
(76) (a) Walser, A. D.; Priestley, R.; Dorsinville, R. *Synth. Met.* **1999**, *102*, 1552-1553; (b) Martin, R. L.; Kress, J. D.; Campbell, I. H.; Smith, D. L. *Phys. Rev. B* **2000**, *61*, 15804; (c) Colle, M.; Garditz, C. *Appl. Phys. Lett.* **2004**, *84*, 3160-3162.

(77) Seo, J. H.; Kim, I. J.; Kim, Y. K.; Kim, Y. S. *Thin Solid Films* **2008**, *516*, 3614-3617.
(78) (a) Du, Y.; Fu, Y.; Shi, Y.; Lü, X.; Lü, C.; Su, Z. *J. Solid State Chem.* **2009**, *182*, 1430-1437; (b) Kai, Y.; Morita, M.; Yasuoka, N.; Kasai, N. *Bull. Chem. Soc. Jpn.* **1985**, *58*, 1631-1635.
(79) (a) Tao, X. T.; Suzuki, H.; Wada, T.; Miyata, S.; Sasabe, H. *J. Am. Chem. Soc.* **1999**, *121*, 9447-9448; (b) Tao, X. T.; Suzuki, H.; Wada, T.; Sasabe, H.; Miyata, S. *Appl. Phys. Lett.* **1999**, *75*, 1655-1657; (c) Vinyard, D. J.; Richter, M. M. *Dalton Trans.* **2006**, 4461-4464.
(80) Pangborn, A. B.; Giardello, M. A.; Grubbs, R. H.; Rosen, R. K.; Timmers, F. J. *Organometallics* **1996**, *15*, 1518-1520.
(81) (a) Adams, R. D.; Cotton, F. A. *Catalysis by Di- and Polynuclear Metal Cluster Complexes*; Wiley-VCH: New York, 1998; (b) Sculfort, S.; Braunstein, P. *Chem. Soc. Rev.* **2011**, *40*, 2741-2760; (c) Moret, M.-E.; Chen, P. *J. Am. Chem. Soc.* **2009**, *131*, 5675-5690.
(82) (a) Pyykkö, P. *Chem. Rev.* **1997**, *97*, 597-636; (b) Pan, Q. J.; Guo, Y. R.; Zhang, H. X. *Organometallics* **2010**, *29*, 3261-3270; (c) Lin, Z. Y. *Acc. Chem. Res.* **2010**, *43*, 602-611.
(83) (a) Adams, R. D.; Captain, B. *Acc. Chem. Res.* **2009**, *42*, 409-418; (b) Adams, R. D.; Barnard, T. S.; Li, Z.; Wu, W.; Yamamoto, J. *J. Am. Chem. Soc.* **1994**, *116*, 9103-9113; (c) Yoshikai, N.; Yamanaka, M.; Ojima, I.; Morokuma, K.; Nakamura, E. *Organometallics* **2006**, *25*, 3867-3875.
(84) (a) Katz, M. J.; Sakai, K.; Leznoff, D. B. *Chem. Soc. Rev.* **2008**, *37*, 1884-1895; (b) Zheng, X.-D.; Jiang, L.; Feng, X.-L.; Lu, T.-B. *Inorg. Chem.* **2008**, *47*, 10858-10865.
(85) (a) Yip, H.-K.; Lin, H.-M.; Cheung, K.-K.; Che, C.-M.; Wang, Y. *Inorg. Chem.* **1994**, *33*, 1644-1651; (b) Gil, B.; Forniés, J.; Gómez, J.; Lalinde, E.; Martín, A.; Moreno, M. T. *Inorg. Chem.* **2006**, *45*, 7788-7798; (c) Fornies, J.; Sicilia, V.; Casas, J. M.; Martin, A.; Lopez, J. A.; Larraz, C.; Borja, P.; Ovejero, C. *Dalton Trans.* **2011**, *40*, 2898-2912.
(86) (a) Uson, R.; Fornies, J.; Tomas, M.; Cotton, F. A.; Falvello, L. R. *J. Am. Chem. Soc.* **1984**, *106*, 2482-2483; (b) Uson, R.; Fornies, J.; Menjon, B.; Cotton, F. A.; Falvello, L. R.; Tomas, M. *Inorg. Chem.* **1985**, *24*, 4651-4656; (c) Balch, A. L.; Catalano, V. J.; Olmstead, M. M. *Inorg. Chem.* **1990**, *29*, 585-586; (d) Balch, A. L.; Catalano, V. J. *Inorg. Chem.* **1991**, *30*, 1302-1308; (e) Kim, M.; Taylor, T. J.; Gabbaï, F. P. *Journal of the American Chemical Society* **2008**, *130*, 6332-6333.
(87) Bauer, J.; Braunschweig, H.; Dewhurst, R. D. *Chem. Rev.* **2012**, *112*, 4329-4346.
(88) (a) Arsenault, G. J.; Anderson, C. M.; Puddephatt, R. J. *Organometallics* **1988**, *7*, 2094-2097; (b) Yamaguchi, T.; Yamazaki, F.; Ito, T. *J. Am. Chem. Soc.* **2001**, *123*, 743-744; (c) Fornies, J.; Fortuno, C.; Ibanez, S.; Martin, A. *Inorg. Chem.* **2008**, *47*, 5978-5987.
(89) Jamali, S.; Mazloomi, Z.; Nabavizadeh, S. M.; Milic, D.; Kia, R.; Rashidi, M. *Inorg. Chem.* **2010**, *49*, 2721-2726.
(90) Scholten, J. D.; Dupont, J. *Organometallics* **2008**, *27*, 4439-4442.
(91) (a) Markó, I. E.; Stérin, S.; Buisine, O.; Mignani, G.; Branlard, P.; Tinant, B.; Declercq, J.-P. *Science* **2002**, *298*, 204; (b) Herrmann, W. A.; Goossen, L. J.; Kocher, C.; Artus, G. R. J. *Angew. Chem. Int. Ed. Engl.* **1996**, *35*, 2805-2807.
(92) (a) Lee, H. M.; Jiang, T.; Stevens, E. D.; Nolan, S. P. *Organometallics* **2001**, *20*, 1255-1258; (b) Türkmen, H.; Pape, T.; Hahn, F. E.; Çetinkaya, B. *Eur. J. Inorg. Chem.* **2008**, *2008*, 5418-5423.

(93) Vehlow, K.; Wang, D.; Buchmeiser, M. R.; Blechert, S. *Angew. Chem. Int. Ed.* **2008**, *47*, 2615-2618.
(94) (a) Valente, C.; Belowich, M. E.; Hadei, N.; Organ, M. G. *Eur. J. Org. Chem.* **2010**, *2010*, 4343-4354; (b) Broggi, J.; Clavier, H.; Nolan, S. P. *Organometallics* **2008**, *27*, 5525-5531.
(95) Mata, J. A.; Poyatos, M.; Peris, E. *Coord. Chem. Rev.* **2007**, *251*, 841-859.
(96) (a) Marion, N.; Ecarnot, E. C.; Navarro, O.; Amoroso, D.; Bell, A.; Nolan, S. P. *J. Org. Chem.* **2006**, *71*, 3816-3821; (b) Demir, S.; Özdemir, I.; Çetinkaya, B.; Arslan, H.; VanDerveer, D. *Polyhedron* **2011**, *30*, 195-200.
(97) (a) Fujihara, T.; Obora, Y.; Tokunaga, M.; Sato, H.; Tsuji, Y. *Chem. Commun.* **2005**, 4526-4528; (b) Ohta, H.; Fujihara, T.; Tsuji, Y. *Dalton Trans.* **2008**, 379-385.
(98) Beletskaya, I. P.; Kashin, A. N.; Litvinov, A. E.; Tyurin, V. S.; Valetsky, P. M.; van Koten, G. *Organometallics* **2006**, *25*, 154-158.
(99) (a) Sajoto, T.; Djurovich, P. I.; Tamayo, A.; Yousufuddin, M.; Bau, R.; Thompson, M. E.; Holmes, R. J.; Forrest, S. R. *Inorg. Chem.* **2005**, *44*, 7992-8003; (b) Wu, Y.; Wu, S. X.; Li, H. B.; Geng, Y.; Su, Z. M. *Dalton Trans.* **2011**, *40*, 4480-4488; (c) Mizuhata, Y.; Sasamori, T.; Tokitoh, N. *Chem. Rev.* **2009**, *109*, 3479-3511; (d) Hindi, K. M.; Panzner, M. J.; Tessier, C. A.; Cannon, C. L.; Youngs, W. J. *Chem. Rev.* **2009**, *109*, 3859-3884; (e) Arnold, P. L.; Casely, I. J. *Chem. Rev.* **2009**, *109*, 3599-3611.
(100) (a) Crocker, C.; Errington, R. J.; McDonald, W. S.; Odell, K. J.; Shaw, B. L.; Goodfellow, R. J. *J. Chem. Soc., Chem. Commun.* **1979**, 498-499; (b) Morales-Morales, D.; Jensen, C. M.; *The Chemistry of Pincer Compounds*; Elsevier: New York, **2007**; (c) Jones, N. D.; Cavell, R. G. *J. Organomet. Chem.* **2005**, *690*, 5485-5496; (d) Gagliardo, M.; Snelders, D. J. M.; Chase, P. A.; Klein Gebbink, R. J. M.; van Klink, G. P. M.; van Koten, G. *Angew. Chem. Int. Ed.* **2007**, *46*, 8558-8573.
(101) (a) Peris, E.; Crabtree, R. H. *Coord. Chem. Rev.* **2004**, *248*, 2239-2246; (b) Poyatos, M.; Mata, J. A.; Peris, E. *Chem. Rev.* **2009**, *109*, 3677-3707; (c) Pugh, D.; Danopoulos, A. A. *Coord. Chem. Rev.* **2007**, *251*, 610-641; (d) Corberan, R.; Mas-Marza, E.; Peris, E. *Eur. J. Inorg. Chem.* **2009**, 1700-1716; (e) Melaimi, M.; Soleilhavoup, M.; Bertrand, G. *Angew. Chem. Int. Ed.* **2010**, *49*, 8810-8849; (f) Normand, A. T.; Yen, S. K.; Huynh, H. V.; Hor, T. S. A.; Cavell, K. J. *Organometallics* **2008**, *27*, 3153-3160; (g) Bacciu, D.; Cavell, K. J.; Fallis, I. A.; Ooi, L.-l. *Angew. Chem., Int. Ed.* **2005**, *44*, 5282-5284.
(102) (a) Tam, A. Y.-Y.; Wong, K. M.-C.; Yam, V. W.-W. *J. Am. Chem. Soc.* **2009**, *131*, 6253-6260; (b) Shirakawa, M.; Fujita, N.; Tani, T.; Kaneko, K.; Shinkai, S. *Chem. Commun.* **2005**, *0*, 4149-4151; (c) Huang, M.; Soyez, H.; Dunn, B.; Zink, J.; Sellinger, A.; Brinker, C. J. *J Sol-Gel Sci Technol* **2008**, *47*, 300-310.
(103) Schneider, N.; Bellemin-Laponnaz, S.; Wadepohl, H.; Gade, L. H. *Eur. J. Inorg. Chem.* **2008**, *2008*, 5587-5598.
(104) (a) Khan, M. S.; Al-Suti, M. K.; Shah, H. H.; Al-Humaimi, S.; Al-Battashi, F. R.; Bjernemose, J. K.; Male, L.; Raithby, P. R.; Zhang, N.; Kohler, A.; Warren, J. E. *Dalton Trans.* **2011**, *40*, 10174-10183; (b) Mintcheva, N.; Georgieva, I.; Mihaylov, T.; Trendafilova, N.; Tanabe, M.; Osakada, K. *J. Organomet. Chem.* **2012**, *697*, 23-32; (c) Moret, M.-E.; Chen, P. *Organometallics* **2008**, *27*, 4903-4916; (d) Swartz, B. D.; Brennessel, W. W.; Jones, W. D. *Organometallics* **2011**, *30*, 1523-1529.

(105) (a) Janzen, D. E.; Mehne, L. F.; VanDerveer, D. G.; Grant, G. J. *Inorg. Chem.* **2005**, *44*, 8182-8184; (b) Forniés, J.; Martínez, F.; Navarro, R.; Urriolabeitia, E. P. *Organometallics* **1996**, *15*, 1813-1819.
(106) Shannon, R. D. *Acta Cryst A* **1976**, *32*, 751-767.
(107) (a) Orpen, A. G.; Brammer, L.; Allen, F. H.; Kennard, O.; Watson, D. G.; Taylor, R. *J. Chem. Soc., Dalton Trans.* **1989**, S1-S83; (b) Cordero, B.; Gomez, V.; Platero-Prats, A. E.; Reves, M.; Echeverria, J.; Cremades, E.; Barragan, F.; Alvarez, S. *Dalton Trans.* **2008**, 2832-2838; (c) Allen, F. H.; Kennard, O.; Watson, D. G.; Brammer, L.; Orpen, A. G.; Taylor, R. *J. Chem. Soc., Perkin Trans. 2* **1987**, S1-S19.
(108) (a) Cramer, R. D.; Lindsey, R. V.; Prewitt, C. T.; Stolberg, U. G. *J. Am. Chem. Soc.* **1965**, *87*, 658-658; (b) De Felice, V.; Ferrara, M. L.; Panunzi, A.; Ruffo, F. *J. Organomet. Chem.* **1992**, *439*, C49-C51; (c) Aizawa, S.-i.; Kobayashi, T.; Kawamoto, T. *Inorg. Chim. Acta* **2005**, *358*, 2319-2326.
(109) Asensio, G.; Medio-Simon, M.; Alemán, P.; de Arellano, C. R. *Cryst. Growth Des.* **2006**, *6*, 2769-2778.
(110) (a) Shimoni, L.; Carrell, H. L.; Glusker, J. P.; Coombs, M. M. *J. Am. Chem. Soc.* **1994**, *116*, 8162-8168; (b) Ottaviani, P.; Caminati, W.; Favero, L. B.; Blanco, S.; López, J. C.; Alonso, J. L. *Chem. Eur. J.* **2006**, *12*, 915-920.
(111) (a) van den Berg, J.-A.; Seddon, K. R. *Cryst. Growth Des.* **2003**, *3*, 643-661; (b) Desiraju, G. R. *Acc. Chem. Res.* **2002**, *35*, 565-573; (c) Hyla-Kryspin, I.; Haufe, G.; Grimme, S. *Chem. Eur. J.* **2004**, *10*, 3411-3422.
(112) Parr, R. G.; Weitao, Y. *Density-Functional Theory of Atoms and Molecules*; Oxford University Press, 1994.
(113) (a) Tao, J.; Perdew, J. P.; Staroverov, V. N.; Scuseria, G. E. *Phys. Rev. Lett.* **2003**, *91*, 146401; (b) Staroverov, V. N.; Scuseria, G. E.; Tao, J. M.; Perdew, J. P. *J. Chem. Phys.* **2003**, *119*, 12129-12137.
(114) (a) Perdew, J. P.; Burke, K.; Ernzerhof, M. *Phys. Rev. Lett.* **1996**, *77*, 3865-3868; (b) Perdew, J. P.; Burke, K.; Ernzerhof, M. *Phys. Rev. Lett.* **1997**, *78*, 1396-1396.
(115) (a) Becke, A. D. *J. Chem. Phys.* **1993**, *98*, 5648-5652; (b) Lee, C.; Yang, W.; Parr, R. G. *Phys. Rev. B* **1988**, *37*, 785.
(116) Zhao, Y.; Truhlar, D. G. *Theor. Chem. Acc.* **2008**, *120*, 215-241.
(117) Hay, P. J.; Wadt, W. R. *J. Chem. Phys.* **1985**, *82*, 299-310.
(118) (a) Hariharan, P. C.; Pople, J. A. *Theor. Chim. Acta* **1973**, *28*, 213-222; (b) Hehre, W. J.; Ditchfie.R; Pople, J. A. *J. Chem. Phys.* **1972**, *56*, 2257-2261.
(119) Frisch, M. J. et al. *Gaussian 09, Revisions, A.02, Gaussian, Inc.* Wallingford, CT, 2009.
(120) Couty, M.; Hall, M. B. *J. Comput. Chem.* **1996**, *17*, 1359-1370.
(121) (a) Nolan, S. P. *N-Heterocyclic Carbenes in Synthesis*; Wiley, 2006; (b) Díez-González, S. *N-Heterocyclic Carbenes: From Laboratory Curiosities to Efficient Synthetic Tools*; Royal Society of Chemistry, 2010.
(122) Öfele, K.; Herrmann, W. A.; Mihalios, D.; Elison, M.; Herdtweck, E.; Scherer, W.; Mink, J. *J. Organomet. Chem.* **1993**, *459*, 177-184.
(123) (a) Crabtree, R. H. *J. Organomet. Chem.* **2005**, *690*, 5451-5457; (b) Weskamp, T.; Schattenmann, W. C.; Spiegler, M.; Herrmann, W. A. *Angew. Chem. Int. Ed.* **1998**, *37*, 2490-2493; (c) Huang, J.; Stevens, E. D.; Nolan, S. P.; Petersen, J. L. *J. Am. Chem. Soc.*

1999, *121*, 2674-2678; (d) Scholl, M.; Ding, S.; Lee, C. W.; Grubbs, R. H. *Org. Lett.* **1999**, *1*, 953-956.
(124) (a) A.Herrmann, W.; Weskamp, T.; Bohm, V. P. W. In *Adv. Organomet. Chem.*; Academic Press: 2001; Vol. Volume 48, p 1-69; (b) Jafarpour, L.; Nolan, S. P. In *Adv. Organomet. Chem.*; Academic Press: 2000; Vol. Volume 46, p 181-222.
(125) Tafipolsky, M.; Scherer, W.; Öfele, K.; Artus, G.; Pedersen, B.; Herrmann, W. A.; McGrady, G. S. *J. Am. Chem. Soc.* **2002**, *124*, 5865-5880.
(126) (a) Grundemann, S.; Albrecht, M.; Loch, J. A.; Faller, J. W.; Crabtree, R. H. *Organometallics* **2001**, *20*, 5485-5488; (b) Schultz, K. M.; Goldberg, K. I.; Gusev, D. G.; Heinekey, D. M. *Organometallics* **2011**, *30*, 1429-1437; (c) Lv, K.; Cui, D. *Organometallics* **2010**, *29*, 2987-2993.
(127) (a) Loch, J. A.; Albrecht, M.; Peris, E.; Mata, J.; Faller, J. W.; Crabtree, R. H. *Organometallics* **2002**, *21*, 700-706; (b) McGuinness, D. S.; Gibson, V. C.; Steed, J. W. *Organometallics* **2004**, *23*, 6288-6292; (c) Serra, D.; Cao, P.; Cabrera, J.; Padilla, R.; Rominger, F.; Limbach, M. *Organometallics* **2011**, *30*, 1885-1895.
(128) Nielsen, D. J.; Cavell, K. J.; Skelton, B. W.; White, A. H. *Inorg. Chim. Acta* **2002**, *327*, 116-125.
(129) Zuo, W.; Braunstein, P. *Organometallics* **2011**.
(130) Miecznikowski, J. R.; Grundemann, S.; Albrecht, M.; Megret, C.; Clot, E.; Faller, J. W.; Eisenstein, O.; Crabtree, R. H. *Dalton Trans.* **2003**, *0*, 831-838.
(131) Schwartsburd, L.; Poverenov, E.; Shimon, L. J. W.; Milstein, D. *Organometallics* **2007**, *26*, 2931-2936.
(132) Lee, C.-S.; Zhuang, R. R.; Sabiah, S.; Wang, J.-C.; Hwang, W.-S.; Lin, I. J. B. *Organometallics* **2011**, *30*, 3897-3900.
(133) (a) Cave, G. W. V.; Fanizzi, F. P.; Deeth, R. J.; Errington, W.; Rourke, J. P. *Organometallics* **2000**, *19*, 1355-1364; (b) Lai, S.-W.; Lam, H.-W.; Lu, W.; Cheung, K.-K.; Che, C.-M. *Organometallics* **2001**, *21*, 226-234; (c) Newman, C. P.; Cave, G. W. V.; Wong, M.; Errington, W.; Alcock, N. W.; Rourke, J. P. *J. Chem. Soc., Dalton Trans.* **2001**, *0*, 2678-2682; (d) Sanna, G.; Minghetti, G.; Zucca, A.; Pilo, M. I.; Seeber, R.; Laschi, F. *Inorg. Chim. Acta* **2000**, *305*, 189-205; (e) Baik, C.; Han, W.-S.; Kang, Y.; Kang, S. O.; Ko, J. *J. Organomet. Chem.* **2006**, *691*, 5900-5910; (f) Petz, W.; Neumüller, B. *Polyhedron* **2011**, *30*, 1779-1784; (g) Grove, D. M.; Van Koten, G.; Louwen, J. N.; Noltes, J. G.; Spek, A. L.; Ubbels, H. J. C. *J. Am. Chem. Soc.* **1982**, *104*, 6609-6616; (h) Vuzman, D.; Poverenov, E.; Diskin-Posner, Y.; Leitus, G.; Shimon, L. J. W.; Milstein, D. *Dalton Trans.* **2007**, *0*, 5692-5700; (i) Adams, J. J.; Lau, A.; Arulsamy, N.; Roddick, D. M. *Inorg. Chem.* **2007**, *46*, 11328-11334; (j) Poverenov, E.; Gandelman, M.; Shimon, L. J. W.; Rozenberg, H.; Ben-David, Y.; Milstein, D. *Organometallics* **2005**, *24*, 1082-1090.

Appendix

X-RAY CRYSTALLOGRAPHY

X-ray crystallography details of complexes 1, 2, and 4-7

2-(1,3-Bis(N-butylimidazol-2-ylidene)phenylene)(chloro) platinum (II), (1)

Data collection

The specimen was loose light yellow color, prismatic crystals. A small specimen (0.18 x 0.23 x 0.34mm) was retrieved from the sample; it was representative of the crystals. The crystal was mounted atop a fine glass fiber, which was fixed to a stout glass fiber, and mounted on a pin; the pin was placed on a goniometer head. The crystallographic properties and data were collected using MoKα radiation and the charge-coupled area detector (CCD) detector on an Oxford Diffraction Systems Gemini S diffractometer at 298(2)K (1). A preliminary set of cell constants was calculated from reflections observed on three sets of 5 frames which were oriented approximately in mutually orthogonal directions of reciprocal space. Data collection was carried out using MoKα radiation (graphite monochromator) with 5 runs consisting of 300 frames with a frame time of 42.3sec and a crystal-to-CCD distance of 50.000mm. The runs were collected by omega scans of 1.0° width, and at detector position of 28.624, -30.187° in 2θ. The intensity data were corrected for absorption with an analytical correction (4). Final cell constants were calculated from 9680 stronger reflections reflections from the actual data collection after integration. See Table S1-1 through Table S1-6 for crystal and refinement information.

Structure solution and refinement

The crystal is orthorhombic, space group $P2_12_12_1$ (#19; chiral) as determined from systematic absences, reflections statistics, and successful solution and refinement. The structure was solved using by direct methods in SHELXS-86(2b), and all non-H atoms were found in the E-map. Refinements were done using SHELXL-97(2a). All non-H atoms were refined and with anisotropic vibrational factors. H-atoms were observable in difference electron density maps, and placed in idealize positions; all were refined as riding atoms with relative isotropic displacement parameters of 120% of the U(eq) of the attached atom. One of the butyl side chains is disordered over two alternate conformations; the major conformer has occupancy 0.640(9). The final full-matrix least-squares refinement converged to $R_1 = 0.0169$ and $wR_2 = 0.0317$ (5320 reflections, F^2, $I > 2\sigma(I)$); $R_1 = 0.0200$

and wR_2 =.0319 for all 5896 data, 255 parameters, 0 restraints, goodness-of-fit (S) 1.003, and a small extinction parameter [0.00746(13)].

Structure description

Individual molecules comprise the asymmetric unit. The rings are nearly planar, and the Pt is approximately square planar in its coordination geometry.

2-(1,3-Bis(N-butylimidazol-2-ylidene)phenylene)(bromo) platinum (II), (2)

Data collection

Crystals were light yellow prisms, some well formed as rectangular tablets or shallow prisms. A single such specimen (dimensions 0.071 x 0.305 x 0.351 mm^3) was glued to the tip of a glass fibre and mounted on a goniometer head. The crystallographic properties and data were collected using MoKα radiation and the charge-coupled area detector (CCD) detector on an Oxford Diffraction Systems Gemini diffractometer at 173(1)K. A preliminary set of cell constants was calculated from reflections observed on three sets of 5 frames which were oriented approximately in mutually orthogonal directions of reciprocal space. Data collection was carried out using MoK radiation (graphite monochromator) with 12 runs consisting of 596 frames with a frame time of 7.99sec, and a crystal-to-CCD distance of 50.000mm. A randomly oriented region of reciprocal space was surveyed to the extent of one sphere and to a resolution of 0.70 Å. The runs were collected with phi and omega scans of 1.0° width, and at detector positions of 28.468 and -30.187° in 2θ. The intensity data were corrected for absorption (analytical) and decay. Final cell constants were calculated from 14714 strong reflections from the actual data collection after integration. See Table S2-1 through Table S2-6 for crystal and refinement information.

Structure solution and refinement

The structure was solved using SHELXS-86(2) and refined using SHELXL-97(2) The space group $P2_12_12_1$ (#19) is a polar space group, and the crystals are, apparently, a conglomerate. The cell was determined based on cell geometry, reflection statistics, systematic absences and successful solution and refinement. All non-H atoms of the molecule were found in the best E-map. Full-matrix least squares cycles were performed

to refined the positions and isotropic vibrational factors. Then, the positions and anisotropic displacement parameters for the non-H atoms were similarly refined. All hydrogen atoms on carbons were placed in ideal positions and refined as riding atoms with relative isotropic displacement parameters equal to 120% of the equivalent isotropic vibrational factor of the attached atom. One of the two butyl side chains is disordered (about 81:19), and this was modeled with an occupancy factor which refined to 0.808(16), and weak restraints applied to the displacement parameters. The final full-matrix least-squares refinement converged to R_1 = 0.030 (5202 F^2, F>2σF^2), and 0.042 (all 5991) data; wR_2 = 0.0764 for all data, 263 parameters, 2 restraints, and S (goodness-of-fit) = 1.075. The final difference features were +1.93, -1.73 e/Å^3 (in the vicinity of the Pt atom).

Structure description

A molecule comprises the asymmetric unit, with four in the cell. All bond distances, angles and torsions have typical values. There are no close contacts of importance between molecules. The platinum (IV) ion is approximately square planar, coordinated to a bromide and three carbanions.

2-(1,3-Bis(trimethylsilylmethyl-imidazol-2-ylidene)phenylene)(chloro) platinum (II), (4)

Data collection

The specimens were thin needles that nicely extinguished polarized light, but showed signs of twinning. The first specimen studied was twinned; a second is nicely ordered. The crystals were yellow, and a representative long needle specimen was cut (0.063 x 0.109 x 0.690 mm, and affixed to a fine glass fibre attached to a stout glass fibre mounted on a pin; the pin was placed on a goniometer head. The crystallographic properties and data were collected using MoKα radiation and the charge-coupled area detector (CCD) detector on an Oxford Diffraction Systems Gemini S diffractometer at 298(1)K (1). A preliminary set of cell constants was calculated from reflections observed on three sets of 5 frames which were oriented approximately in mutually orthogonal directions of reciprocal space. Data collection was carried out using MoKα radiation (graphite monochromator) with 8 runs consisting of 512 frames with a frame time of 20.68 sec and a crystal-to-CCD distance of

50.000mm, and a strategy to achieve a resolution of 0.7Å. The runs were collected by omega scans of 1.0° width, and at detector position of 28.624, -30.187° in 2θ. The intensity data were corrected for absorption with an analytical correction (4). Final cell constants were calculated from 7655 stronger reflections from the actual data collection after integration. See Table S1-1 through Table S1-6 for crystal and refinement information.

Structure solution and refinement

The crystal is monoclinic, C-centered, and the space group C2/c was determined from the cell geometry, reflections statistics, systematic absences, and successful solution and refinement. The structure was also solved in space group Cc, but the complex showed chemically unreasonable distortions, and it was clear that Cc was incorrect (Cc and C2/c cannot be told apart from systematic absences). The structure was solved by using direct methods in SHELXS-86(2b), and all non-H atoms were found in the E-map. Refinements were done using SHELXL-97(2a). All non-H atoms were refined and with anisotropic vibrational factors. H-atoms were observable in difference electron density maps, and placed in idealize positions; all were refined as riding atoms with relative isotropic displacement parameters of 120% of the U(eq) of the attached atom. One of the butyl side chains is disordered over two alternate conformations; the major conformer has occupancy 0.640(9). The final full-matrix least-squares refinement converged to R_1 = 0.0208 (2983 reflections, F^2, I > 2σ(I)); R_1 = 0.0290 and wR_2 =.0383 for all 3663 data, 129 parameters, 0 restraints, goodness-of-fit (S) 0.999, and no extinction.

Structure description

A half-molecule comprises the asymmetric unit, and complexes lie on the two-fold axis with the C-Pt-Cl exactly on the two-fold axis. The molecule has C_2 symmetry, and therefore can be limitingly close-packed in space group C_2/c. Pt-C(1) is 2.024(3)Å, Pt-C(7) is 1.929(3)Å, while Pt-Cl is 2.4052(9)Å. All other bond distances and angles are in normal ranges. There are no exceptional close contacts between molecules.

Pt_2Ag_2 cluster, (5)

Data collection

The crystals were virgulate and extinguished nicely under crossed polarized light. One of the specimens, representative of the sample had dimensions 0.019 x 0.094 x 0.829 mm^3. It was fixed to a fine glass fibre attached to a stout glass fibre mounted on a pin; the pin was placed on a goniometer head. The crystallographic properties and data were collected using MoKα radiation and the charge-coupled area detector (CCD) detector on an Oxford Diffraction Systems Gemini S diffractometer at 150(1) K (1). A preliminary set of cell constants was calculated from reflections observed on three sets of 5 frames which were oriented approximately in mutually orthogonal directions of reciprocal space. Data collection was carried out using MoKα radiation (graphite monochromator) with 6 runs consisting of 510 frames with a frame time of 60.0 sec and a crystal-to-CCD distance of 50.000mm, and a strategy to achieve a resolution of 0.7Å. The runs were collected by omega scans of 1.0° width, and at detector position of 28.624 and -30.187° in 2θ. The intensity data were corrected for absorption with an analytical correction (4). Final cell constants were calculated from 17346 stronger reflections from the actual data collection after integration. See Table S2-1 through Table S2-6 for crystal and refinement information.

Structure solution and refinement

The crystal is triclinic, space group P-1 (#2) as determined from the cell geometry, reflections statistics and successful solution and refinement. The structure was solved using by direct methods in SHELXS-86(2b), and all non-H atoms were found in the E-map. Refinements were done using SHELXL-97(2a). All non-H atoms were refined and with anisotropic vibrational factors. H-atoms were observable in difference electron density maps, and placed in idealize positions; all were refined as riding atoms with relative isotropic displacement parameters of 120% of the U(eq) of the attached atom. The trifluoroacetate salt was prepared with silver trifluoroacetate, and two equivalents of silver trifluoroacetate are incorporated into the dimerized structure. Solvent was located in the cell, which refined as a 0.77 pentane and an 0.23 hexane occupying a solvent location; the non-H atoms were modeled with isotropic vibrational parameters; the hexane is fairly non-thermal, occupying the location tightly while the pentane is rather more thermal. The final full-matrix least-squares refinement converged to R_1 = 0.0297 (13754 reflections, F2, I >

$2\sigma(I)$); R_1 = 0.0529 and wR_2 =0.0523 for all 20422 data, 794 parameters, 12 restraints (on C-C distances in the solvent), goodness-of-fit (S) 0.845, and no extinction.

Structure description

The structure is nominally the Pt complex as the trifluoroacetate, but dimerized on either side of two silver trifluoroacetates.

$PtAg_2$ triangles are formed, with Pt-Ag distances of 2.93 and 3.14Å, with Ag-Ag distances of 2.94Å. The remaining Pt-Ag distance is 2.91Å.

Other Information

Data collection and structure solution were conducted at the University of Portland Diffraction Facility, 112A Swindells Hall, Department of Chemistry, University of Portland, Portland, OR, 97203. All calculations were performed using Pentium computers using the current SHELX suite of programs.

2-(1,3-Bis(trimethylsilylmethyl-imidazol-2-ylidene)phenylene)(trifluoroacetato) platinum (II), (6)

Data collection

The specimens were thin needles that nicely extinguished polarized light, but showed signs of twinning. The first specimen studied was twinned; a second is nicely ordered. The crystals were yellow, and a representative long needle specimen was cut (0.063 x 0.109 x 0.690 mm, and affixed to a fine glass fibre attached to a stout glass fibre mounted on a pin; the pin was placed on a goniometer head. The crystallographic properties and data were collected using MoKα radiation and the charge-coupled area detector (CCD) detector on an Oxford Diffraction Systems Gemini S diffractometer at 298(1)K (1). A preliminary set of cell constants was calculated from reflections observed on three sets of 5 frames which were oriented approximately in mutually orthogonal directions of reciprocal space. Data collection was carried out using MoKα radiation (graphite monochromator) with 8 runs consisting of 512 frames with a frame time of 20.68 sec and a crystal-to-CCD distance of 50.000mm, and a strategy to achieve a resolution of 0.7Å. The runs were collected by omega scans of 1.0° width, and at detector position of 28.624, -30.187° in 2θ. The intensity

data were corrected for absorption with an analytical correction (4). Final cell constants were calculated from 7655 stronger reflections from the actual data collection after integration. See Table S1-1 through Table S1-6 for crystal and refinement information.

Structure solution and refinement

The crystal is monoclinic, C-centered, and the space group C2/c was determined from the cell geometry, reflections statistics, systematic absences, and successful solution and refinement. The structure was also solved in space group Cc, but the complex showed chemically unreasonable distortions, and it was clear that Cc was incorrect (Cc and C2/c cannot be told apart from systematic absences). The structure was solved by using direct methods in SHELXS-86(2b), and all non-H atoms were found in the E-map. Refinements were done using SHELXL-97(2a). All non-H atoms were refined and with anisotropic vibrational factors. H-atoms were observable in difference electron density maps, and placed in idealize positions; all were refined as riding atoms with relative isotropic displacement parameters of 120% of the U(eq) of the attached atom. One of the butyl side chains is disordered over two alternate conformations; the major conformer has occupancy 0.640(9). The final full-matrix least-squares refinement converged to R_1 = 0.0208 (2983 reflections, F^2, I > 2σ(I)); R_1 = 0.0290 and wR_2 =.0383 for all 3663 data, 129 parameters, 0 restraints, goodness-of-fit (S) 0.999, and no extinction.

Structure description

A half-molecule comprises the asymmetric unit, and complexes lie on the two-fold axis with the C-Pt-Cl exactly on the two-fold axis. The molecule has C_2 symmetry, and therefore can be limitingly close-packed in space group C_2/c. Pt-C(1) is 2.024(3)Å, Pt-C(7) is 1.929(3)Å, while Pt-Cl is 2.4052(9)Å. All other bond distances and angles are in normal ranges. There are no exceptional close contacts between molecules.

2-(1,3-Bis(butyl-imidazol-2-ylidene)phenylene)(carbonyl)trifluoromethyl sulfonate platinum (II), (7)

Data collection

The specimens were loose crystals, light yellow color, plates and arrowheads (some with

acute reentrant angles); twining was suspected. The specimens were examined, two plates and one arrowhead. The data were twinned in all cases, In the best treatment, a small arrowhead specimen (0.04 x 0.06 x 0.32 mm) was retrieved from the sample. The crystal was mounted atop a fine glass fibre, which was fixed to a stout glass fibre, and mounted on a pin; the pin was placed on a goniometer head. The crystallographic properties and data were collected using MoK radiation and the charge-coupled area detector (CCD) detector on an Oxford Diffraction Systems Gemini S diffractometer at 299(2)K (1). A preliminary set of cell constants was calculated from reflections observed on three sets of 5 frames which were oriented approximately in mutually orthogonal directions of reciprocal space. Data collection was carried out using MoK α radiation (graphite monochromator) with 5 runs consisting of 478 frames with a frame time of 60.0sec and a crystal-to-CCD distance of 50.000mm. The runs were collected by omega scans of 1.0 degree width, and at detector position of 28.468, -30.031 degrees in 2 . The intensity data were corrected for absorption with an analytical correction (4). Final cell constants were calculated from 2600 stronger reflections reflections from the actual data collection after integration. See Table 1 for crystal and refinement information.

Structure solution and refinement

The crystal displays a pseudo C-centered monoclinic cell with dimensions 63.2, 8.05, 32.51Å, β = 112.0deg., but the crystal is twinned, and on separation into the two twin components (and the specimen has only two), the cell is triclinic, as determined from lack of systematic absences, reflections statistics, and successful solution and refinement. The structure was solved using by direct methods in SHELXS-86(2b), and all non-H atoms were found in the E-map. Refinements were done using SHELXL-97(2a). All non-H atoms were refined and with anisotropic vibrational factors. H-atoms were observable in difference electron density maps, and placed in idealize positions; all were refined as riding atoms with relative isotropic displacement parameters of 120% of the U(eq) of the attached atom. Butyl side chains are ordered. The two twin components converge on the same model, but the stronger diffracting one (56% vs 44%) of the two data sets finishes with slightly better agreement factors. It is for the stronger twin component that this report concerns. The final full-matrix least-squares refinement converged to R1 = 0.0647 (3129

reflections, F2, I > 2 (I)); R1 = 0.1361 and wR2 = 0.1016 for all 5616 data, 316 parameters, 0 restraints, goodness-of-fit (S) 0.990, and no extinction.

Structure description

Ion pairs comprise the asymmetric unit. The rings are nearly planar, and the Pt is approximately square planar in its coordination geometry. In the coordinate CO, the C-O distance is 1.130(14)Å; the Pt-C distance to the carbonyl is 1.902(16) Å. The three other Pt-C macrocycle distances are 2.048, 2.038 1.963Å (esd's about 0.010Å). The triflate anions are ordered, and show staggered geometry. The C-F distances are 1.292(14), 1.328(16), and 1.291(14)Å, and the S-O distances are 1.413(7), 1.405(8), 1.415(6)Å , and C-S is 1.768(14)Å. Bond length and angle esd's are larger than ordinarily found due to the twinning, the smallness of the crystal, and the temperature of the study.

Other Information

Data collection and structure solution were conducted at the University of Portland Diffraction Facility, 112A Swindells Hall, Department of Chemistry, University of Portland, Portland, OR, 97203. All calculations were performed using Pentium computers using the current SHELX suite of programs.

Relevant References

1. CrysalisPro (2007), Version 171.32.5, Oxford Diffraction Ltd., Abingdon, Oxfordshire, OX14 4RX, United Kingdom.

2a. SHELX97 [Includes SHELXS97, SHELXL97, CIFTAB] - Programs for Crystal Structure Analysis (Release 97-2). G. M. Sheldrick, Institüt für Anorganische Chemie der Universität, Tammanstrasse 4, D-3400 Göttingen, Germany, 1998.

2b. SHELXS86 - G. M. Sheldrick, In "Crystallographic Computing 3", Ed. G. M. Sheldrick, C. Kruger and R. Goddard, Oxford University Press. pp. 175-189, 1985.

SHELXS86 - Program for Crystal Structure solution. G. M. Sheldrick, Institüt für Anorganische Chemie der Universität, Tammanstrasse 4, D-3400 Göttingen, Germany, 1986

3. ORTEP3 for Windows - L. J. Farrugia, J. Appl. Crystallogr. 1997, 30, 565.

4. ABSORPTION CORRECTION (ANALYTICAL) - C. Katayama, Acta Crystallogr., Sect A 1986, 42, 19-23.

5. Wingx L.J. Farrugia, J. Appl. Cryst., 1999, 32, 837-838.

6. PLATON/PLUTON - (a) A. L. Spek, Acta Crystallogr., Sect A 1990, 46, C34. (b) PLATON, A Multipurpose Crystallographic Tool, Utrecht University, Utrecht, The Netherlands, A. L. Spek, 1998.

Relevant Equations used in this report:

$$R_{int} = \Sigma \left| F_o^2 - < F_o^2 > \right| / \Sigma \left| F_o^2 \right|$$

$$R_1 = \Sigma \left| \left| F_o \right| - \left| F_c \right| \right| / \Sigma \left| F_o \right|$$

$$wR2 = [\Sigma[w(F_o^2 - F_c^2)^2] / \Sigma [w(F_o^2)^2]]^{1/2}$$

$$\text{where } w = q / [\sigma^2 (F_o^2) + (a*P)^2 + b*P + d + e*\sin(\theta)]$$

$$\text{GooF} = S = [\Sigma[w(F_o^2 - F_c^2)^2] / (n-p)]^{1/2}$$

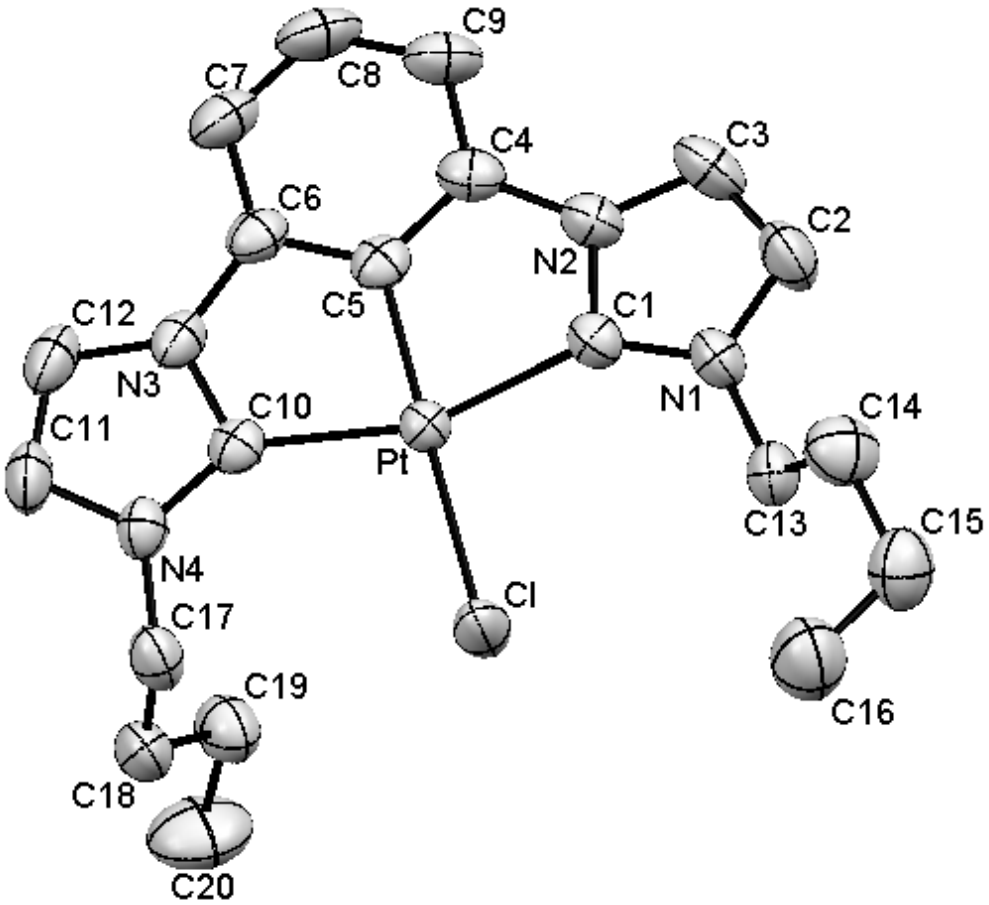

Figure A1. CCC^{Bu}-NHC-Pt-Cl **1**

Table A1-1. Crystal data and structure refinement for **1.**

Empirical formula	C_{20} H_{25} Cl N_4 Pt
Formula weight	551.98
Temperature	293(2) K
Wavelength	0.71073 A
Crystal system, space group	Orthorhombic, P 2_1 2_1 2_1
Unit cell dimensions	a = 10.51850(10) A alpha = 90 º b = 11.14600(10) A beta = 90 º c = 16.7776(2) A gamma = 90 º
Volume	1966.99(3) A^3
Z, Calculated density	4, 1.864 Mg/m^3
Absorption coefficient	7.281 mm^{-1}
F(000)	1072
Crystal size	0.2 x 0.2 x 0.2 mm
Theta range for data collection	3.60 to 30.57 deg.
Limiting indices	$-12\leq h \leq 15$, $-15\leq k \leq 14$, $-24\leq l \leq 23$
Reflections collected / unique	12969 / 5896 [R(int) = 0.0185]
Completeness to theta = 30.57	99.6 %
Absorption correction	Analytical
Max. and min. transmission	0.347 and 0.178
Refinement method	Full-matrix least-squares on F^2
Data / restraints / parameters	5896 / 0 / 255
Goodness-of-fit on F^2	1.003
Final R indices [I>2sigma(I)]	R_1 = 0.0169, wR_2 = 0.0317
R indices (all data)	R_1 = 0.0200, wR_2 = 0.0319
Absolute structure parameter	-0.005(5)
Extinction coefficient	0.00746(13)
Largest diff. peak and hole	0.474 and -0.544 $e.A^{-3}$

Table A1-2. Atomic coordinates (x 10^4) and equivalent isotropic displacement parameters (A^2 x 10^3) for **1.** U(eq) is defined as one third of the trace of the orthogonalized Uij tensor.

Atom	x	y	z	U(eq)
N(1)	5956(2)	6459(2)	8848(1)	42(1)
C(2)	6368(2)	7046(2)	8197(2)	36(1)
N(3)	5664(2)	6552(2)	7592(1)	43(1)
C(4)	4835(3)	5695(3)	7869(2)	57(1)
C(5)	5016(3)	5647(3)	8662(2)	59(1)
C(6)	5892(3)	7016(3)	6812(2)	44(1)
C(7)	6816(2)	7878(2)	6832(2)	38(1)
C(8)	7167(2)	8443(2)	6132(1)	42(1)

C(9)	6597(3)	8134(3)	5405(2)	55(1)
C(10)	5675(3)	7260(3)	5417(2)	63(1)
C(11)	5292(3)	6685(3)	6108(2)	57(1)
N(12)	8093(2)	9340(2)	6279(1)	41(1)
C(13)	8460(2)	9494(2)	7065(2)	36(1)
N(14)	9309(2)	10391(2)	7032(1)	39(1)
C(15)	9468(3)	10802(3)	6259(2)	51(1)
C(16)	8697(3)	10150(3)	5789(2)	52(1)
C(17)	6399(3)	6660(3)	9668(2)	47(1)
C(18)	6958(3)	5539(3)	10040(2)	63(1)
C(19)	7395(4)	5736(3)	10891(2)	67(1)
C(20)	8562(4)	6474(4)	10949(2)	83(1)
C(21)	9932(3)	10928(3)	7719(2)	46(1)
C(22)	9382(6)	12166(6)	7918(4)	52(2)
C(23)	7995(5)	12201(5)	8036(3)	58(2)
C(24)	7620(5)	13530(3)	8229(3)	97(1)
C(22A)	9086(11)	11756(11)	8162(6)	49(3)
C(23A)	8554(8)	12744(8)	7663(5)	44(3)
Pt	7577(1)	8358(1)	7836(1)	31(1)
Cl	8497(1)	8951(1)	9085(1)	53(1)

Table A1-3. Bond lengths [Å] and angles [º] for **1.**

N(1)-C(2)	1.344(3)	N(14)-C(21)	1.454(4)
N(1)-C(5)	1.377(4)	C(15)-C(16)	1.344(4)
N(1)-C(17)	1.469(3)	C(15)-H(15A)	0.9300
C(2)-N(3)	1.371(3)	C(16)-H(16A)	0.9300
C(2)-Pt	2.030(3)	C(17)-C(18)	1.516(4)
N(3)-C(4)	1.374(4)	C(17)-H(17A)	0.9700
N(3)-C(6)	1.428(4)	C(17)-H(17B)	0.9700
C(4)-C(5)	1.345(5)	C(18)-C(19)	1.517(5)
C(4)-H(4A)	0.9300	C(18)-H(18A)	0.9700
C(5)-H(5A)	0.9300	C(18)-H(18B)	0.9700
C(6)-C(7)	1.367(4)	C(19)-C(20)	1.481(5)
C(6)-C(11)	1.390(4)	C(19)-H(19A)	0.9700
C(7)-C(8)	1.383(4)	C(19)-H(19B)	0.9700
C(7)-Pt	1.941(3)	C(20)-H(20A)	0.9600
C(8)-C(9)	1.401(4)	C(20)-H(20B)	0.9600
C(8)-N(12)	1.418(3)	C(20)-H(20C)	0.9600
C(9)-C(10)	1.374(5)	C(21)-C(22A)	1.482(11)
C(9)-H(9A)	0.9300	C(21)-C(22)	1.533(7)
C(10)-C(11)	1.384(5)	C(21)-H(21A)	0.9700
C(10)-H(10A)	0.9300	C(21)-H(21B)	0.9700
C(11)-H(11A)	0.9300	C(21)-H(21C)	0.9700
N(12)-C(16)	1.377(4)	C(21)-H(21D)	0.9700
N(12)-C(13)	1.384(3)	C(22)-C(23)	1.473(9)
C(13)-N(14)	1.342(3)	C(22)-H(22A)	0.9700
C(13)-Pt	2.035(3)	C(22)-H(22B)	0.9700
N(14)-C(15)	1.387(4)	C(23)-C(24)	1.567(6)

C(23)-H(23A)	0.9700	C(16)-N(12)-C(8)	132.5(2)
C(23)-H(23B)	0.9700	C(13)-N(12)-C(8)	116.4(2)
C(23)-H(24F)	1.5765	N(14)-C(13)-N(12)	103.9(2)
C(24)-C(23A)	1.623(9)	N(14)-C(13)-Pt	142.5(2)
C(24)-H(24A)	0.9600	N(12)-C(13)-Pt	113.70(18)
C(24)-H(24B)	0.9600	C(13)-N(14)-C(15)	111.3(2)
C(24)-H(24C)	0.9600	C(13)-N(14)-C(21)	125.1(2)
C(24)-H(24D)	0.9600	C(15)-N(14)-C(21)	123.4(2)
C(24)-H(24E)	0.9600	C(16)-C(15)-N(14)	107.3(3)
C(24)-H(24F)	0.9600	C(16)-C(15)-H(15A)	126.3
C(22A)-C(23A)	1.492(15)	N(14)-C(15)-H(15A)	126.3
C(22A)-H(22A)	0.9700	C(15)-C(16)-N(12)	106.4(3)
C(22A)-H(22B)	0.9700	C(15)-C(16)-H(16A)	126.8
C(23A)-H(23A)	0.9700	N(12)-C(16)-H(16A)	126.8
C(23A)-H(23B)	0.9700	N(1)-C(17)-C(18)	112.5(3)
Pt-Cl	2.3997(7)	N(1)-C(17)-H(17A)	109.1
		C(18)-C(17)-H(17A)	109.1
C(2)-N(1)-C(5)	111.5(2)	N(1)-C(17)-H(17B)	109.1
C(2)-N(1)-C(17)	125.8(2)	C(18)-C(17)-H(17B)	109.1
C(5)-N(1)-C(17)	122.7(2)	H(17A)-C(17)-H(17B)	107.8
N(1)-C(2)-N(3)	103.4(2)	C(17)-C(18)-C(19)	112.7(3)
N(1)-C(2)-Pt	142.57(19)	C(17)-C(18)-H(18A)	109.1
N(3)-C(2)-Pt	114.00(19)	C(19)-C(18)-H(18A)	109.1
C(2)-N(3)-C(4)	111.8(3)	C(17)-C(18)-H(18B)	109.1
C(2)-N(3)-C(6)	116.3(2)	C(19)-C(18)-H(18B)	109.1
C(4)-N(3)-C(6)	131.9(3)	H(18A)-C(18)-H(18B)	107.8
C(5)-C(4)-N(3)	105.8(3)	C(20)-C(19)-C(18)	113.1(3)
C(5)-C(4)-H(4A)	127.1	C(20)-C(19)-H(19A)	109.0
N(3)-C(4)-H(4A)	127.1	C(18)-C(19)-H(19A)	109.0
C(4)-C(5)-N(1)	107.5(3)	C(20)-C(19)-H(19B)	109.0
C(4)-C(5)-H(5A)	126.3	C(18)-C(19)-H(19B)	109.0
N(1)-C(5)-H(5A)	126.3	H(19A)-C(19)-H(19B)	107.8
C(7)-C(6)-C(11)	122.0(3)	C(19)-C(20)-H(20A)	109.5
C(7)-C(6)-N(3)	110.6(2)	C(19)-C(20)-H(20B)	109.5
C(11)-C(6)-N(3)	127.4(3)	H(20A)-C(20)-H(20B)	109.5
C(6)-C(7)-C(8)	119.3(2)	C(19)-C(20)-H(20C)	109.5
C(6)-C(7)-Pt	120.5(2)	H(20A)-C(20)-H(20C)	109.5
C(8)-C(7)-Pt	120.2(2)	H(20B)-C(20)-H(20C)	109.5
C(7)-C(8)-C(9)	120.9(3)	N(14)-C(21)-C(22A)	112.5(5)
C(7)-C(8)-N(12)	110.8(2)	N(14)-C(21)-C(22)	111.9(3)
C(9)-C(8)-N(12)	128.3(2)	C(22A)-C(21)-C(22)	26.3(3)
C(10)-C(9)-C(8)	117.6(3)	N(14)-C(21)-H(21A)	109.2
C(10)-C(9)-H(9A)	121.2	C(22A)-C(21)-H(21A)	128.8
C(8)-C(9)-H(9A)	121.2	C(22)-C(21)-H(21A)	109.2
C(9)-C(10)-C(11)	123.0(3)	N(14)-C(21)-H(21B)	109.2
C(9)-C(10)-H(10A)	118.5	C(22A)-C(21)-H(21B)	85.0
C(11)-C(10)-H(10A)	118.5	C(22)-C(21)-H(21B)	109.2
C(10)-C(11)-C(6)	117.2(3)	H(21A)-C(21)-H(21B)	107.9
C(10)-C(11)-H(11A)	121.4	N(14)-C(21)-H(21C)	108.8
C(6)-C(11)-H(11A)	121.4	C(22A)-C(21)-H(21C)	108.2
C(16)-N(12)-C(13)	111.1(2)	C(22)-C(21)-H(21C)	84.3

H(21A)-C(21)-H(21C)	28.1	C(23A)-C(24)-H(24D)	109.5
H(21B)-C(21)-H(21C)	130.4	H(24A)-C(24)-H(24D)	69.0
N(14)-C(21)-H(21D)	109.4	H(24B)-C(24)-H(24D)	42.0
C(22A)-C(21)-H(21D)	110.0	H(24C)-C(24)-H(24D)	113.4
C(22)-C(21)-H(21D)	129.9	C(23)-C(24)-H(24E)	111.9
H(21A)-C(21)-H(21D)	81.8	C(23A)-C(24)-H(24E)	109.7
H(21B)-C(21)-H(21D)	28.2	H(24A)-C(24)-H(24E)	112.7
H(21C)-C(21)-H(21D)	107.9	H(24B)-C(24)-H(24E)	103.6
C(23)-C(22)-C(21)	115.3(5)	H(24C)-C(24)-H(24E)	5.9
C(23)-C(22)-H(22A)	108.5	H(24D)-C(24)-H(24E)	109.5
C(21)-C(22)-H(22A)	108.5	C(23)-C(24)-H(24F)	72.8
C(23)-C(22)-H(22B)	108.5	C(23A)-C(24)-H(24F)	109.2
C(21)-C(22)-H(22B)	108.5	H(24A)-C(24)-H(24F)	42.2
H(22A)-C(22)-H(22B)	107.5	H(24B)-C(24)-H(24F)	143.2
C(22)-C(23)-C(24)	107.6(5)	H(24C)-C(24)-H(24F)	103.7
C(22)-C(23)-H(23A)	110.2	H(24D)-C(24)-H(24F)	109.5
C(24)-C(23)-H(23A)	110.2	H(24E)-C(24)-H(24F)	109.5
C(22)-C(23)-H(23B)	110.2	C(21)-C(22A)-C(23A)	113.8(8)
C(24)-C(23)-H(23B)	110.2	C(21)-C(22A)-H(22A)	108.8
H(23A)-C(23)-H(23B)	108.5	C(23A)-C(22A)-H(22A)	108.8
C(22)-C(23)-H(24F)	139.8	C(21)-C(22A)-H(22B)	108.8
C(24)-C(23)-H(24F)	35.6	C(23A)-C(22A)-H(22B)	108.8
H(23A)-C(23)-H(24F)	81.8	H(22A)-C(22A)-H(22B)	107.7
H(23B)-C(23)-H(24F)	101.1	C(22A)-C(23A)-C(24)	107.3(7)
C(23)-C(24)-C(23A)	38.4(3)	C(22A)-C(23A)-H(23A)	110.3
C(23)-C(24)-H(24A)	109.5	C(24)-C(23A)-H(23A)	110.3
C(23A)-C(24)-H(24A)	135.2	C(22A)-C(23A)-H(23B)	110.3
C(23)-C(24)-H(24B)	109.5	C(24)-C(23A)-H(23B)	110.3
C(23A)-C(24)-H(24B)	73.2	H(23A)-C(23A)-H(23B)	108.5
H(24A)-C(24)-H(24B)	109.5	C(7)-Pt-C(2)	78.58(11)
C(23)-C(24)-H(24C)	109.5	C(7)-Pt-C(13)	78.87(11)
C(23A)-C(24)-H(24C)	111.4	C(2)-Pt-C(13)	157.44(11)
H(24A)-C(24)-H(24C)	109.5	C(7)-Pt-Cl	179.40(8)
H(24B)-C(24)-H(24C)	109.5	C(2)-Pt-Cl	101.01(8)
C(23)-C(24)-H(24D)	134.7	C(13)-Pt-Cl	101.53(7)

Table A1-4. Anisotropic displacement parameters ($A^2 \times 10^3$) for **1**
The anisotropic displacement factor exponent takes the form:
$-2\pi^2 [h^2 a^{*2} U11 + ... + 2 h k a^* b^* U12]$

Atom	U11	U22	U33	U23	U13	U12
N(1)	40(1)	36(1)	50(1)	3(1)	1(1)	-8(1)
C(2)	34(1)	35(1)	41(1)	0(1)	-1(1)	0(1)
N(3)	42(1)	39(1)	47(1)	-4(1)	-5(1)	-5(1)
C(4)	49(2)	43(2)	79(2)	-3(2)	-9(2)	-16(1)
C(5)	53(2)	55(2)	67(2)	9(2)	1(2)	-23(2)
C(6)	45(1)	39(2)	48(2)	-8(1)	-5(1)	3(1)

C(7)	40(1)	34(1)	39(1)	-4(1)	3(1)	9(1)
C(8)	51(1)	38(1)	36(1)	-5(1)	1(1)	8(1)
C(9)	72(2)	59(2)	33(1)	-7(1)	-1(1)	8(2)
C(10)	81(2)	68(2)	42(2)	-17(2)	-18(2)	7(2)
C(11)	63(2)	55(2)	53(2)	-15(2)	-15(1)	-2(2)
N(12)	54(1)	36(1)	32(1)	2(1)	6(1)	8(1)
C(13)	36(1)	35(1)	37(1)	-1(1)	3(1)	7(1)
N(14)	41(1)	37(1)	39(1)	7(1)	4(1)	2(1)
C(15)	59(2)	47(2)	46(2)	13(2)	17(2)	-3(2)
C(16)	69(2)	51(2)	35(1)	9(1)	14(1)	8(2)
C(17)	52(1)	45(2)	43(1)	6(2)	6(1)	-9(2)
C(18)	71(2)	52(2)	67(2)	1(2)	-6(2)	3(2)
C(19)	68(2)	70(2)	62(2)	16(2)	2(2)	0(2)
C(20)	77(2)	96(3)	76(3)	8(3)	-1(2)	-15(2)
C(21)	40(1)	48(2)	49(2)	10(2)	-4(2)	-10(1)
C(22)	56(3)	54(4)	47(3)	-2(3)	4(3)	-18(3)
C(23)	52(3)	55(3)	67(3)	-6(3)	11(2)	-7(2)
C(24)	121(3)	76(2)	95(3)	-31(2)	-3(3)	25(3)
C(22A)	70(7)	50(6)	28(4)	4(4)	7(4)	-23(5)
C(23A)	44(5)	41(5)	45(5)	-3(4)	-2(4)	1(4)
Pt	31(1)	30(1)	32(1)	1(1)	0(1)	2(1)
Cl	62(1)	60(1)	36(1)	7(1)	-10(1)	-24(1)

Table A1-5. Hydrogen coordinates (x 10^4) and isotropic displacement parameters (A^2 x 10^3) for **1.**

Atom	x	y	z	U(eq)
H(4A)	4266	5243	7570	68
H(5A)	4585	5155	9019	70
H(9A)	6834	8506	4932	66
H(10A)	5291	7045	4939	76
H(11A)	4660	6102	6101	68
H(15A)	10009	11414	6095	61
H(16A)	8591	10231	5241	62
H(17A)	5690	6933	9991	56
H(17B)	7037	7288	9667	56
H(18A)	7676	5274	9722	76
H(18B)	6325	4906	10032	76
H(19A)	6719	6128	11187	80
H(19B)	7551	4963	11139	80
H(20A)	8784	6580	11499	99
H(20B)	8414	7242	10709	99
H(20C)	9245	6076	10676	99
H(21A)	10834	11006	7610	55
H(21B)	9833	10404	8176	55
H(21C)	10664	11381	7536	55
H(21D)	10235	10299	8070	55

H(22A)	9789	12458	8399	63
H(22B)	9600	12714	7490	63
H(23A)	7753	11679	8472	70
H(23B)	7562	11932	7557	70
H(24A)	6718	13582	8305	116
H(24B)	7868	14039	7794	116
H(24C)	8047	13784	8706	116
H(24D)	7268	14182	7927	116
H(24E)	8092	13843	8672	116
H(24F)	6946	13028	8421	116
H(22A)	9559	12104	8601	59
H(22B)	8388	11298	8386	59
H(23A)	8083	12415	7216	52
H(23B)	9235	13242	7456	52

Table A1-6. Torsion angles [°] for **1.**

C(5)-N(1)-C(2)-N(3)	-1.1(3)	C(9)-C(8)-N(12)-C(16)	0.1(5)
C(17)-N(1)-C(2)-N(3)	-179.2(3)	C(7)-C(8)-N(12)-C(13)	-0.5(3)
C(5)-N(1)-C(2)-Pt	177.2(3)	C(9)-C(8)-N(12)-C(13)	177.4(3)
C(17)-N(1)-C(2)-Pt	-0.9(5)	C(16)-N(12)-C(13)-N(14)	-1.2(3)
N(1)-C(2)-N(3)-C(4)	0.7(3)	C(8)-N(12)-C(13)-N(14)	-179.0(2)
Pt-C(2)-N(3)-C(4)	-178.2(2)	C(16)-N(12)-C(13)-Pt	178.54(18)
N(1)-C(2)-N(3)-C(6)	179.5(2)	C(8)-N(12)-C(13)-Pt	0.7(3)
Pt-C(2)-N(3)-C(6)	0.6(3)	N(12)-C(13)-N(14)-C(15)	0.6(3)
C(2)-N(3)-C(4)-C(5)	0.0(4)	Pt-C(13)-N(14)-C(15)	-179.0(2)
C(6)-N(3)-C(4)-C(5)	-178.6(3)	N(12)-C(13)-N(14)-C(21)	176.9(2)
N(3)-C(4)-C(5)-N(1)	-0.7(4)	Pt-C(13)-N(14)-C(21)	-2.6(4)
C(2)-N(1)-C(5)-C(4)	1.2(4)	C(13)-N(14)-C(15)-C(16)	0.2(3)
C(17)-N(1)-C(5)-C(4)	179.4(3)	C(21)-N(14)-C(15)-C(16)	-176.2(3)
C(2)-N(3)-C(6)-C(7)	1.0(3)	N(14)-C(15)-C(16)-N(12)	-0.9(3)
C(4)-N(3)-C(6)-C(7)	179.5(3)	C(13)-N(12)-C(16)-C(15)	1.3(3)
C(2)-N(3)-C(6)-C(11)	-178.8(3)	C(8)-N(12)-C(16)-C(15)	178.8(3)
C(4)-N(3)-C(6)-C(11)	-0.2(5)	C(2)-N(1)-C(17)-C(18)	-121.1(3)
C(11)-C(6)-C(7)-C(8)	0.2(4)	C(5)-N(1)-C(17)-C(18)	61.0(4)
N(3)-C(6)-C(7)-C(8)	-179.6(2)	N(1)-C(17)-C(18)-C(19)	-179.0(2)
C(11)-C(6)-C(7)-Pt	177.4(2)	C(17)-C(18)-C(19)-C(20)	-72.1(4)
N(3)-C(6)-C(7)-Pt	-2.3(3)	C(13)-N(14)-C(21)-C(22A)	-76.5(6)
C(6)-C(7)-C(8)-C(9)	-0.7(4)	C(15)-N(14)-C(21)-C(22A)	99.4(6)
Pt-C(7)-C(8)-C(9)	-178.0(2)	C(13)-N(14)-C(21)-C(22)	-105.0(4)
C(6)-C(7)-C(8)-N(12)	177.4(2)	C(15)-N(14)-C(21)-C(22)	70.9(4)
Pt-C(7)-C(8)-N(12)	0.1(3)	N(14)-C(21)-C(22)-C(23)	54.4(7)
C(7)-C(8)-C(9)-C(10)	0.5(4)	C(22A)-C(21)-C(22)-C(23)	-42.4(10)
N(12)-C(8)-C(9)-C(10)	-177.2(3)	C(21)-C(22)-C(23)-C(24)	-179.8(4)
C(8)-C(9)-C(10)-C(11)	0.2(5)	C(22)-C(23)-C(24)-C(23A)	39.7(6)
C(9)-C(10)-C(11)-C(6)	-0.6(5)	N(14)-C(21)-C(22A)-C(23A)	-56.7(10)
C(7)-C(6)-C(11)-C(10)	0.5(4)		
N(3)-C(6)-C(11)-C(10)	-179.8(3)	C(22)-C(21)-C(22A)-C(23A)	37.5(9)
C(7)-C(8)-N(12)-C(16)	-177.8(3)		

C(21)-C(22A)-C(23A)-C(24)	178.1(6)	N(3)-C(2)-Pt-C(7)	-1.40(18)
		N(1)-C(2)-Pt-C(13)	-177.6(3)
C(23)-C(24)-C(23A)-C(22A)	-41.7(7)	N(3)-C(2)-Pt-C(13)	0.7(4)
		N(1)-C(2)-Pt-Cl	-0.1(3)
C(6)-C(7)-Pt-C(2)	2.1(2)	N(3)-C(2)-Pt-Cl	178.16(17)
C(8)-C(7)-Pt-C(2)	179.4(2)	N(14)-C(13)-Pt-C(7)	179.1(3)
C(6)-C(7)-Pt-C(13)	-177.1(2)	N(12)-C(13)-Pt-C(7)	-0.44(17)
C(8)-C(7)-Pt-C(13)	0.2(2)	N(14)-C(13)-Pt-C(2)	177.0(3)
C(6)-C(7)-Pt-Cl	-45(8)	N(12)-C(13)-Pt-C(2)	-2.5(4)
C(8)-C(7)-Pt-Cl	133(8)	N(14)-C(13)-Pt-Cl	-0.5(3)
N(1)-C(2)-Pt-C(7)	-179.6(3)	N(12)-C(13)-Pt-Cl	-179.99(16)

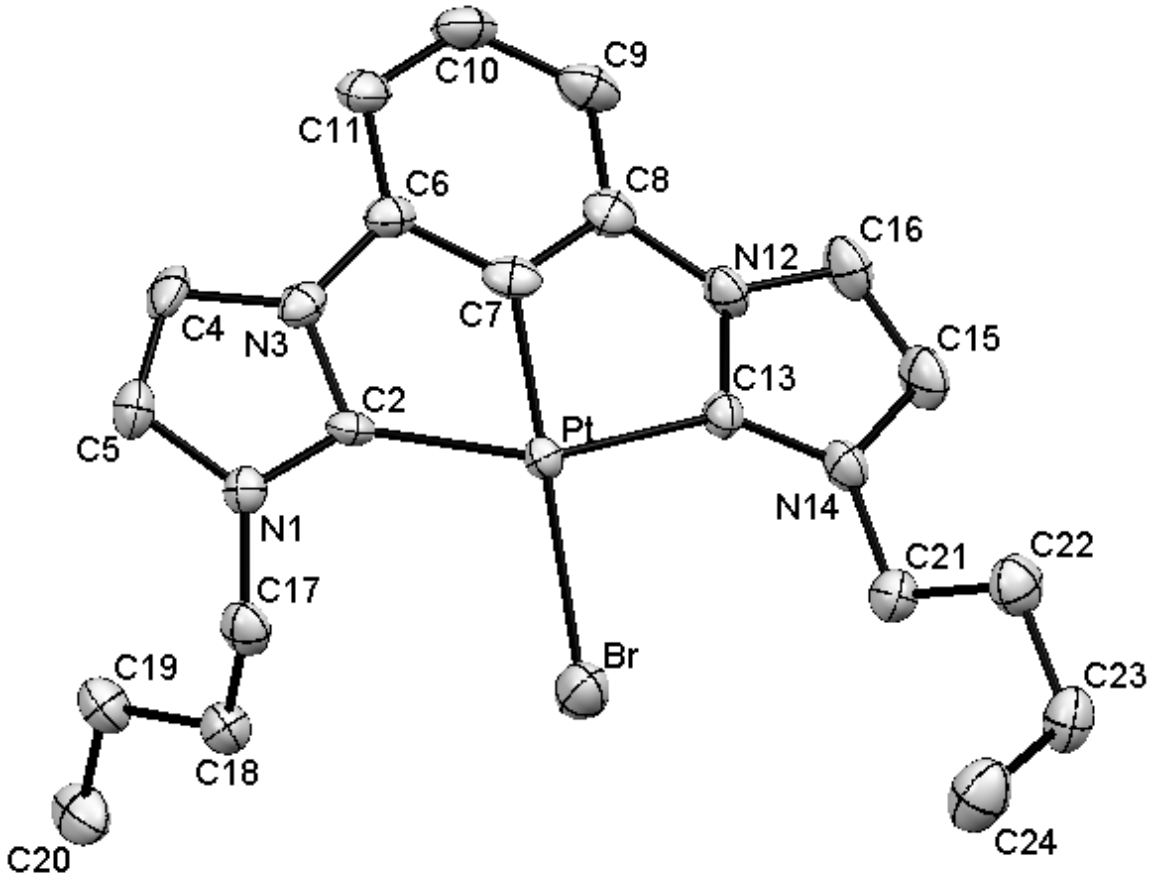

Figure A2. CCC^{Bu}-NHC-Pt-Br **2**

Table A2-1. Crystal data and structure refinement for **2.**

Empirical formula	C_{20} H_{25} Br N_4 Pt
Formula weight	596.43
Temperature	173(2) K
Wavelength	0.71073 A

Crystal system, space group	Orthorhombic, P 2_1 2_1 2_1
Unit cell dimensions	a = 10.31400(10) A alpha = 90 °
	b = 11.1814(2) A beta = 90 °
	c = 16.9083(2) A gamma = 90 °
Volume	1949.95(5) A^3
Z, Calculated density	4, 2.032 Mg/m^3
Absorption coefficient	9.256 mm^{-1}
F(000)	1144
Crystal size	0.35 x 0.30 x 0.07 mm
Theta range for data collection	2.94 to 30.68 °
Limiting indices	-14≤ h ≤14, -16≤ k ≤14, -24≤ l ≤22
Reflections collected / unique	25185 / 5991 [R(int) = 0.0398]
Completeness to theta = 30.68	99.4 %
Absorption correction	Analytical
Max. and min. transmission	0.5635 and 0.1400
Refinement method	Full-matrix least-squares on F^2
Data / restraints / parameters	5991 / 18 / 263
Goodness-of-fit on F^2	1.009
Final R indices [I>2sigma(I)]	R_1 = 0.0299, wR_2 = 0.0639
R indices (all data)	R_1 = 0.0419, wR_2 = 0.0716
Absolute structure parameter	-0.043(12)
Largest diff. peak and hole	1.933 and -1.740 $e.A^{-3}$

Table A2-2. Atomic coordinates (x 10^4) and equivalent isotropic displacement parameters (A^2 x 10^3) for **2.** U(eq) is defined as one third of the trace of the orthogonalized Uij tensor.

Atom	x	y	z	U(eq)
C(2)	3483(6)	4468(5)	7028(3)	21(1)
C(4)	3696(7)	5145(6)	5757(4)	29(1)
C(5)	4465(7)	5815(6)	6231(4)	29(1)
C(6)	2170(5)	3409(6)	6098(3)	24(1)
C(7)	1806(6)	2863(6)	6796(4)	26(1)
C(8)	855(6)	2012(6)	6790(4)	27(1)
C(9)	226(6)	1696(7)	6096(4)	34(1)
C(10)	617(7)	2253(7)	5399(4)	36(2)
C(11)	1588(7)	3120(6)	5389(4)	30(1)
C(13)	1354(6)	2031(5)	8165(4)	22(1)
C(15)	-13(7)	620(7)	8629(5)	36(2)
C(16)	-223(6)	703(6)	7837(5)	36(2)
C(17)	4947(6)	5943(6)	7687(4)	29(1)
C(18)	4078(9)	6824(8)	8107(6)	31(2)
C(19)	3519(8)	7791(7)	7595(5)	32(2)
C(18A)	4390(30)	7230(30)	7810(20)	24(7)
C(19A)	2950(20)	7240(20)	7979(15)	14(7)
C(20A)	2400(40)	8460(40)	8180(30)	24(8)
C(20)	2770(11)	8713(11)	8049(7)	39(3)

C(21)	1437(6)	1608(6)	9621(4)	30(1)
C(22)	1974(7)	470(7)	9976(4)	36(2)
C(23)	2413(8)	640(6)	10815(4)	37(1)
C(24)	3628(8)	1415(8)	10909(5)	49(2)
N(3)	3095(5)	4313(5)	6252(3)	24(1)
N(1)	4318(5)	5399(5)	6997(3)	22(1)
N(12)	617(5)	1564(5)	7562(3)	27(1)
N(14)	954(5)	1439(5)	8815(3)	27(1)
Br	3555(1)	3992(1)	9089(1)	38(1)
Pt	2588(1)	3340(1)	7801(1)	19(1)

Table A2-3. Bond lengths [Å] and angles [º] for **2.**

C(2)-N(1)	1.352(7)	N(3)-C(2)-Pt	113.6(4)
C(2)-N(3)	1.381(7)	C(5)-C(4)-N(3)	105.8(6)
C(2)-Pt	2.037(6)	C(4)-C(5)-N(1)	107.7(6)
C(4)-C(5)	1.354(10)	C(11)-C(6)-C(7)	121.4(6)
C(4)-N(3)	1.397(8)	C(11)-C(6)-N(3)	128.4(6)
C(5)-N(1)	1.386(8)	C(7)-C(6)-N(3)	110.0(5)
C(6)-C(11)	1.379(8)	C(8)-C(7)-C(6)	119.8(6)
C(6)-C(7)	1.381(9)	C(8)-C(7)-Pt	119.6(5)
C(6)-N(3)	1.414(8)	C(6)-C(7)-Pt	120.6(5)
C(7)-C(8)	1.366(9)	C(7)-C(8)-C(9)	121.3(7)
C(7)-Pt	1.955(6)	C(7)-C(8)-N(12)	111.3(6)
C(8)-C(9)	1.387(9)	C(9)-C(8)-N(12)	127.4(6)
C(8)-N(12)	1.419(8)	C(8)-C(9)-C(10)	117.8(6)
C(9)-C(10)	1.393(10)	C(9)-C(10)-C(11)	121.9(6)
C(10)-C(11)	1.394(10)	C(6)-C(11)-C(10)	117.8(6)
C(13)-N(14)	1.346(8)	N(14)-C(13)-N(12)	104.4(5)
C(13)-N(12)	1.375(8)	N(14)-C(13)-Pt	142.4(5)
C(13)-Pt	2.036(6)	N(12)-C(13)-Pt	113.2(4)
C(15)-C(16)	1.360(11)	C(16)-C(15)-N(14)	107.0(6)
C(15)-N(14)	1.389(8)	C(15)-C(16)-N(12)	106.2(6)
C(16)-N(12)	1.377(8)	N(1)-C(17)-C(18)	112.5(6)
C(17)-N(1)	1.466(8)	N(1)-C(17)-C(18A)	109.1(14)
C(17)-C(18)	1.510(11)	C(18)-C(17)-C(18A)	28.1(14)
C(17)-C(18A)	1.57(3)	C(19)-C(18)-C(17)	115.3(8)
C(18)-C(19)	1.501(13)	C(20)-C(19)-C(18)	113.5(8)
C(19)-C(20)	1.499(14)	C(19A)-C(18A)-C(17)	113(2)
C(18A)-C(19A)	1.51(4)	C(20A)-C(19A)-C(18A)	114(3)
C(19A)-C(20A)	1.51(5)	N(14)-C(21)-C(22)	112.7(6)
C(21)-N(14)	1.465(8)	C(23)-C(22)-C(21)	112.3(6)
C(21)-C(22)	1.512(10)	C(22)-C(23)-C(24)	114.6(6)
C(22)-C(23)	1.501(10)	C(2)-N(3)-C(4)	111.0(5)
C(23)-C(24)	1.532(11)	C(2)-N(3)-C(6)	117.3(5)
Br-Pt	2.5028(8)	C(4)-N(3)-C(6)	131.6(5)
		C(2)-N(1)-C(5)	111.3(5)
N(1)-C(2)-N(3)	104.2(5)	C(2)-N(1)-C(17)	124.9(5)
N(1)-C(2)-Pt	142.1(4)	C(5)-N(1)-C(17)	123.8(5)

C(13)-N(12)-C(16)	111.2(6)	C(7)-Pt-C(13)	79.0(3)
C(13)-N(12)-C(8)	116.9(5)	C(7)-Pt-C(2)	78.4(2)
C(16)-N(12)-C(8)	131.8(6)	C(13)-Pt-C(2)	157.3(2)
C(13)-N(14)-C(15)	111.1(6)	C(7)-Pt-Br	178.66(18)
C(13)-N(14)-C(21)	126.2(5)	C(13)-Pt-Br	101.26(17)
C(15)-N(14)-C(21)	122.7(6)	C(2)-Pt-Br	101.41(15)

Table A2-4. Anisotropic displacement parameters (A^2 x 10^3) for **2.**
The anisotropic displacement factor exponent takes the form:
$-2\pi^2$ [h^2 a^{*2} U11 + ... + 2 h k a* b* U12]

Atom	U11	U22	U33	U23	U13	U12
C(2)	25(3)	19(2)	19(3)	-7(2)	-1(2)	0(2)
C(4)	36(3)	33(3)	19(3)	7(3)	11(2)	1(3)
C(5)	31(3)	28(3)	28(3)	9(3)	4(3)	-2(3)
C(6)	27(3)	25(3)	21(2)	-4(2)	-1(2)	4(2)
C(7)	22(3)	28(3)	28(3)	-10(3)	1(2)	5(2)
C(8)	26(3)	25(3)	30(3)	-4(3)	1(2)	3(2)
C(9)	32(3)	34(3)	37(4)	-9(3)	-9(3)	-4(3)
C(10)	43(4)	39(4)	26(3)	-10(3)	-9(3)	0(3)
C(11)	42(3)	25(3)	24(3)	-6(3)	-2(3)	3(3)
C(13)	23(3)	20(3)	23(3)	2(2)	4(2)	-3(2)
C(15)	29(3)	34(4)	44(4)	3(3)	6(3)	-14(3)
C(16)	30(3)	30(3)	47(4)	3(4)	1(4)	-13(3)
C(17)	25(3)	28(3)	34(4)	1(3)	-3(3)	-7(2)
C(18)	37(4)	27(5)	29(4)	0(4)	0(3)	-4(4)
C(19)	34(4)	24(4)	38(5)	-1(3)	0(3)	-1(3)
C(18A)	22(9)	22(10)	26(10)	1(9)	0(8)	-7(8)
C(19A)	12(9)	13(9)	17(10)	-6(7)	-1(6)	3(7)
C(20A)	26(15)	14(12)	31(14)	-3(12)	8(12)	-4(13)
C(20)	34(6)	38(6)	45(6)	-5(5)	15(4)	-7(4)
C(21)	34(3)	29(3)	27(3)	2(3)	2(2)	-3(3)
C(22)	38(4)	31(3)	39(4)	5(3)	-3(3)	3(3)
C(23)	34(3)	39(3)	37(3)	11(3)	2(3)	-3(3)
C(24)	41(4)	63(6)	43(4)	11(4)	-3(3)	-5(4)
N(3)	26(2)	27(3)	20(2)	-1(2)	3(2)	4(2)
N(1)	21(2)	22(2)	23(3)	1(2)	1(2)	0(2)
N(12)	24(2)	23(3)	33(3)	0(2)	-2(2)	-8(2)
N(14)	25(2)	24(3)	31(3)	1(2)	0(2)	-8(2)
Br	41(1)	41(1)	32(1)	3(1)	-3(1)	-11(1)
Pt	19(1)	17(1)	20(1)	0(1)	0(1)	0(1)

Table A2-5. Hydrogen coordinates (x 10^4) and isotropic displacement parameters (A^2 x 10^3) for **2.**

Atom	x	y	z	U(eq)

H(4A)	3587	5223	5201	35
H(5A)	5008	6455	6067	35
H(9A)	-449	1118	6096	41
H(10A)	209	2036	4916	43
H(11A)	1841	3498	4910	36
H(15A)	-445	102	8988	43
H(16A)	-829	255	7534	43
H(17A)	5745	6359	7513	35
H(17B)	5203	5305	8061	35
H(17C)	5896	5978	7603	35
H(17D)	4776	5456	8164	35
H(18A)	3354	6377	8353	37
H(18B)	4579	7204	8539	37
H(19A)	4233	8192	7307	38
H(19B)	2939	7422	7197	38
H(18C)	4847	7616	8260	28
H(18D)	4559	7716	7333	28
H(19C)	2485	6932	7508	17
H(19D)	2768	6689	8423	17
H(20D)	2997	8868	8545	29
H(20E)	1557	8362	8437	29
H(20F)	2306	8930	7698	29
H(20A)	2287	8323	8476	47
H(20B)	2163	9119	7693	47
H(20C)	3372	9300	8274	47
H(21A)	722	1905	9959	36
H(21B)	2126	2224	9616	36
H(22A)	1298	-158	9960	43
H(22B)	2716	192	9653	43
H(23A)	2587	-156	11049	44
H(23B)	1698	1009	11119	44
H(24A)	4362	1026	10646	59
H(24B)	3823	1514	11473	59
H(24C)	3476	2200	10669	59

Table A2-6. Torsion angles [°] for **2.**

N(3)-C(4)-C(5)-N(1)	-0.5(7)	N(12)-C(8)-C(9)-C(10)	179.9(7)
C(11)-C(6)-C(7)-C(8)	0.4(9)	C(8)-C(9)-C(10)-C(11)	-1.3(11)
N(3)-C(6)-C(7)-C(8)	175.8(5)	C(7)-C(6)-C(11)-C(10)	-0.1(9)
C(11)-C(6)-C(7)-Pt	-177.2(5)	N(3)-C(6)-C(11)-C(10)	-174.6(6)
N(3)-C(6)-C(7)-Pt	-1.7(7)	C(9)-C(10)-C(11)-C(6)	0.6(10)
C(6)-C(7)-C(8)-C(9)	-1.2(10)	N(14)-C(15)-C(16)-N(12)	0.1(8)
Pt-C(7)-C(8)-C(9)	176.4(5)	N(1)-C(17)-C(18)-C(19)	-53.9(9)
C(6)-C(7)-C(8)-N(12)	-179.7(6)	C(18A)-C(17)-C(18)-C(19)	35(3)
Pt-C(7)-C(8)-N(12)	-2.1(7)	C(17)-C(18)-C(19)-C(20)	-174.3(8)
C(7)-C(8)-C(9)-C(10)	1.6(10)	N(1)-C(17)-C(18A)-C(19A)	62(3)

C(18)-C(17)-C(18A)-C(19A)	-41(2)
C(17)-C(18A)-C(19A)-C(20A)	174(3)
N(14)-C(21)-C(22)-C(23)	-177.5(6)
C(21)-C(22)-C(23)-C(24)	-69.6(8)
N(1)-C(2)-N(3)-C(4)	0.1(7)
Pt-C(2)-N(3)-C(4)	177.3(4)
N(1)-C(2)-N(3)-C(6)	-178.0(5)
Pt-C(2)-N(3)-C(6)	-0.8(7)
C(5)-C(4)-N(3)-C(2)	0.2(7)
C(5)-C(4)-N(3)-C(6)	178.0(6)
C(11)-C(6)-N(3)-C(2)	176.6(6)
C(7)-C(6)-N(3)-C(2)	1.6(7)
C(11)-C(6)-N(3)-C(4)	-1.1(11)
C(7)-C(6)-N(3)-C(4)	-176.1(6)
N(3)-C(2)-N(1)-C(5)	-0.5(7)
Pt-C(2)-N(1)-C(5)	-176.3(6)
N(3)-C(2)-N(1)-C(17)	176.8(5)
Pt-C(2)-N(1)-C(17)	1.0(10)
C(4)-C(5)-N(1)-C(2)	0.6(7)
C(4)-C(5)-N(1)-C(17)	-176.7(6)
C(18)-C(17)-N(1)-C(2)	-81.5(8)
C(18A)-C(17)-N(1)-C(2)	-111.3(17)
C(18)-C(17)-N(1)-C(5)	95.5(8)
C(18A)-C(17)-N(1)-C(5)	65.7(17)
N(14)-C(13)-N(12)-C(16)	0.2(7)
Pt-C(13)-N(12)-C(16)	-178.6(4)
N(14)-C(13)-N(12)-C(8)	-178.6(5)
Pt-C(13)-N(12)-C(8)	2.5(7)
C(15)-C(16)-N(12)-C(13)	-0.1(8)
C(15)-C(16)-N(12)-C(8)	178.5(7)
C(7)-C(8)-N(12)-C(13)	-0.4(8)
C(9)-C(8)-N(12)-C(13)	-178.9(6)
C(7)-C(8)-N(12)-C(16)	-178.9(7)
C(9)-C(8)-N(12)-C(16)	2.6(12)
N(12)-C(13)-N(14)-C(15)	-0.1(7)
Pt-C(13)-N(14)-C(15)	178.1(6)
N(12)-C(13)-N(14)-C(21)	-179.8(6)
Pt-C(13)-N(14)-C(21)	-1.6(11)
C(16)-C(15)-N(14)-C(13)	0.1(8)
C(16)-C(15)-N(14)-C(21)	179.7(6)
C(22)-C(21)-N(14)-C(13)	-122.2(7)
C(22)-C(21)-N(14)-C(15)	58.1(8)
C(8)-C(7)-Pt-C(13)	2.8(5)
C(6)-C(7)-Pt-C(13)	-179.7(5)
C(8)-C(7)-Pt-C(2)	-176.5(5)
C(6)-C(7)-Pt-C(2)	1.1(5)
C(8)-C(7)-Pt-Br	-97(9)
C(6)-C(7)-Pt-Br	81(9)
N(14)-C(13)-Pt-C(7)	179.1(8)
N(12)-C(13)-Pt-C(7)	-2.8(4)
N(14)-C(13)-Pt-C(2)	-179.0(6)
N(12)-C(13)-Pt-C(2)	-0.9(9)
N(14)-C(13)-Pt-Br	-2.2(8)
N(12)-C(13)-Pt-Br	175.9(4)
N(1)-C(2)-Pt-C(7)	175.5(7)
N(3)-C(2)-Pt-C(7)	-0.1(4)
N(1)-C(2)-Pt-C(13)	173.6(6)
N(3)-C(2)-Pt-C(13)	-2.0(9)
N(1)-C(2)-Pt-Br	-3.2(7)
N(3)-C(2)-Pt-Br	-178.8(4)

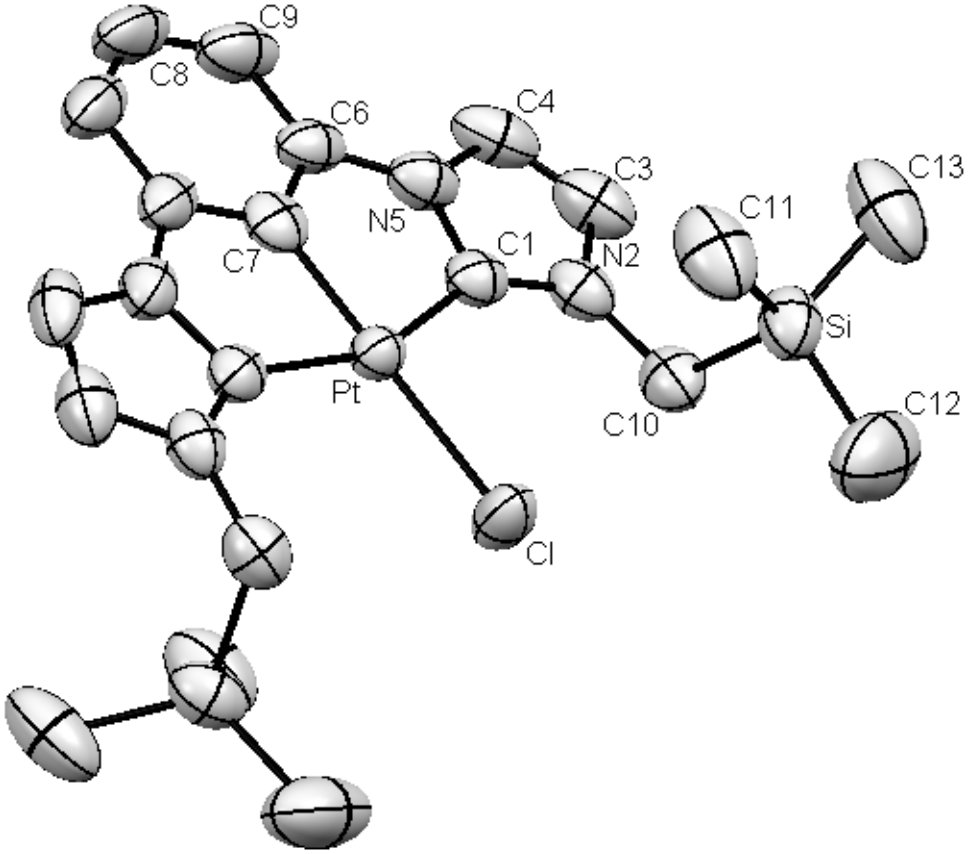

Figure A3. CCC-NHC-Pt-Cl **4**

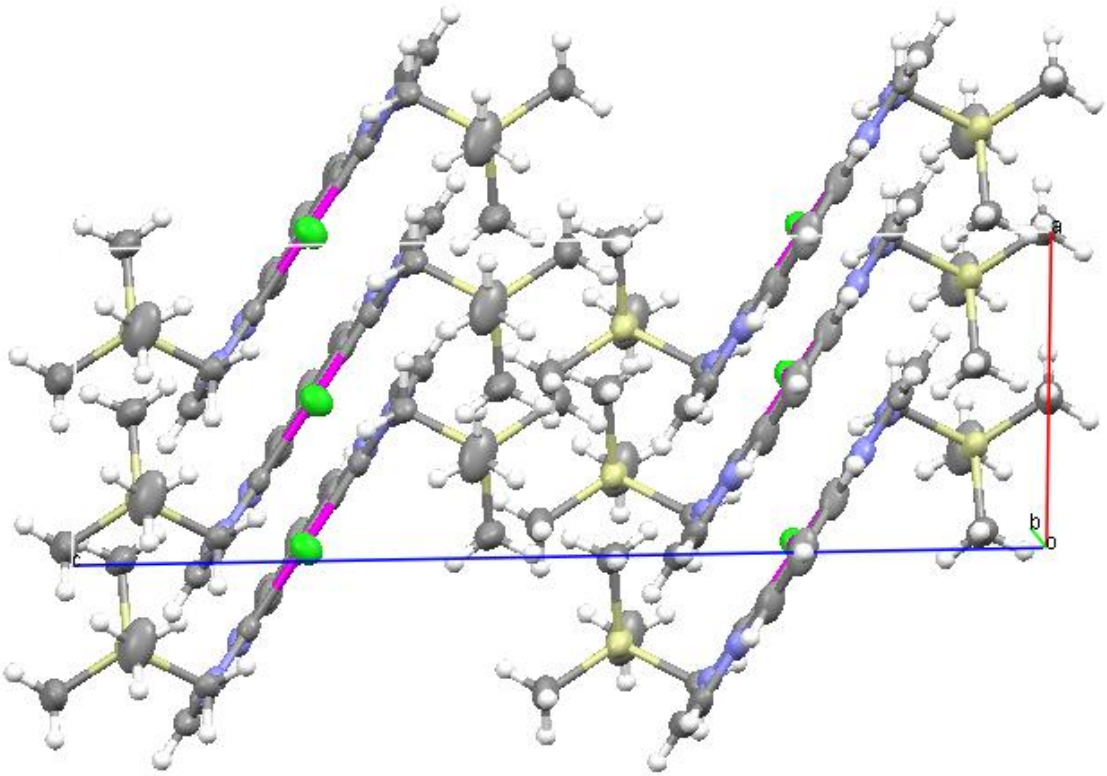

Figure A5. Unit cell of CCC-NHC-Pt-Cl **4**

Table A4-1. Crystal data and structure refinement for **4.**

Empirical formula	C_{20} H_{29} Cl N_4 Pt Si_2
Formula weight	612.19
Temperature	298(2) K
Wavelength	0.71073 Å
Crystal system, space group	Monoclinic, C 1 2/c 1
Unit cell dimensions	a = 6.2984(2) Å alpha = 90 º
	b = 19.4917(6) Å beta = 91.865(3) º
	c = 19.4312(7) Å gamma = 90 º
Volume	2384.24(14) $Å^3$
Z, Calculated density	4, 1.705 Mg/m^3
Absorption coefficient	6.111 mm^{-1}
F(000)	1200
Crystal size	0.69 x 0.11x 0.06 mm
Theta range for data collection	3.40 to 30.60 º
Limiting indices	-9≤ h ≤8, -27≤ k ≤27 -27≤ l ≤27
Reflections collected / unique	13513 / 3663 [R(int) = 0.0264]
Completeness to theta = 30.57	99.7 %
Absorption correction	Analytical
Max. and min. transmission	0.7106 and 0.1015
Refinement method	Full-matrix least-squares on F^2

Data / restraints / parameters	3663 / 0 / 129
Goodness-of-fit on F^2	0.999
Final R indices [I>2sigma(I)]	$R_1 = 0.0208$, $wR_2 = 0.0379$
R indices (all data)	$R_1 = 0.0290$, $wR_2 = 0.0385$
Largest diff. peak and hole	0.701 and -0.492 e.A^{-3}

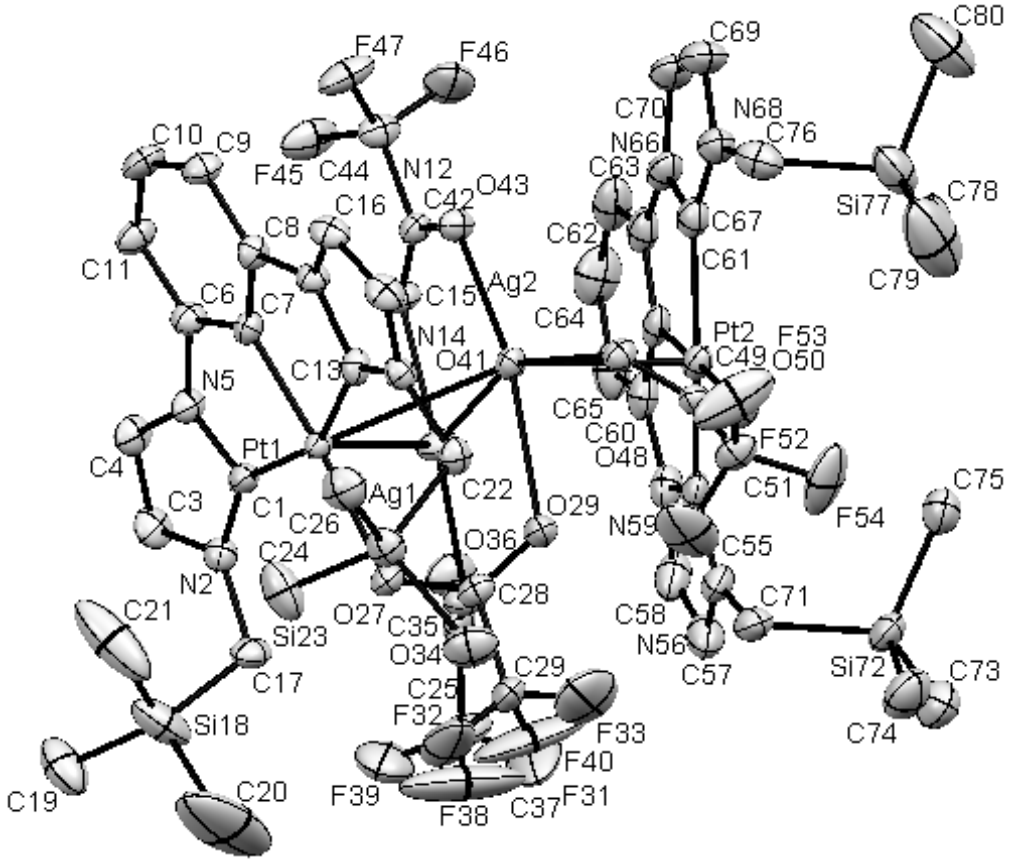

Figure A6. Cluster Pt_2Ag_2 **5**

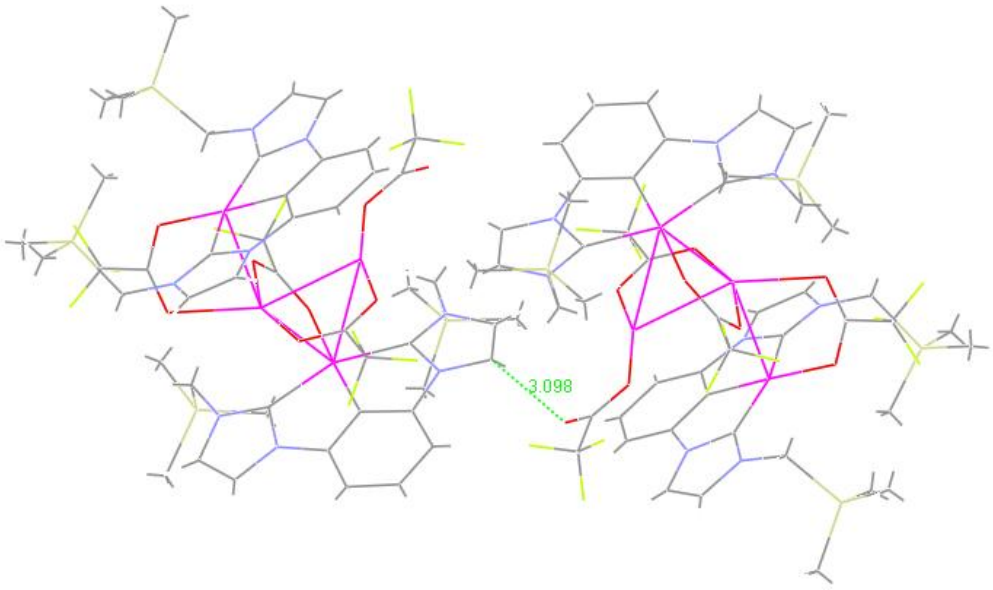

Figure A7. Dimmer configuration of Cluster Pt_2Ag_2 **5**.

* One trifluoroacetate bridges neighboring dimers by H-bonding, with C-H⋯⋯O at 3.09 Å.

Table A5-1. Crystal data and structure refinement for **5.**

Empirical formula	$C_{53}\ H_{70}\ Ag_2\ F_{12}\ N_8\ O_8\ Pt\ Si_4$
Formula weight	1698.36
Temperature	150(2) K
Wavelength	0.71073 Å
Crystal system, space group	Triclinic, P -1 (#2)
Unit cell dimensions	a = 15.2722(6) Å alpha = 65.227(4) °
	b = 15.7319(6) Å beta = 86.256(3) °
	c = 16.6232(6) Å gamma = 69.667(4) °
Volume	3385.2(2) $Å^3$
Z, Calculated density	2, 1.666 Mg/m^3
Absorption coefficient	2.791 mm^{-1}
F(000)	1688
Crystal size	0.50 x 0. 08 x 0.05 mm
Theta range for data collection	3.52 to 30.60 °
Limiting indices	-21≤ h ≤21, -22≤ k ≤22, -23≤ l ≤21
Reflections collected / unique	38505 / 20422 [R(int) = 0.0298]
Completeness to theta = 30.68	97.9 %
Absorption correction	Analytical
Max. and min. transmission	0.8730 and 0.3358
Refinement method	Full-matrix least-squares on F^2
Data / restraints / parameters	20422 / 12 / 794
Goodness-of-fit on F^2	0.845
Final R indices [I>2sigma(I)]	R_1 = 0.0297, wR_2 = 0.0500
R indices (all data)	R_1 = 0.0559, wR_2 = 0.0523

Largest diff. peak and hole	1.195 and -0.840 e. Å $^{-3}$

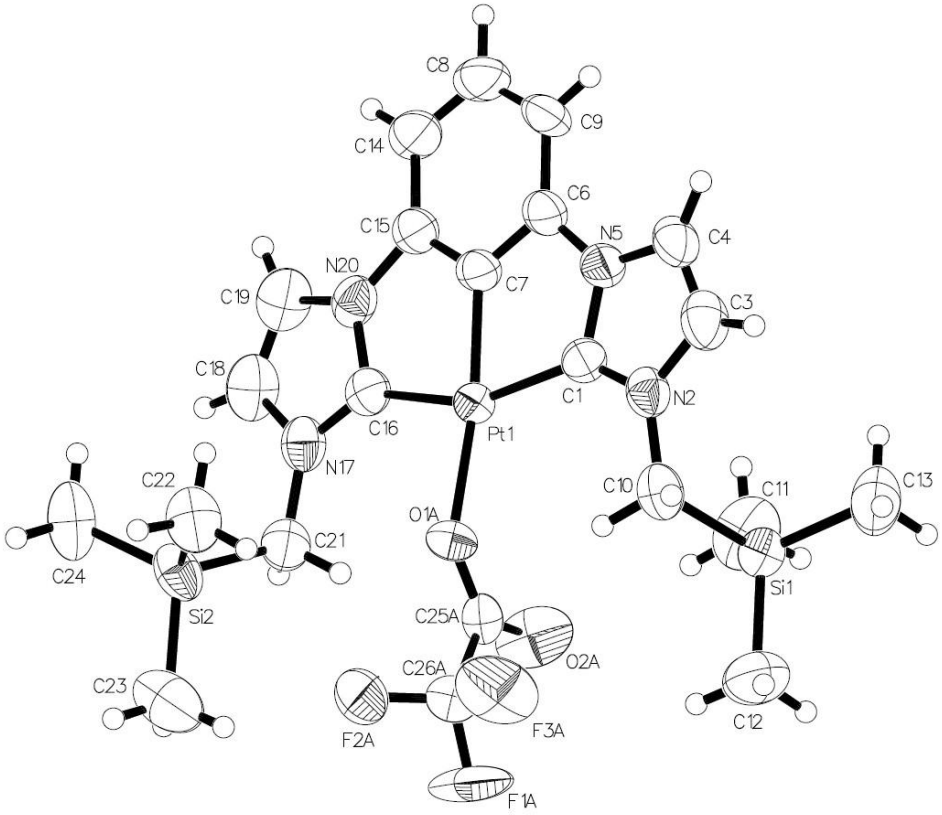

Figure A8. CCC-NHC-Pt-O_2CCF_3 **6**

Table S6-1. Crystal data and structure refinement for **6.**

Empirical formula	C_{22} H_{29} F_3 N_4 O_2 Pt Si_2
Formula weight	689.76
Temperature	293(2) K
Wavelength	0.71075 Å
Crystal system, space group	Monoclinic P $2_1/n$
Unit cell dimensions	a = 6.6502(12) Å alpha = 90 º
	b = 20.061(4) Å beta = 93.427(7) º
	c = 20.159(4) Å gamma = 90 º
Volume	2684.6(9) Å^3
Z, Calculated density	4, 1.707 Mg/m^3
Absorption coefficient	5.362 mm^{-1}
F(000)	1352
Crystal size	0.36 x 0.20x 0.15 mm

Theta range for data collection	3.17 to 27.48 º
Limiting indices	-8≤ h ≤8, -25≤ k ≤26 -26≤ l ≤26
Reflections collected / unique	27869 / 6155 [R(int) = 0.0644]
Absorption correction	Analytical
Max. and min. transmission	0.5001 and 0.2484
Data / restraints / parameters	6155 / 76 / 381
Goodness-of-fit	1.032
Final R indices [I>2sigma(I)]	R_1 = 0.0395, wR_2 = 0.0621
R indices (all data)	R_1 = 0.0620, wR_2 = 0.0684
Largest diff. peak and hole	1.308 and -0.841 e.A^{-3}

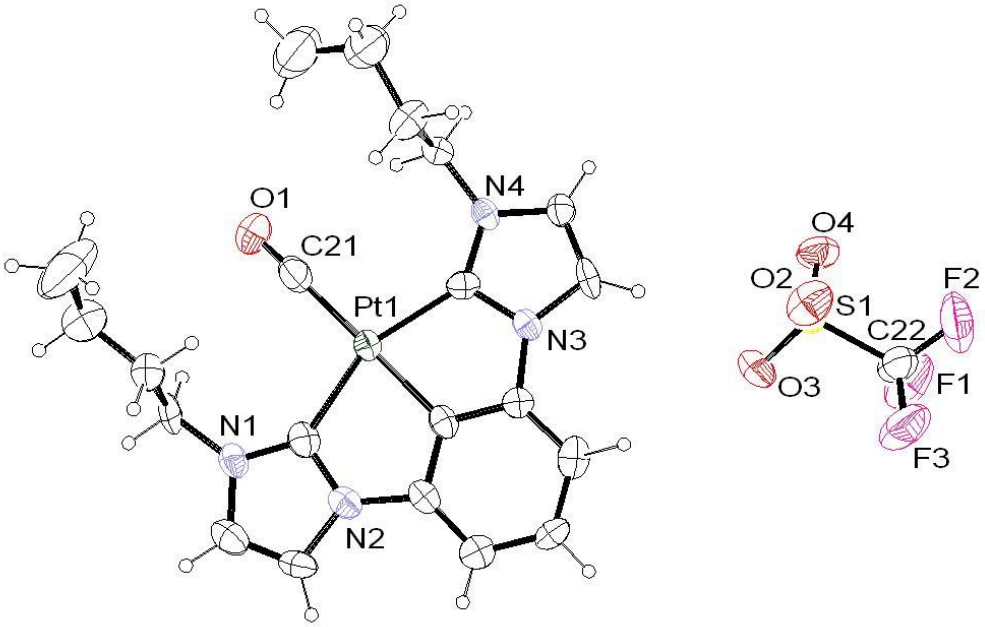

Figure A9. CCC-NHC-Pt-CO/OTf **7**

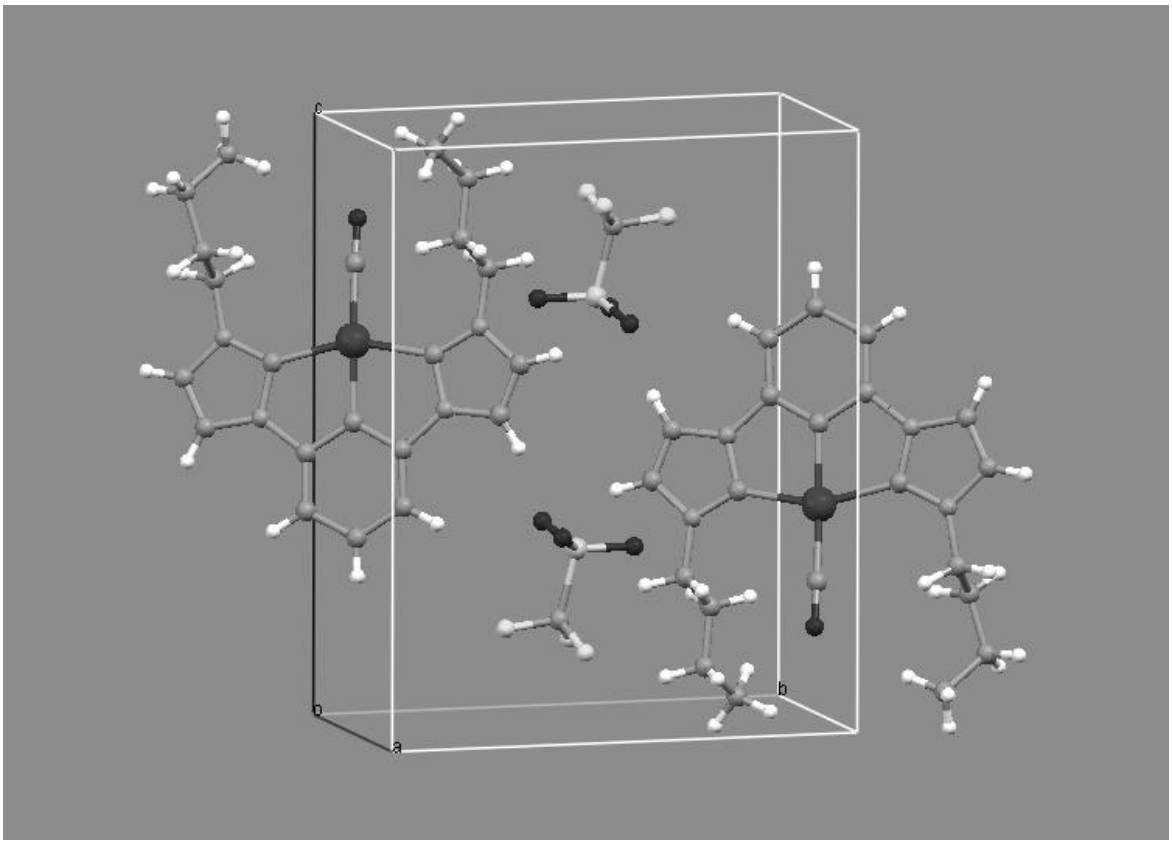

Figure A10. Unit cell of complex CCC-NHC-Pt-CO/OTf **7**

Table A7-1. Crystal data and structure refinement for **7.**

Empirical formula	C_{22} H_{25} F_3 N_4 O_4 Pt S
Formula weight	693.61
Temperature	299(2) K
Wavelength	0.71073 Å
Crystal system, space group	Triclinic, P -1
Unit cell dimensions	a = 8.0262(6)Å alpha = 87.360(5) º
	b = 11.1533(8) Å beta = 87.057(5) º
	c = 14.6244(9) Å gamma = 75.666(6) º
Volume	1265.98(15) $Å^3$
Z, Calculated density	2, 1.820 Mg/m^3
Absorption coefficient	5.682 mm^{-1}
F(000)	676
Crystal size	0.32 x 0.06x 0.04 mm
Theta range for data collection	3.59 to 28.00 º
Limiting indices	$-10\leq h \leq 10$, $-14\leq k \leq 14$ $-18\leq l \leq 19$
Reflections collected / unique	10439 / 5616 [R(int) = 0.0264]
Completeness to theta = 30.57	91.7 %
Absorption correction	Analytical

Max. and min. transmission	0.8046 and 0.2636
Refinement method	Full-matrix least-squares on F^2
Data / restraints / parameters	5616 / 0 / 316
Goodness-of-fit on F^2	0.990
Final R indices [I>2sigma(I)]	R_1 = 0.0647, wR_2 = 0.0896
R indices (all data)	R_1 = 0.1361, wR_2 = 0.1016
Largest diff. peak and hole	1.630 and -1.294 e.A^{-3}

Table A7-2. Atomic coordinates (x 10^4) and equivalent isotropic displacement parameters (A^2 x 10^3) for **7.** U(eq) is defined as one third of the trace of the orthogonalized Uij tensor.

Atom	x	y	z	U(eq)
C(1)	7359(12)	-2126(9)	3925(8)	58(3)
C(2)	6436(14)	-3815(11)	4086(10)	76(4)
C(3)	6250(13)	-3361(10)	4903(9)	66(3)
C(4)	6776(10)	-1342(8)	5441(7)	48(2)
C(5)	7373(11)	-402(9)	4990(7)	49(2)
C(6)	7468(10)	607(9)	5475(7)	44(2)
C(7)	6943(11)	689(10)	6406(8)	62(3)
C(8)	6400(11)	-302(11)	6852(7)	60(3)
C(9)	6321(11)	-1308(10)	6359(8)	58(3)
C(10)	8487(10)	1156(9)	4020(7)	49(2)
C(11)	8437(11)	2605(9)	5051(8)	59(3)
C(12)	9019(12)	2975(9)	4248(7)	56(3)
C(13)	7544(13)	-3300(10)	2537(8)	66(3)
C(14)	6178(14)	-2517(11)	1937(8)	73(3)
C(15)	6592(16)	-2702(13)	965(10)	102(4)
C(16)	5420(30)	-1810(20)	375(12)	200(10)
C(17)	9535(13)	2226(10)	2668(7)	63(3)
C(18)	7961(12)	2745(11)	2092(7)	76(3)
C(19)	8422(18)	3048(16)	1115(10)	112(5)
C(20)	9260(20)	2000(19)	571(12)	158(7)
C(21)	9072(17)	-716(11)	2472(10)	81(4)
C(22)	7320(20)	5176(16)	8415(9)	91(4)
N(1)	7163(10)	-3080(8)	3486(6)	57(2)
N(2)	6795(9)	-2274(8)	4807(7)	59(2)
N(3)	8110(8)	1468(7)	4909(6)	47(2)
N(4)	9068(8)	2098(7)	3619(6)	47(2)
O(1)	9718(14)	-875(10)	1768(7)	122(4)
O(2)	5785(9)	5374(9)	6949(5)	96(3)
O(3)	7834(10)	3483(7)	7286(6)	95(3)
O(4)	8771(9)	5297(8)	6862(5)	87(2)
F(1)	8737(11)	4731(10)	8831(6)	144(4)

F(2)	6961(12)	6394(10)	8502(7)	151(3)
F(3)	6129(11)	4821(10)	8899(5)	137(3)
S(1)	7441(3)	4783(3)	7252(2)	60(1)
Pt(1)	8138(1)	-519(1)	3693(1)	47(1)

Table A7-3. Bond lengths [Å] and angles [°] for **7.**

C(1)-N(1)	1.314(12)	O(2)-S(1)	1.413(7)
C(1)-N(2)	1.361(12)	O(3)-S(1)	1.405(8)
C(1)-Pt(1)	2.048(10)	O(4)-S(1)	1.415(6)
C(2)-C(3)	1.306(15)	N(1)-C(1)-N(2)	106.6(9)
C(2)-N(1)	1.379(13)	N(1)-C(1)-Pt(1)	140.5(9)
C(3)-N(2)	1.387(11)	N(2)-C(1)-Pt(1)	112.9(7)
C(4)-C(9)	1.373(13)	C(3)-C(2)-N(1)	109.8(11)
C(4)-C(5)	1.384(12)	C(2)-C(3)-N(2)	105.5(10)
C(4)-N(2)	1.420(12)	C(9)-C(4)-C(5)	121.8(9)
C(5)-C(6)	1.378(13)	C(9)-C(4)-N(2)	129.5(9)
C(5)-Pt(1)	1.963(10)	C(5)-C(4)-N(2)	108.6(9)
C(6)-C(7)	1.405(13)	C(6)-C(5)-C(4)	118.7(9)
C(6)-N(3)	1.415(11)	C(6)-C(5)-Pt(1)	120.3(7)
C(7)-C(8)	1.407(13)	C(4)-C(5)-Pt(1)	121.0(8)
C(8)-C(9)	1.378(14)	C(5)-C(6)-C(7)	120.6(9)
C(10)-N(4)	1.350(11)	C(5)-C(6)-N(3)	111.0(9)
C(10)-N(3)	1.361(12)	C(7)-C(6)-N(3)	128.4(10)
C(10)-Pt(1)	2.038(10)	C(6)-C(7)-C(8)	119.2(9)
C(11)-C(12)	1.327(13)	C(9)-C(8)-C(7)	119.4(10)
C(11)-N(3)	1.384(11)	C(4)-C(9)-C(8)	120.1(9)
C(12)-N(4)	1.365(12)	N(4)-C(10)-N(3)	105.2(8)
C(13)-N(1)	1.425(13)	N(4)-C(10)-Pt(1)	139.0(8)
C(13)-C(14)	1.512(14)	N(3)-C(10)-Pt(1)	115.7(6)
C(14)-C(15)	1.455(16)	C(12)-C(11)-N(3)	105.8(9)
C(15)-C(16)	1.472(18)	C(11)-C(12)-N(4)	109.2(9)
C(17)-N(4)	1.433(12)	N(1)-C(13)-C(14)	112.3(9)
C(17)-C(18)	1.530(12)	C(15)-C(14)-C(13)	112.6(10)
C(18)-C(19)	1.502(16)	C(14)-C(15)-C(16)	113.0(13)
C(19)-C(20)	1.45(2)	N(4)-C(17)-C(18)	112.0(8)
C(21)-O(1)	1.130(14)	C(19)-C(18)-C(17)	113.2(9)
C(21)-Pt(1)	1.902(16)	C(20)-C(19)-C(18)	115.6(14)
C(22)-F(3)	1.291(12)	O(1)-C(21)-Pt(1)	175.7(13)
C(22)-F(1)	1.292(14)	F(3)-C(22)-F(1)	106.3(13)
C(22)-F(2)	1.328(16)	F(3)-C(22)-F(2)	104.8(14)
C(22)-S(1)	1.768(14)	F(1)-C(22)-F(2)	106.0(11)

F(3)-C(22)-S(1)	113.9(9)	C(12)-N(4)-C(17)	124.3(8)
F(1)-C(22)-S(1)	113.6(11)	O(3)-S(1)-O(2)	115.3(5)
F(2)-C(22)-S(1)	111.5(10)	O(3)-S(1)-O(4)	114.6(5)
C(1)-N(1)-C(2)	108.6(10)	O(2)-S(1)-O(4)	114.2(5)
C(1)-N(1)-C(13)	126.4(9)	O(3)-S(1)-C(22)	103.9(7)
C(2)-N(1)-C(13)	124.9(10)	O(2)-S(1)-C(22)	103.2(7)
C(1)-N(2)-C(3)	109.4(9)	O(4)-S(1)-C(22)	103.6(5)
C(1)-N(2)-C(4)	119.3(8)	C(21)-Pt(1)-C(5)	174.9(5)
C(3)-N(2)-C(4)	131.2(10)	C(21)-Pt(1)-C(10)	103.2(4)
C(10)-N(3)-C(11)	110.3(8)	C(5)-Pt(1)-C(10)	77.3(4)
C(10)-N(3)-C(6)	115.7(8)	C(21)-Pt(1)-C(1)	101.3(5)
C(11)-N(3)-C(6)	134.0(9)	C(5)-Pt(1)-C(1)	78.2(4)
C(10)-N(4)-C(12)	109.5(9)	C(10)-Pt(1)-C(1)	155.4(4)
C(10)-N(4)-C(17)	126.1(8)		

Symmetry transformations used to generate equivalent atoms: #1 -x,y,-z+1/2

Table A7-4. Anisotropic displacement parameters (A^2 x 10^3) for **7**
The anisotropic displacement factor exponent takes the form:
$-2\pi^2 [h^2 a^{*2} U11 + ... + 2 h k a^* b^* U12]$

Atom	U11	U22	U33	U23	U13	U12
C(1)	52(6)	42(7)	72(8)	-5(6)	-7(5)	5(5)
C(2)	75(8)	65(8)	96(11)	8(8)	-20(7)	-32(6)
C(3)	68(7)	59(8)	75(10)	22(7)	-8(6)	-28(6)
C(4)	28(5)	40(6)	72(8)	-2(5)	-11(4)	-1(4)
C(5)	43(6)	36(6)	65(7)	-5(5)	-11(5)	0(4)
C(6)	29(5)	45(6)	53(7)	2(5)	-6(4)	2(4)
C(7)	26(5)	66(8)	79(9)	-28(6)	6(5)	19(4)
C(8)	54(7)	82(9)	41(7)	2(6)	5(5)	-16(6)
C(9)	44(6)	57(8)	65(8)	5(6)	-5(5)	5(5)
C(10)	39(5)	52(7)	53(7)	6(5)	2(4)	-7(4)
C(11)	50(6)	40(6)	87(9)	-31(6)	-9(5)	-6(5)
C(12)	63(7)	49(7)	57(7)	-10(6)	4(5)	-13(5)
C(13)	72(7)	51(7)	81(9)	-37(6)	1(6)	-18(6)
C(14)	82(8)	70(8)	68(9)	-13(6)	-1(6)	-22(6)
C(15)	103(10)	111(12)	90(12)	1(9)	2(8)	-25(8)
C(16)	280(20)	220(20)	68(13)	11(14)	-18(13)	14(18)
C(17)	83(8)	56(7)	57(8)	1(5)	4(6)	-32(6)

C(18)	63(7)	95(9)	58(8)	-2(6)	-3(6)	2(6)
C(19)	118(12)	133(15)	87(13)	3(10)	-4(9)	-38(10)
C(20)	199(19)	180(20)	88(13)	-14(13)	4(11)	-34(15)
C(21)	108(11)	54(8)	86(11)	-2(7)	-17(8)	-26(7)
C(22)	103(11)	121(13)	66(10)	-4(9)	4(8)	-61(10)
N(1)	61(6)	43(6)	66(7)	-8(5)	-9(4)	-7(4)
N(2)	56(5)	53(6)	71(7)	3(5)	-10(4)	-18(4)
N(3)	40(4)	38(5)	60(6)	-2(4)	-8(4)	-5(3)
N(4)	37(4)	39(5)	65(6)	-10(4)	1(4)	-7(4)
O(1)	188(10)	114(8)	71(7)	-32(6)	37(6)	-57(7)
O(2)	74(6)	140(8)	79(6)	0(5)	-18(4)	-34(5)
O(3)	127(7)	52(6)	110(7)	-7(5)	8(5)	-29(5)
O(4)	89(6)	100(7)	79(6)	9(5)	16(4)	-41(5)
F(1)	130(7)	226(11)	77(6)	-20(6)	-30(5)	-36(7)
F(2)	179(9)	116(8)	165(9)	-84(6)	14(6)	-41(6)
F(3)	133(7)	203(10)	83(6)	-14(6)	38(5)	-66(6)
S(1)	64(2)	60(2)	59(2)	-7(1)	5(1)	-24(1)
Pt(1)	45(1)	45(1)	54(1)	-8(1)	-3(1)	-12(1)

Table A7-5. Hydrogen coordinates (x 10^4) and isotropic displacement parameters (A^2 x 10^3) for **7.**

Atom	x	y	z	U(eq)
H(2A)	6125	-4527	3932	91
H(3A)	5838	-3696	5436	79
H(7A)	6953	1391	6724	74
H(8A)	6098	-278	7475	72
H(9A)	5960	-1966	6648	70
H(11A)	8282	3024	5596	71
H(12A)	9341	3715	4132	68
H(13A)	7645	-4168	2432	80
H(13B)	8643	-3121	2365	80
H(14A)	5088	-2720	2093	87
H(14B)	6045	-1651	2061	87
H(15A)	6546	-3535	825	122
H(15B)	7759	-2630	830	122
H(16A)	4400	-1421	728	240
H(16B)	5103	-2235	-120	240
H(16C)	5979	-1191	132	240
H(17A)	10147	1423	2445	76
H(17B)	10305	2773	2596	76
H(18A)	7270	2143	2100	91
H(18B)	7266	3488	2368	91
H(19A)	7379	3487	821	134
H(19B)	9175	3607	1114	134
H(20A)	10482	1868	592	189
H(20B)	8918	2162	-52	189

H(20C)	8922	1275	812	189

Table A7-6. Torsion angles [°] for **7.**

N(1)-C(2)-C(3)-N(2)	3.0(13)	Pt(1)-C(10)-N(3)-C(6)	-2.2(9)
C(9)-C(4)-C(5)-C(6)	-1.7(12)	C(12)-C(11)-N(3)-C(10)	-0.2(10)
N(2)-C(4)-C(5)-C(6)	-179.9(7)	C(12)-C(11)-N(3)-C(6)	-179.4(8)
C(9)-C(4)-C(5)-Pt(1)	176.5(6)	C(5)-C(6)-N(3)-C(10)	0.5(10)
N(2)-C(4)-C(5)-Pt(1)	-1.8(9)	C(7)-C(6)-N(3)-C(10)	-178.7(8)
C(4)-C(5)-C(6)-C(7)	-1.0(12)	C(5)-C(6)-N(3)-C(11)	179.6(8)
Pt(1)-C(5)-C(6)-C(7)	-179.2(6)	C(7)-C(6)-N(3)-C(11)	0.4(14)
C(4)-C(5)-C(6)-N(3)	179.8(7)	N(3)-C(10)-N(4)-C(12)	-1.0(9)
Pt(1)-C(5)-C(6)-N(3)	1.6(10)	Pt(1)-C(10)-N(4)-C(12)	-177.9(7)
C(5)-C(6)-C(7)-C(8)	3.3(13)	N(3)-C(10)-N(4)-C(17)	-176.1(8)
N(3)-C(6)-C(7)-C(8)	-177.7(8)	Pt(1)-C(10)-N(4)-C(17)	6.9(15)
C(6)-C(7)-C(8)-C(9)	-2.9(13)	C(11)-C(12)-N(4)-C(10)	0.9(11)
C(5)-C(4)-C(9)-C(8)	2.1(13)	C(11)-C(12)-N(4)-C(17)	176.1(8)
N(2)-C(4)-C(9)-C(8)	179.9(8)	C(18)-C(17)-N(4)-C(10)	80.9(12)
C(7)-C(8)-C(9)-C(4)	0.3(13)	C(18)-C(17)-N(4)-C(12)	-93.6(10)
N(3)-C(11)-C(12)-N(4)	-0.4(10)	F(3)-C(22)-S(1)-O(3)	-62.0(14)
N(1)-C(13)-C(14)-C(15)	177.8(9)	F(1)-C(22)-S(1)-O(3)	60.0(11)
C(13)-C(14)-C(15)-C(16)	-171.0(13)	F(2)-C(22)-S(1)-O(3)	179.7(9)
N(4)-C(17)-C(18)-C(19)	172.3(10)	F(3)-C(22)-S(1)-O(2)	58.7(14)
C(17)-C(18)-C(19)-C(20)	66.9(16)	F(1)-C(22)-S(1)-O(2)	-179.3(10)
N(2)-C(1)-N(1)-C(2)	1.4(10)	F(2)-C(22)-S(1)-O(2)	-59.6(10)
Pt(1)-C(1)-N(1)-C(2)	-175.7(8)	F(3)-C(22)-S(1)-O(4)	178.0(12)
N(2)-C(1)-N(1)-C(13)	178.3(8)	F(1)-C(22)-S(1)-O(4)	-60.1(12)
Pt(1)-C(1)-N(1)-C(13)	1.3(17)	F(2)-C(22)-S(1)-O(4)	59.6(11)
C(3)-C(2)-N(1)-C(1)	-2.8(13)	O(1)-C(21)-Pt(1)-C(5)	2(19)
C(3)-C(2)-N(1)-C(13)	-179.9(9)	O(1)-C(21)-Pt(1)-C(10)	97(15)
C(14)-C(13)-N(1)-C(1)	-77.4(12)	O(1)-C(21)-Pt(1)-C(1)	-83(15)
C(14)-C(13)-N(1)-C(2)	99.1(12)	C(6)-C(5)-Pt(1)-C(21)	94(5)
N(1)-C(1)-N(2)-C(3)	0.4(10)	C(4)-C(5)-Pt(1)-C(21)	-84(5)
Pt(1)-C(1)-N(2)-C(3)	178.4(6)	C(6)-C(5)-Pt(1)-C(10)	-2.1(7)
N(1)-C(1)-N(2)-C(4)	-177.0(7)	C(4)-C(5)-Pt(1)-C(10)	179.7(7)
Pt(1)-C(1)-N(2)-C(4)	1.0(10)	C(6)-C(5)-Pt(1)-C(1)	180.0(8)
C(2)-C(3)-N(2)-C(1)	-2.1(12)	C(4)-C(5)-Pt(1)-C(1)	1.8(7)
C(2)-C(3)-N(2)-C(4)	174.9(9)	N(4)-C(10)-Pt(1)-C(21)	4.2(11)
C(9)-C(4)-N(2)-C(1)	-177.6(8)	N(3)-C(10)-Pt(1)-C(21)	-172.5(7)
C(5)-C(4)-N(2)-C(1)	0.4(11)	N(4)-C(10)-Pt(1)-C(5)	179.0(10)
C(9)-C(4)-N(2)-C(3)	5.6(15)	N(3)-C(10)-Pt(1)-C(5)	2.3(6)
C(5)-C(4)-N(2)-C(3)	-176.4(9)	N(4)-C(10)-Pt(1)-C(1)	-176.1(8)
N(4)-C(10)-N(3)-C(11)	0.7(9)	N(3)-C(10)-Pt(1)-C(1)	7.2(12)
Pt(1)-C(10)-N(3)-C(11)	178.5(5)	N(1)-C(1)-Pt(1)-C(21)	-9.6(12)
N(4)-C(10)-N(3)-C(6)	-179.9(6)	N(2)-C(1)-Pt(1)-C(21)	173.4(7)

N(1)-C(1)-Pt(1)-C(5)	175.5(11)	N(1)-C(1)-Pt(1)-C(10)	170.6(8)
N(2)-C(1)-Pt(1)-C(5)	-1.4(6)	N(2)-C(1)-Pt(1)-C(10)	-6.3(13)

Symmetry transformations used to generate equivalent atoms: #1 -x,y,-z+1/2

NMR SPECTRA

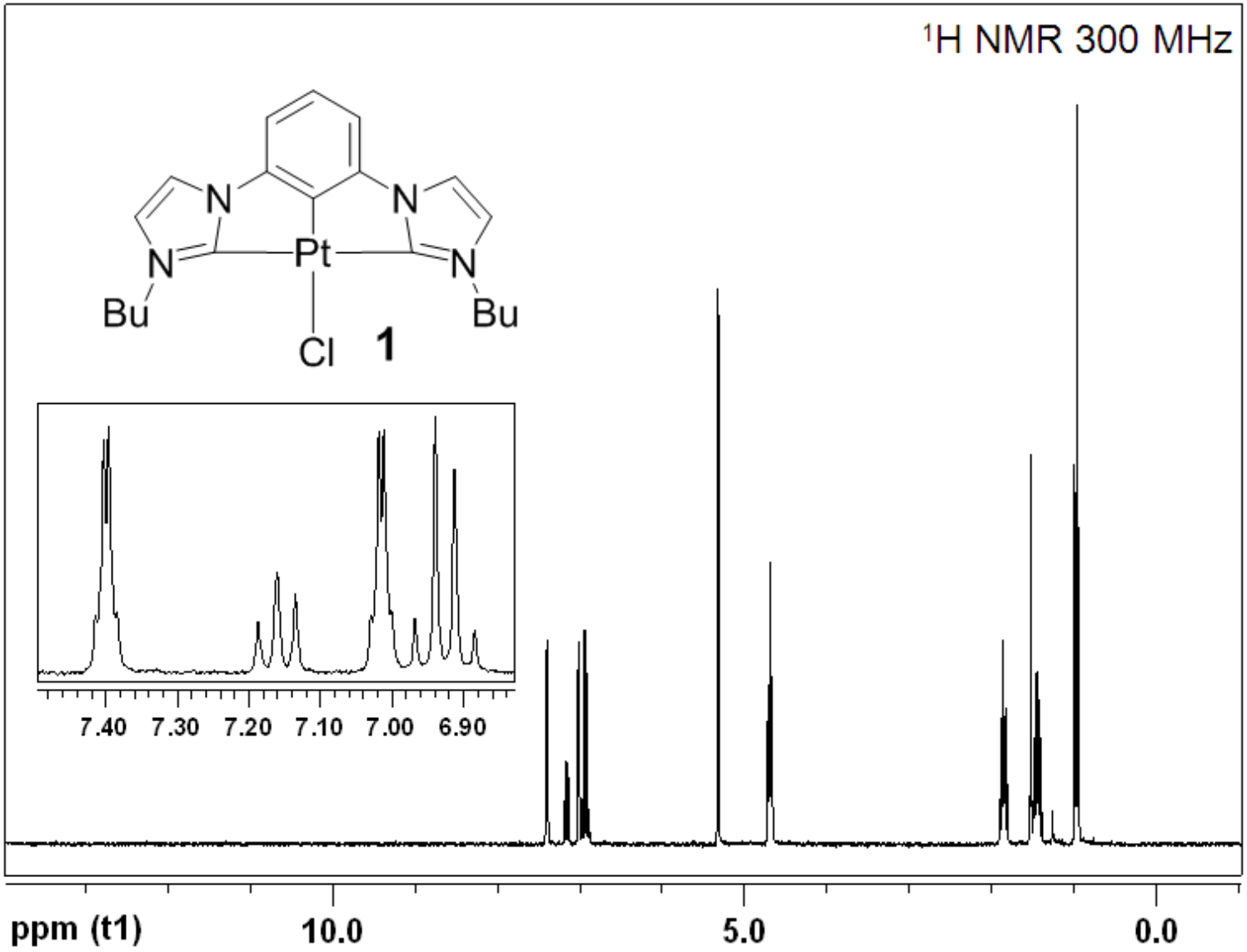
^{1}H NMR 300 MHz
N
N
N
N
Pt
Bu
Bu
Cl
1
7.40
7.30
7.20
7.10
7.00
6.90
ppm (t1)
10.0
5.0
0.0

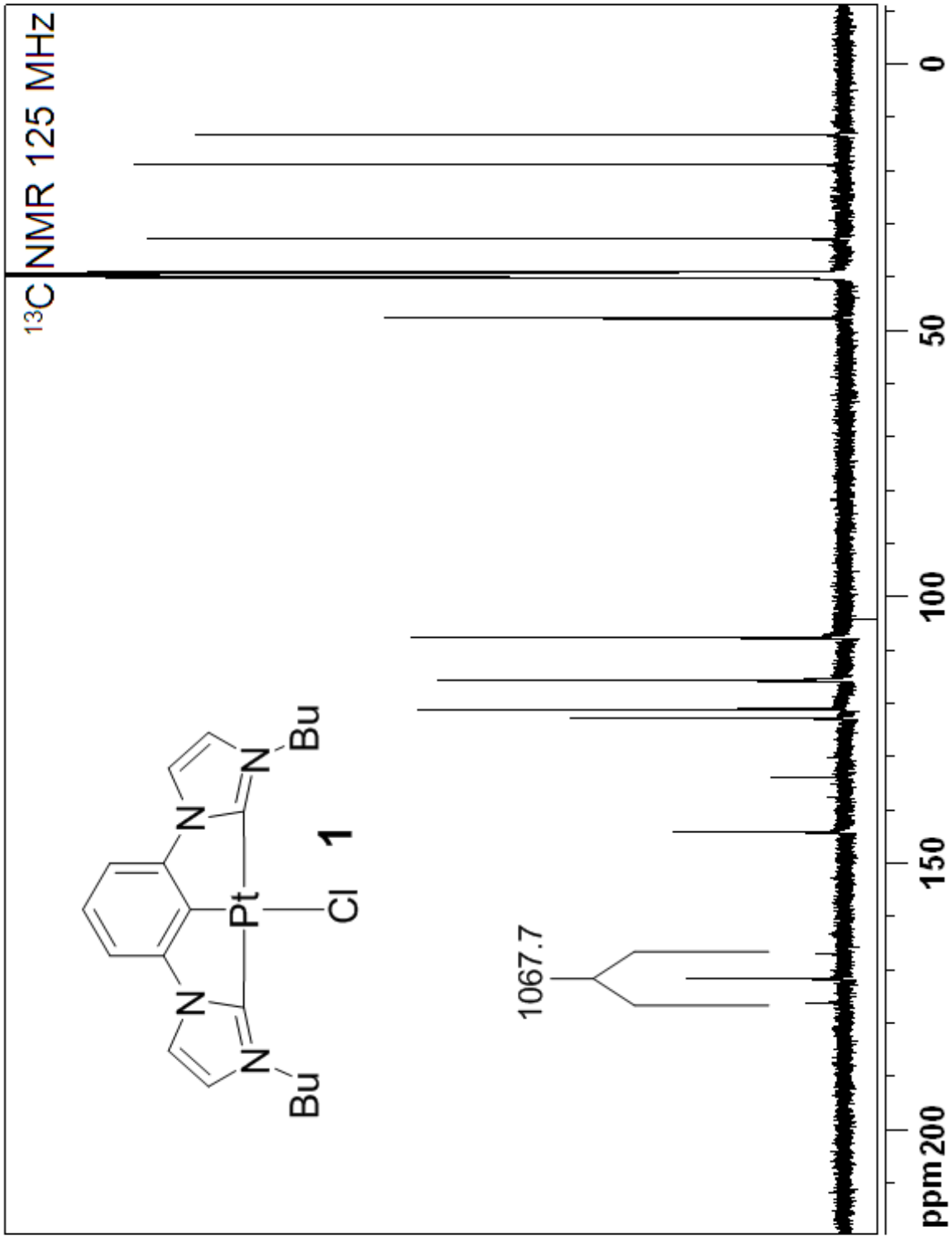
^{13}C NMR 125 MHz
1067.7
Pt
Cl
N
N
N
N
Bu
Bu
1
ppm
200
150
100
50
0

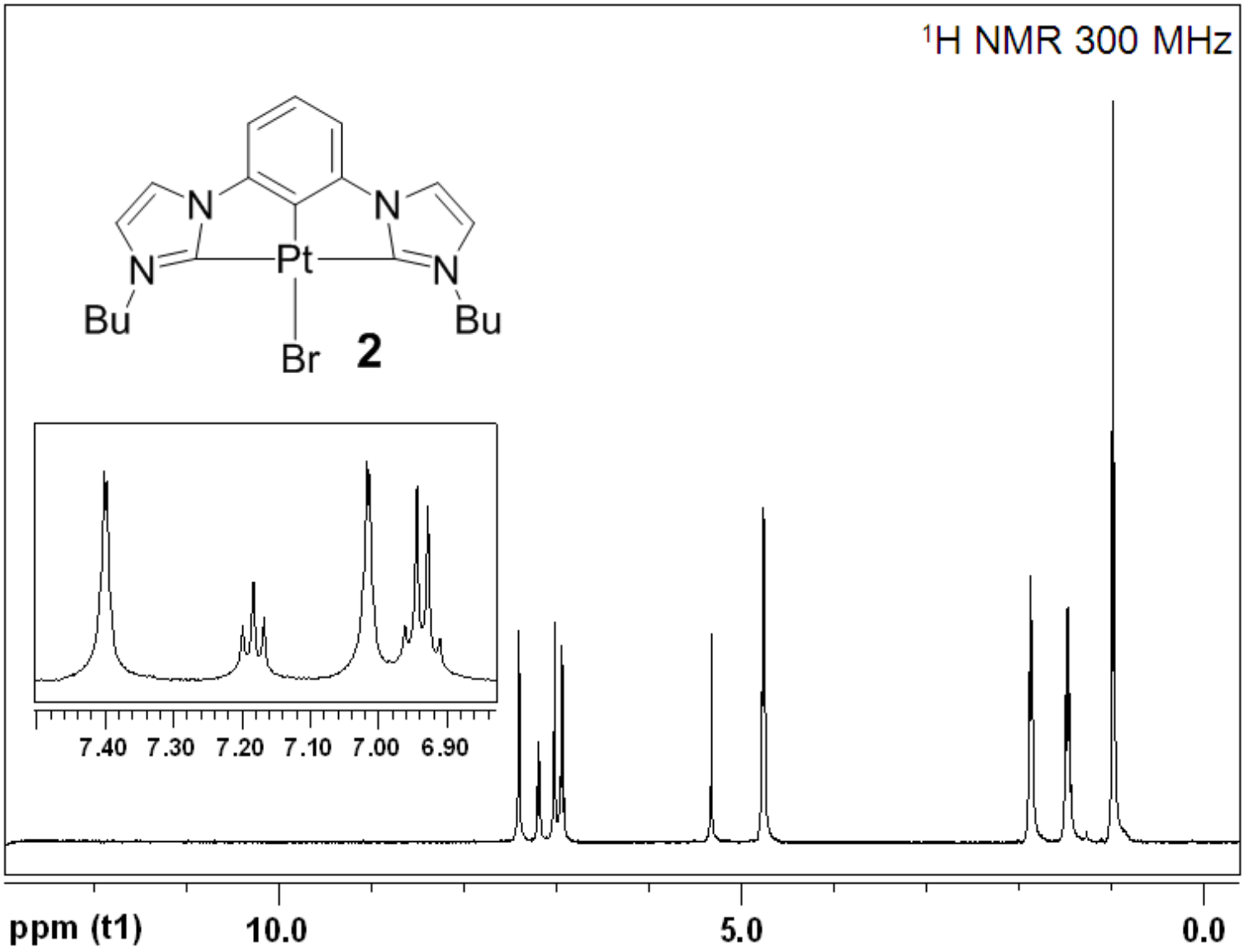
^{1}H NMR 300 MHz
N
N
N
N
Pt
Bu
Bu
Br
2
7.40
7.30
7.20
7.10
7.00
6.90
ppm (t1)
10.0
5.0
0.0

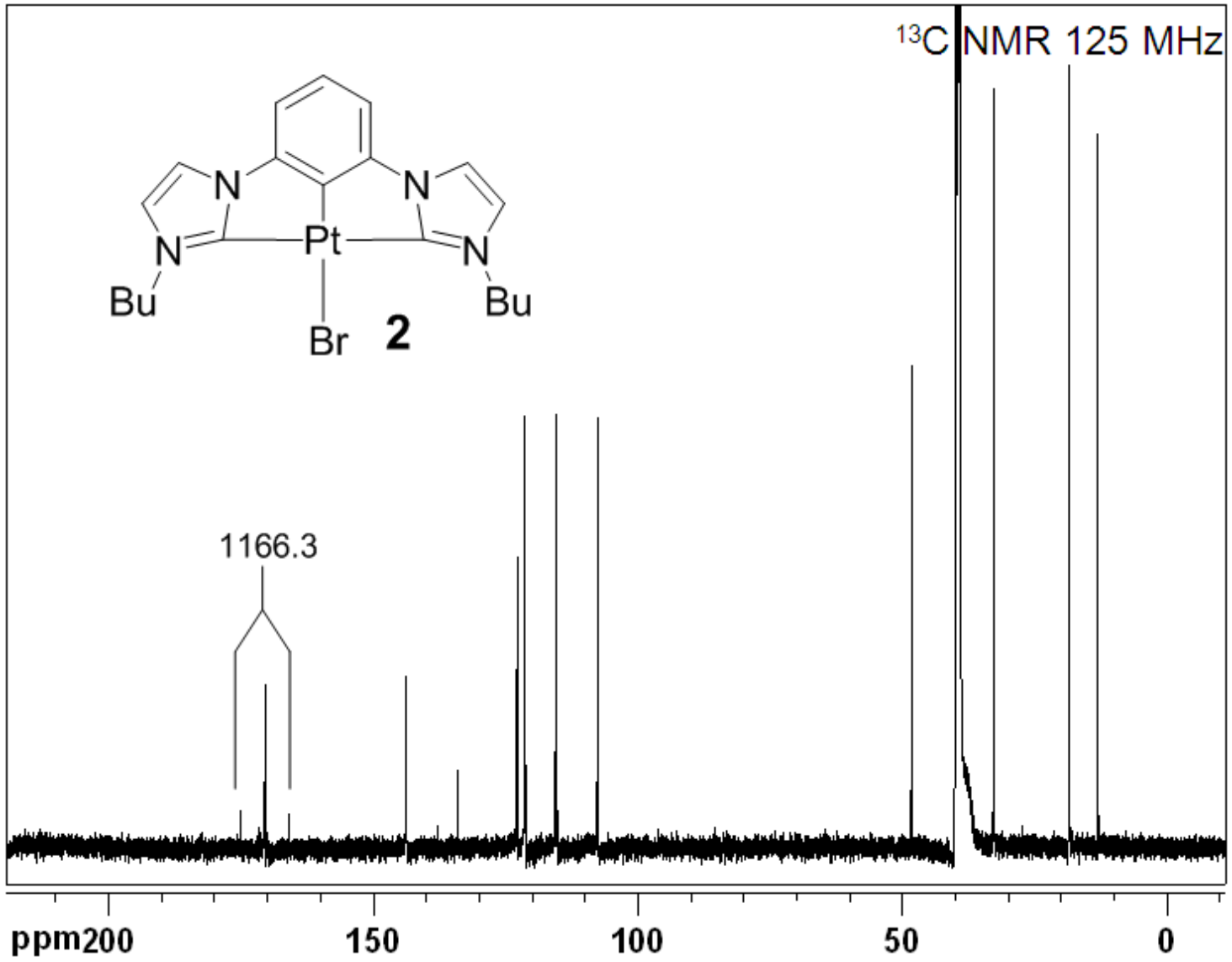
^{13}C NMR 125 MHz
N
N
N
N
Pt
Bu
Bu
Br
2
1166.3
ppm200
150
100
50
0

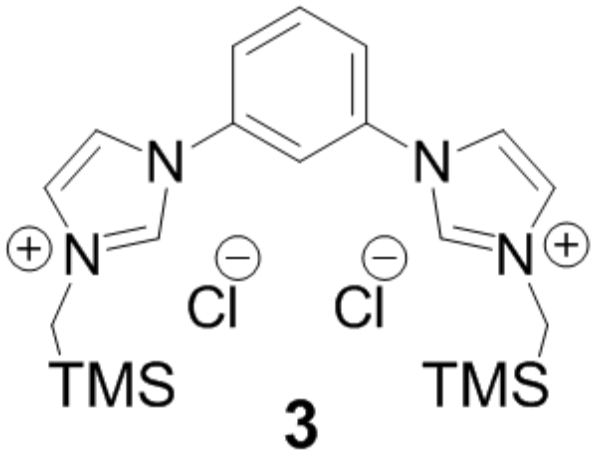

3

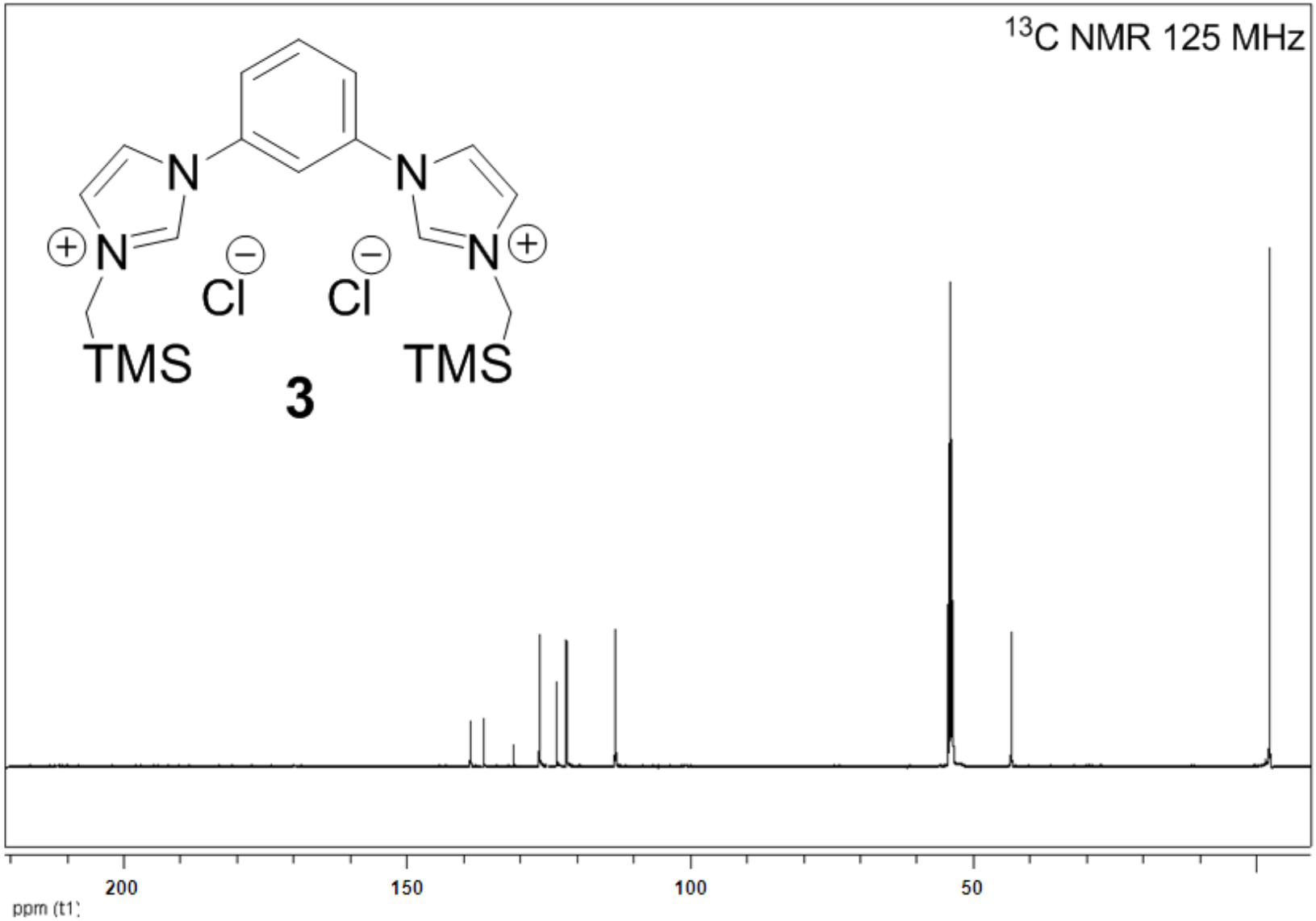
^{13}C NMR 125 MHz
N
N
N
N
Cl
Cl
TMS
TMS
3
200
150
100
50
ppm (t1)

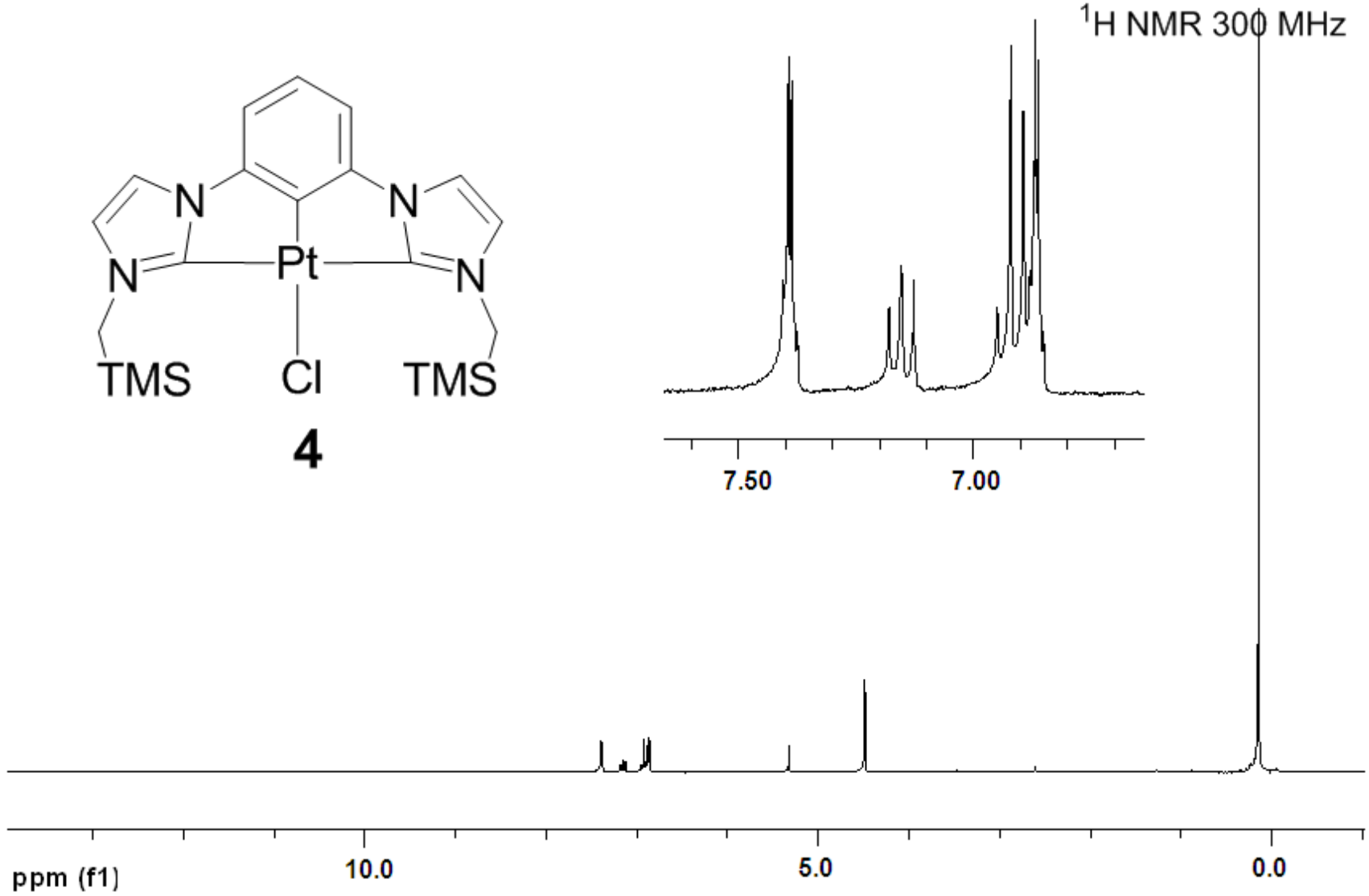
N
N
N
Pt
N
TMS
Cl
TMS
4
^{1}H NMR 300 MHz
7.50
7.00
ppm (f1)
10.0
5.0
0.0

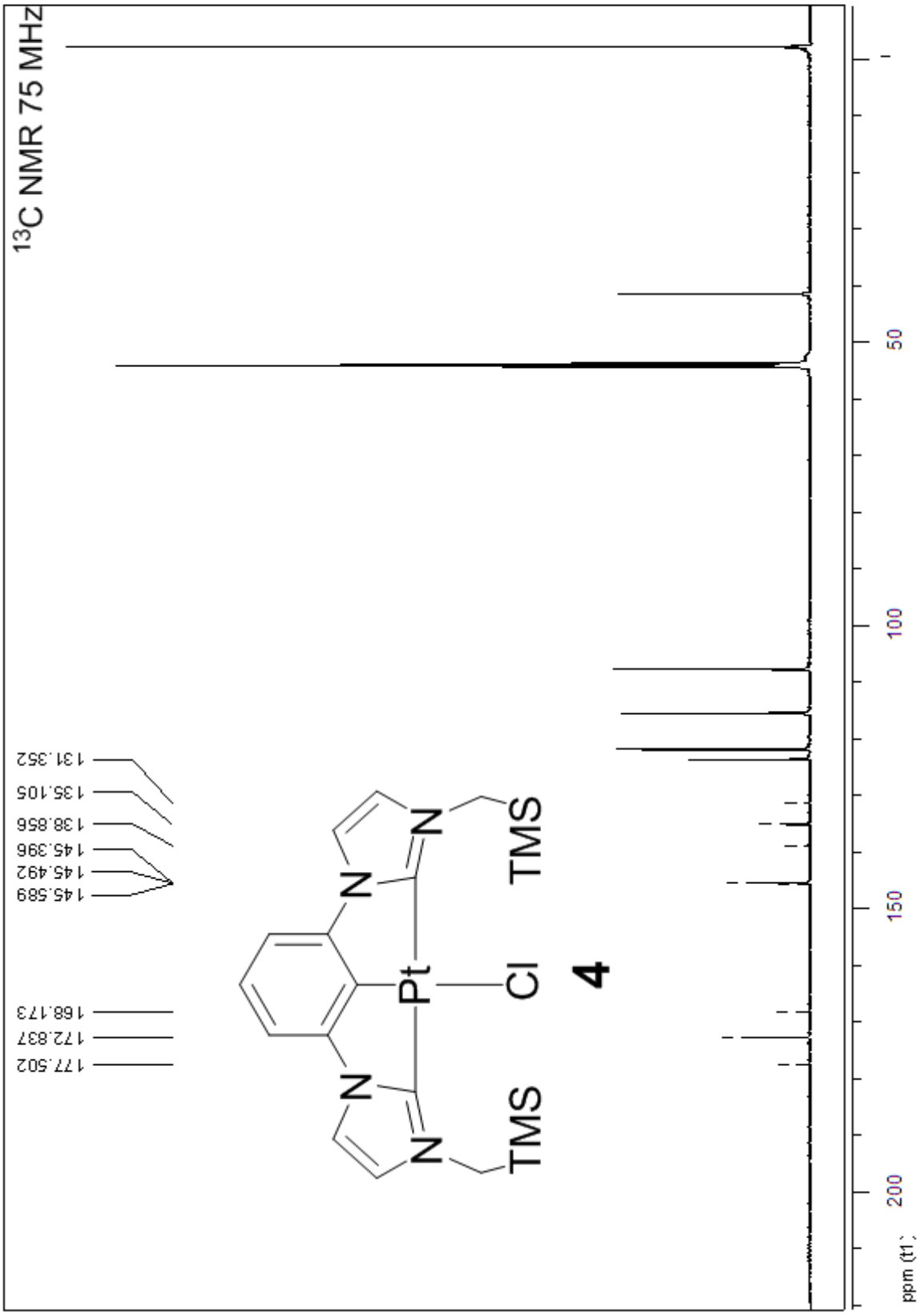
^{13}C NMR 75 MHz
131.352
135.105
138.856
145.396
145.492
145.589
168.173
172.837
177.502
N
N
N
N
Pt
Cl
TMS
TMS
4
50
100
150
200
ppm (t1)

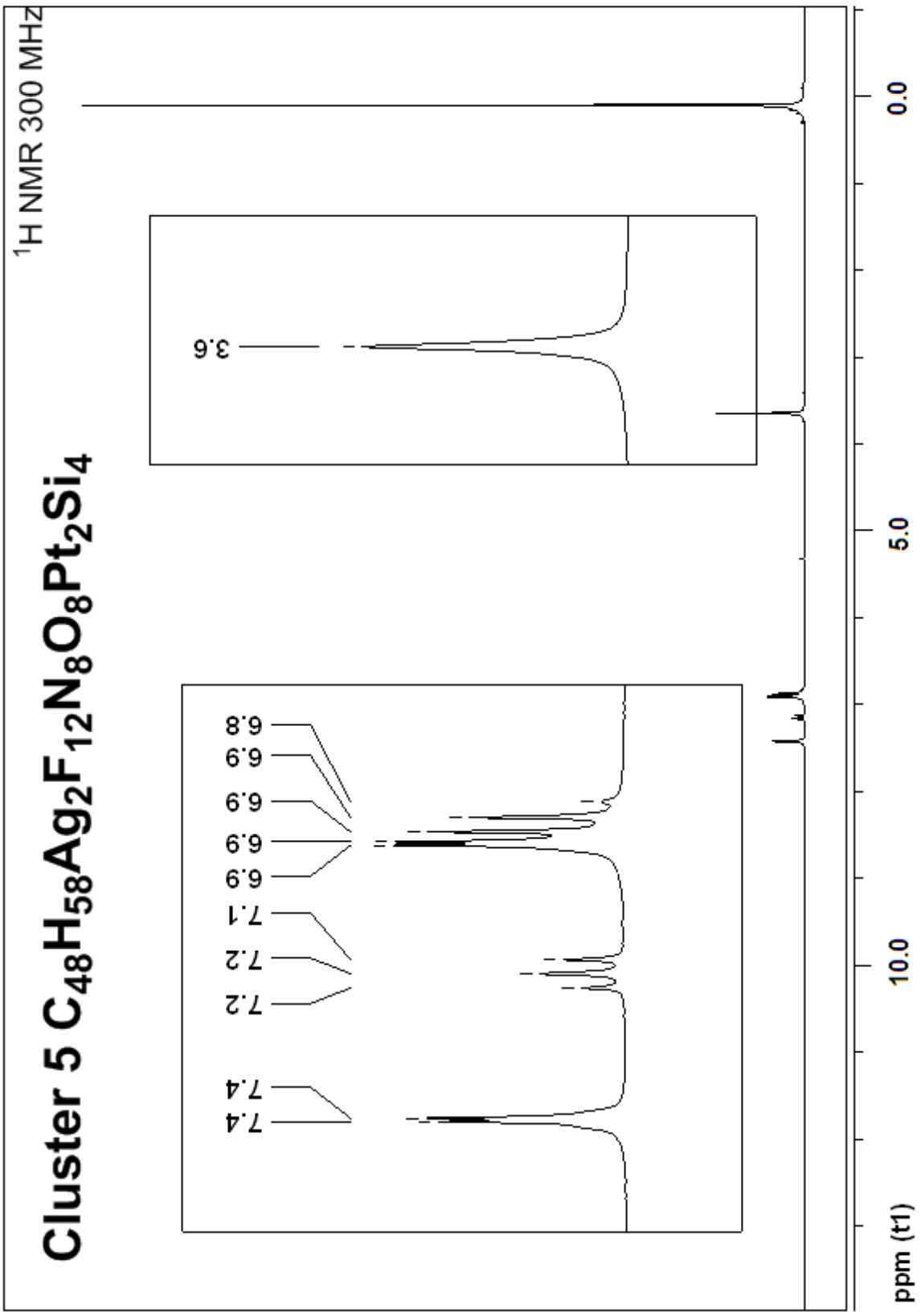
Cluster 5 $C_{48}H_{58}Ag_2F_{12}N_8O_8Pt_2Si_4$
^{1}H NMR 300 MHz
7.4
7.4
7.2
7.2
7.2
7.1
6.9
6.9
6.9
6.9
6.9
6.8
3.6
10.0
5.0
0.0
ppm (t1)

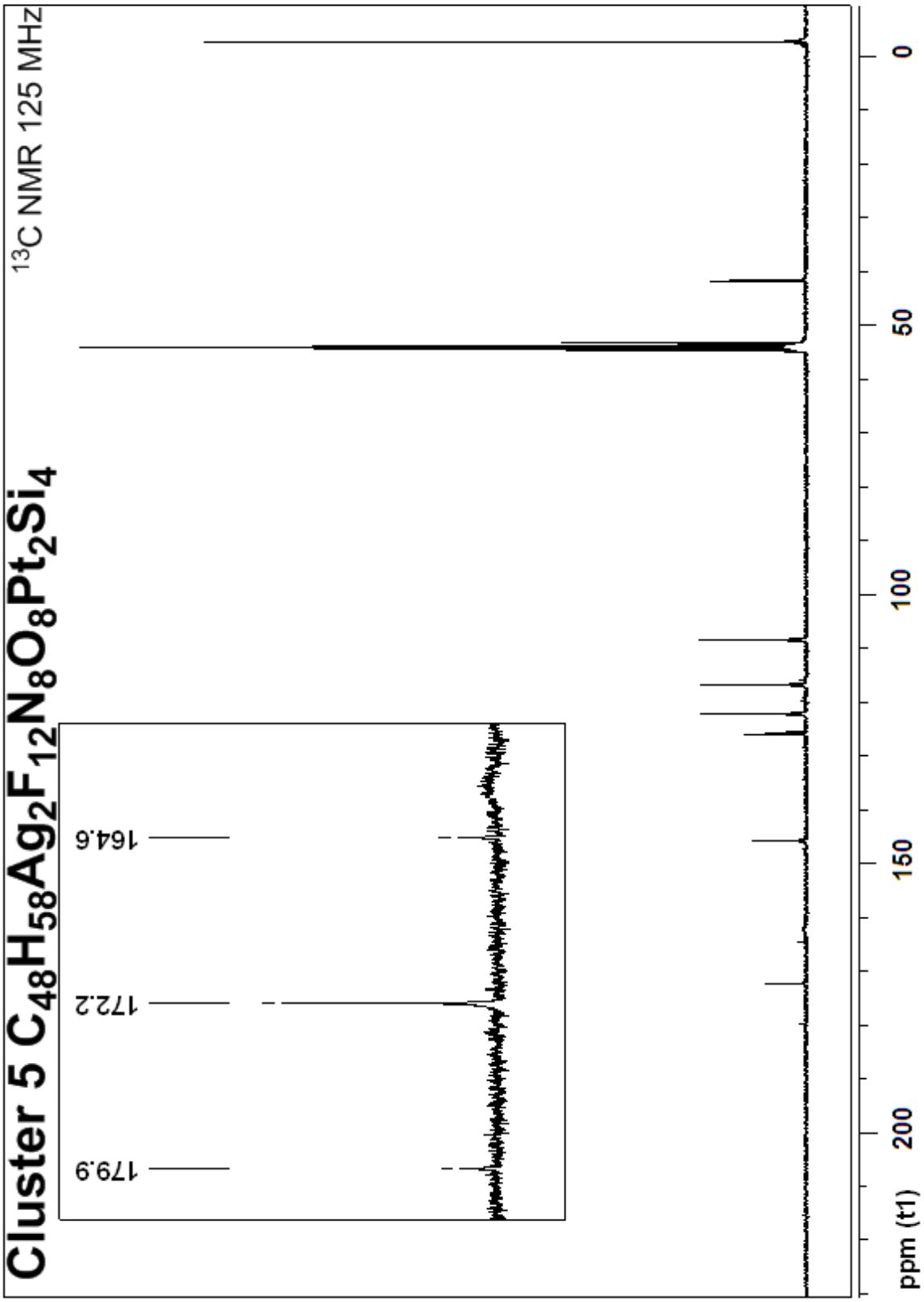
Cluster 5 $C_{48}H_{58}Ag_2F_{12}N_8O_8Pt_2Si_4$
^{13}C NMR 125 MHz
179.9
172.2
164.6
ppm (t1)
200
150
100
50
0

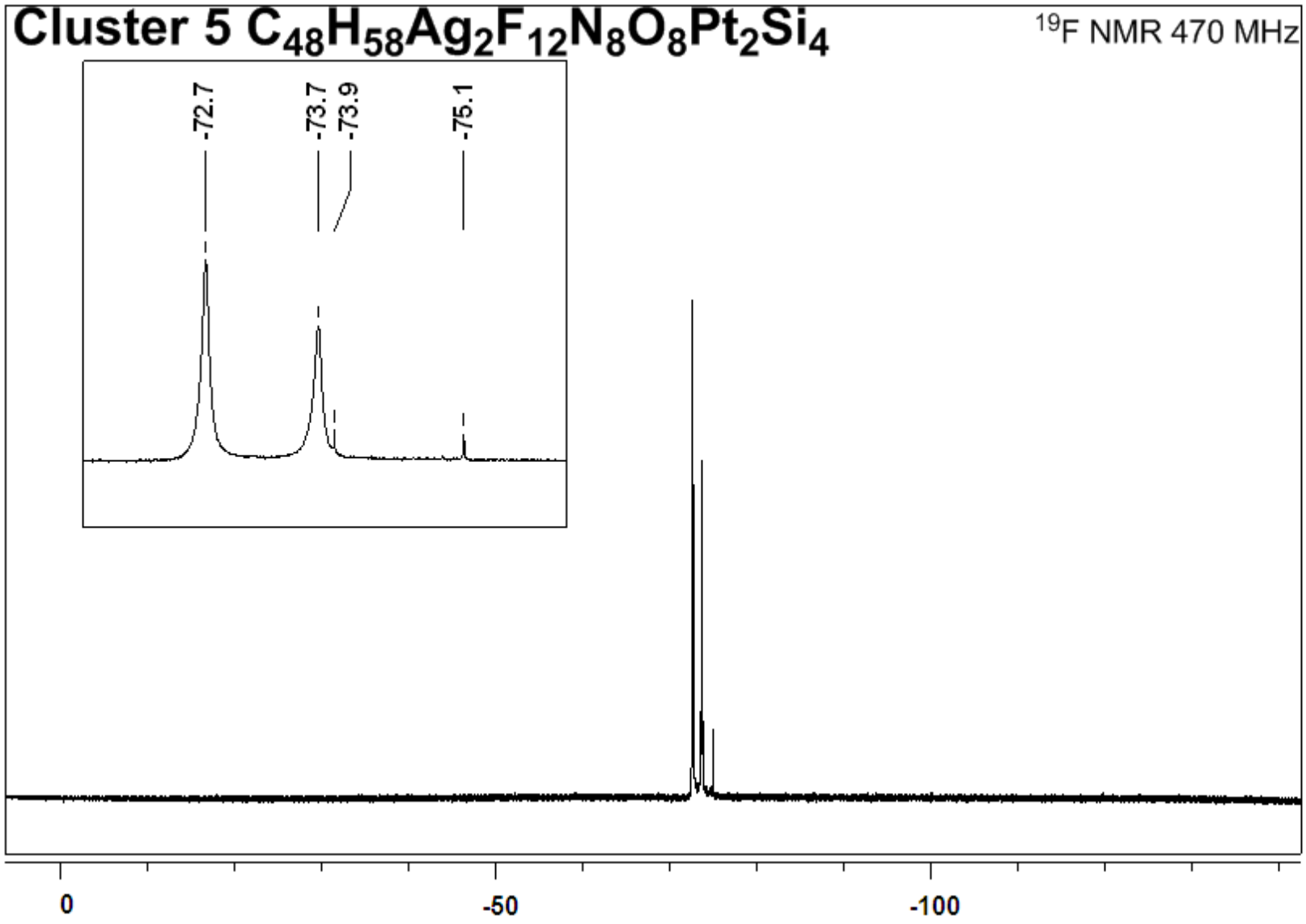
Cluster 5 $C_{48}H_{58}Ag_2F_{12}N_8O_8Pt_2Si_4$
^{19}F NMR 470 MHz
-72.7
-73.7
-73.9
-75.1
0
-50
-100

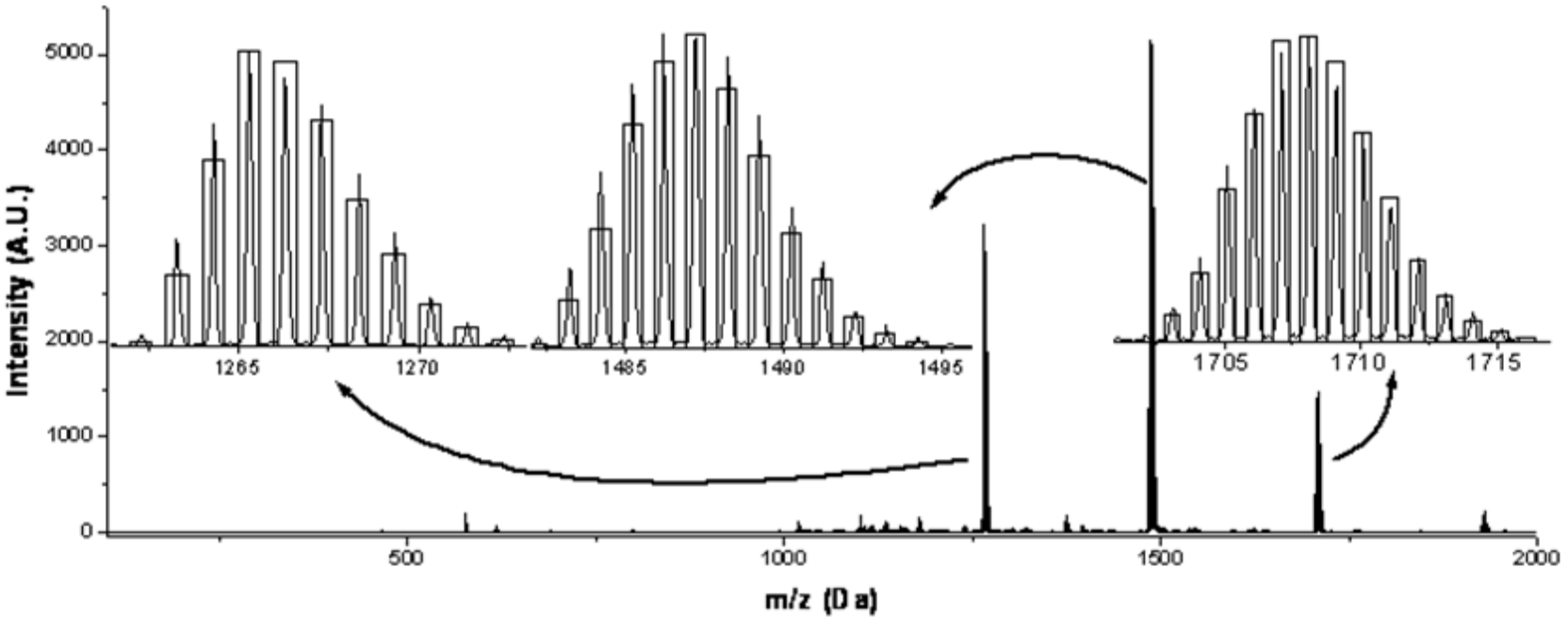

ESI-MS spectra of cluster **5**. Insertions: experimental (line) and calculated (column) isotopic envelope of each peak.

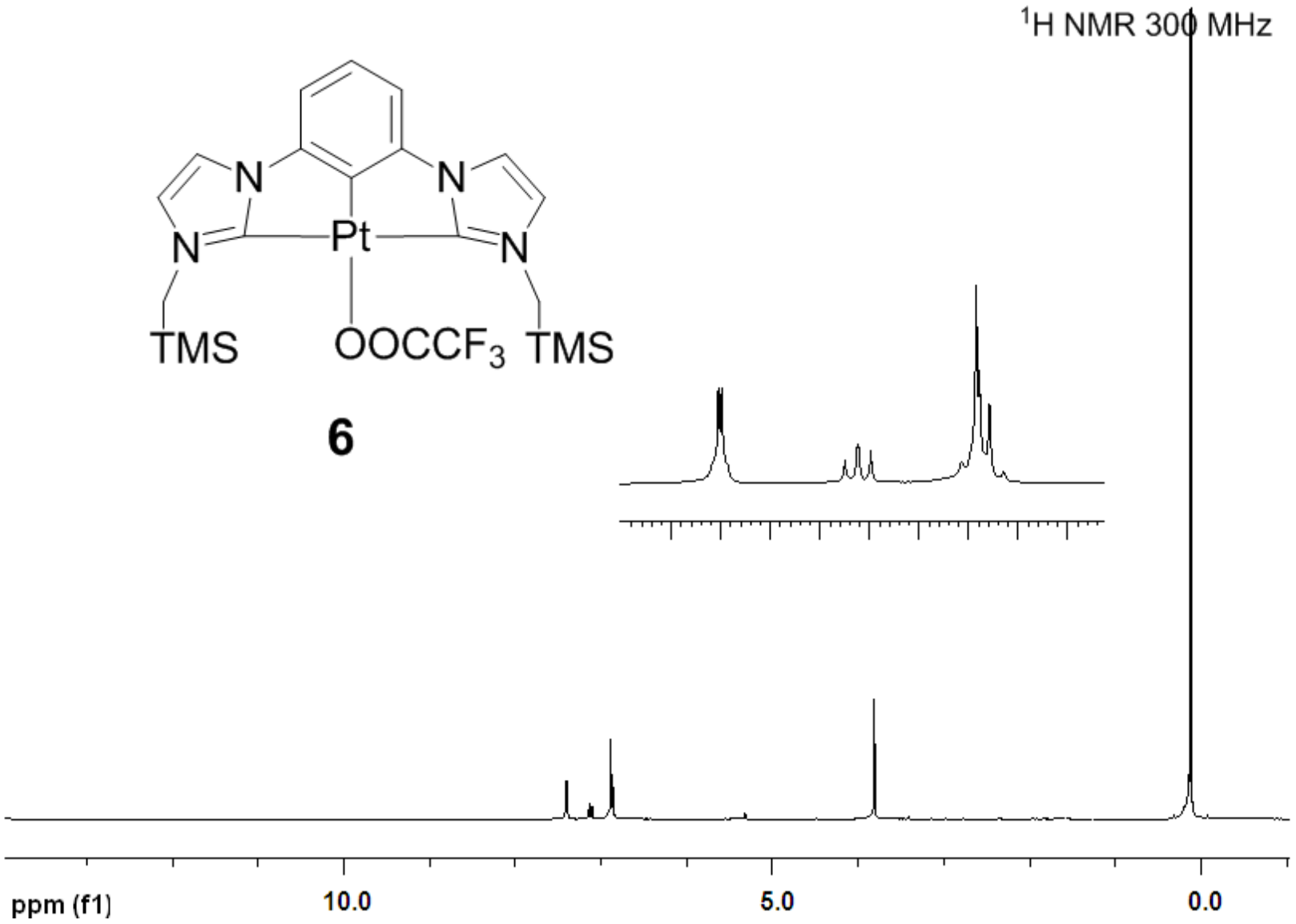
^{1}H NMR 300 MHz
N
N
N
N
Pt
TMS
OOCCF$_3$
TMS
6
ppm (f1)
10.0
5.0
0.0

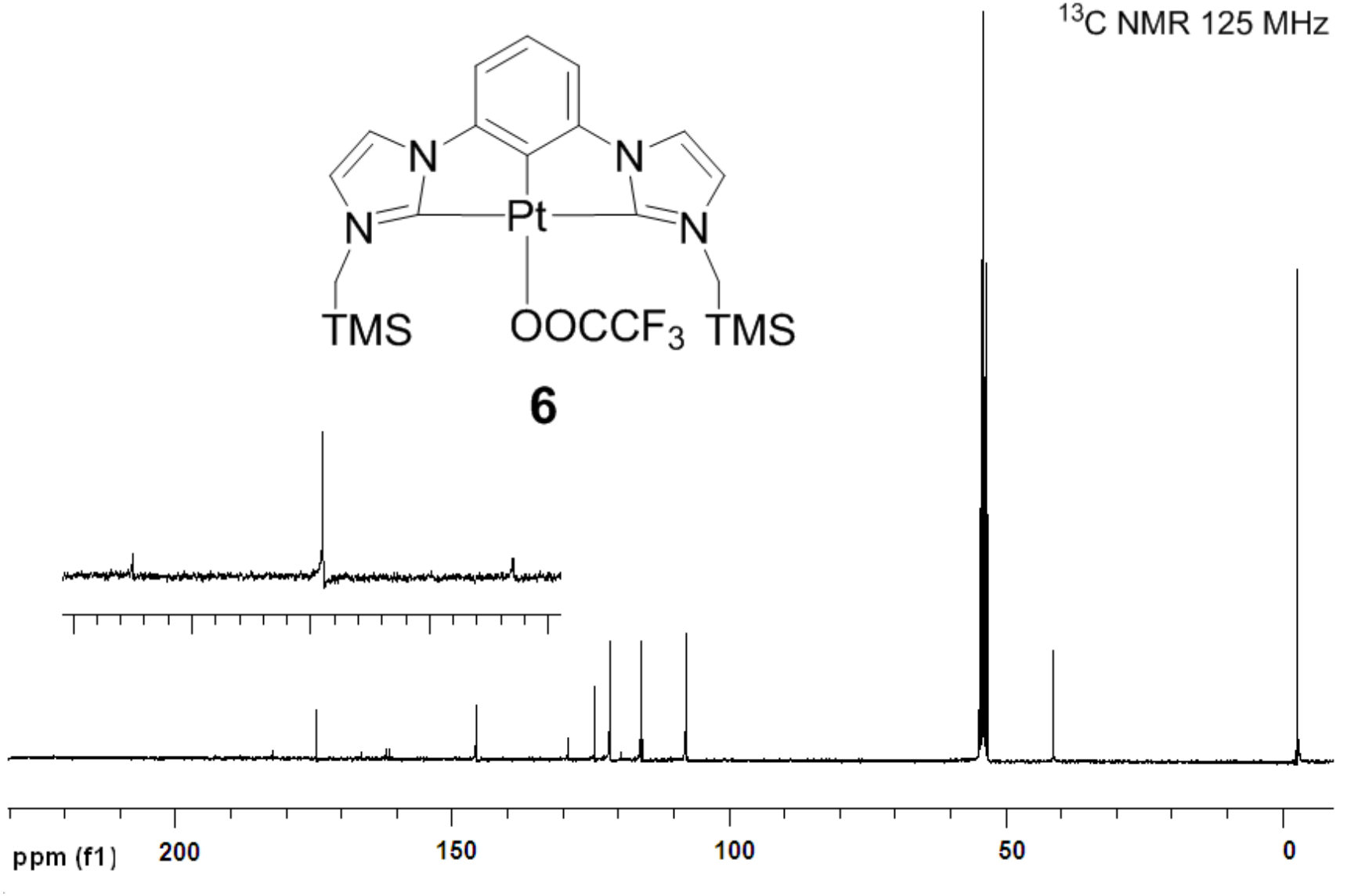
^{13}C NMR 125 MHz
N
N
N
N
Pt
TMS
OOCCF$_3$
TMS
6
ppm (f1)
200
150
100
50
0

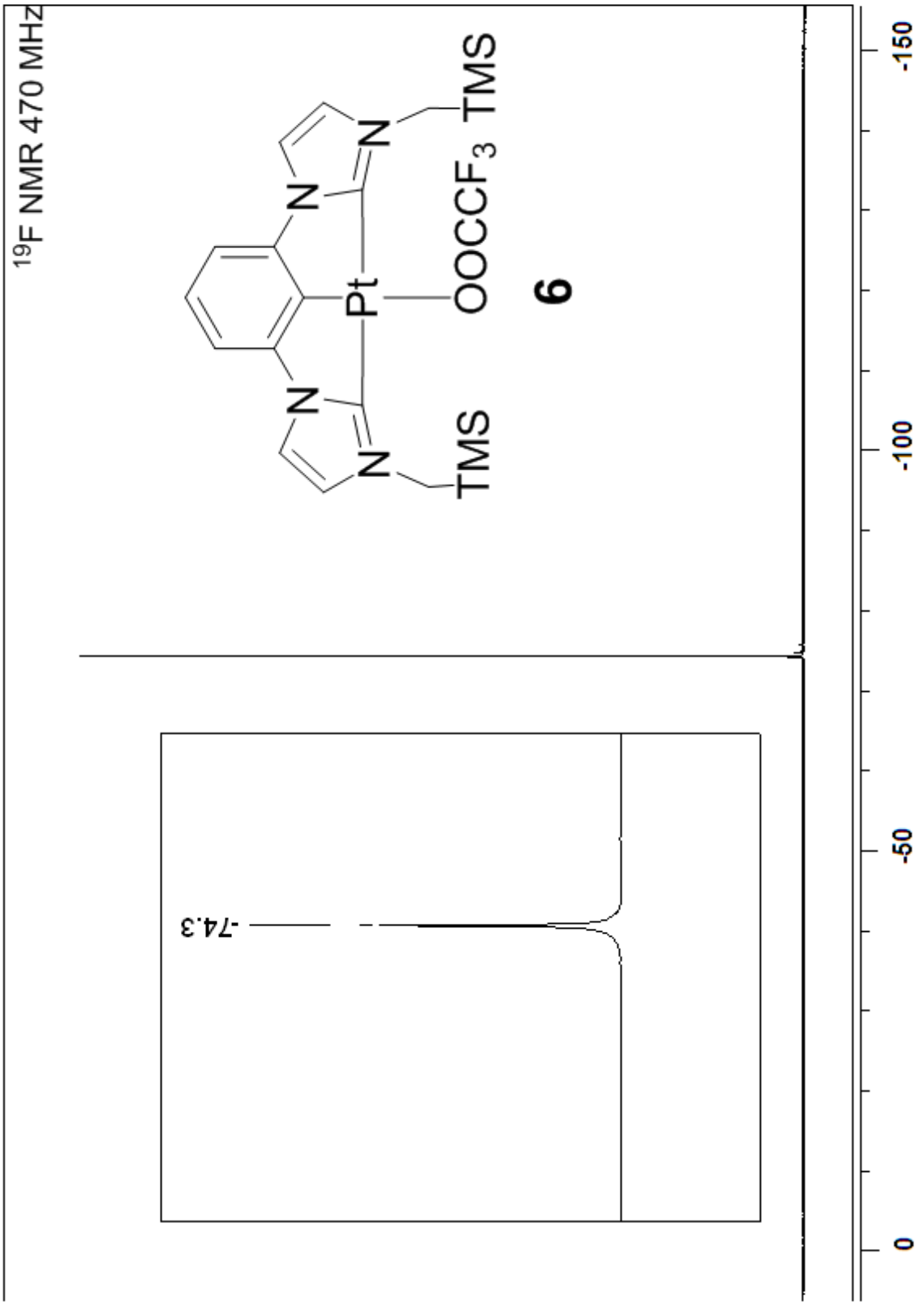
^{19}F NMR 470 MHz
-74.3
0
-50
-100
-150
TMS
N
N
Pt
N
N
OOCCF$_3$
TMS
6

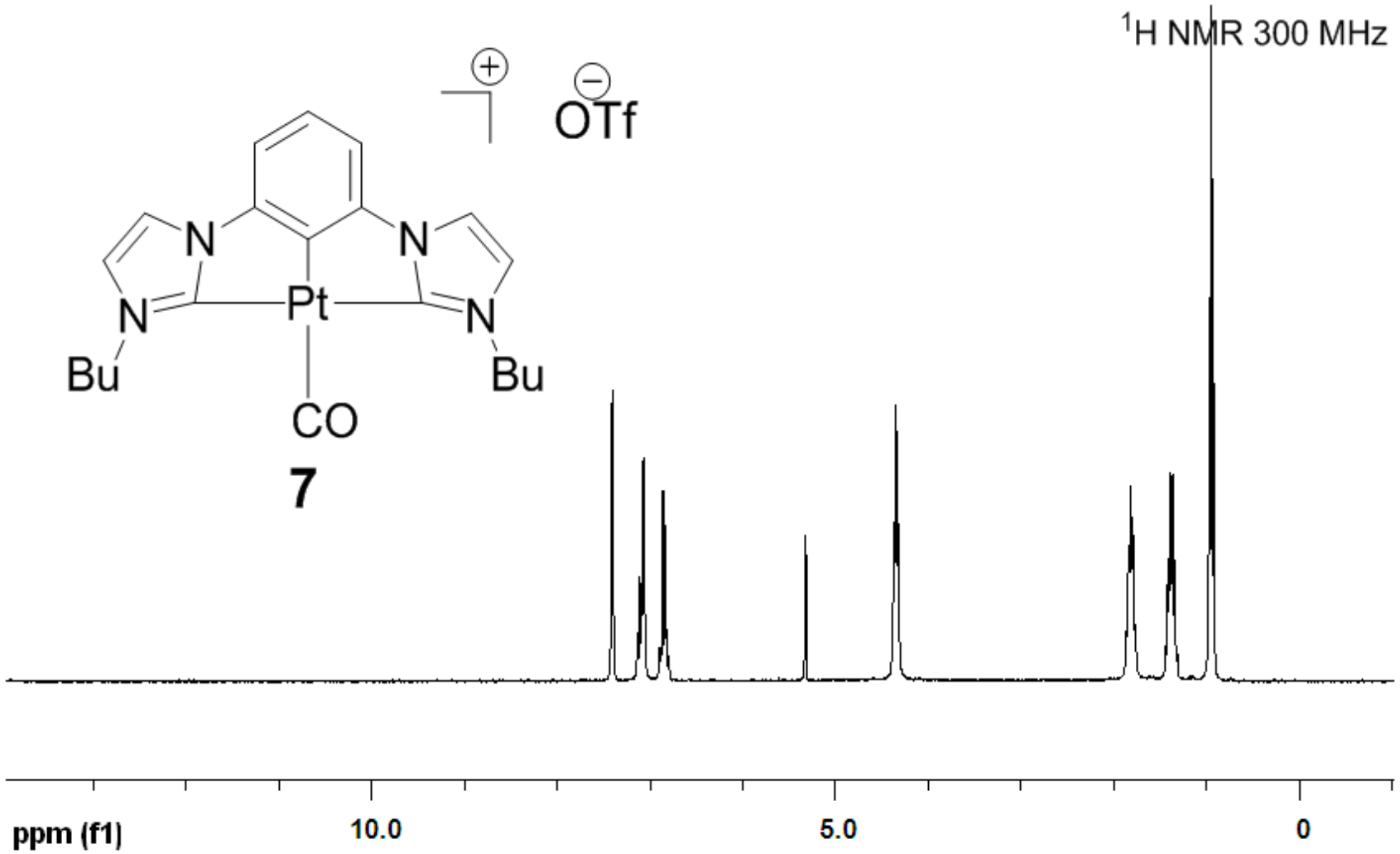
^{1}H NMR 300 MHz
OTf
N
N
N
N
Pt
Bu
Bu
CO
7
ppm (f1)
10.0
5.0
0

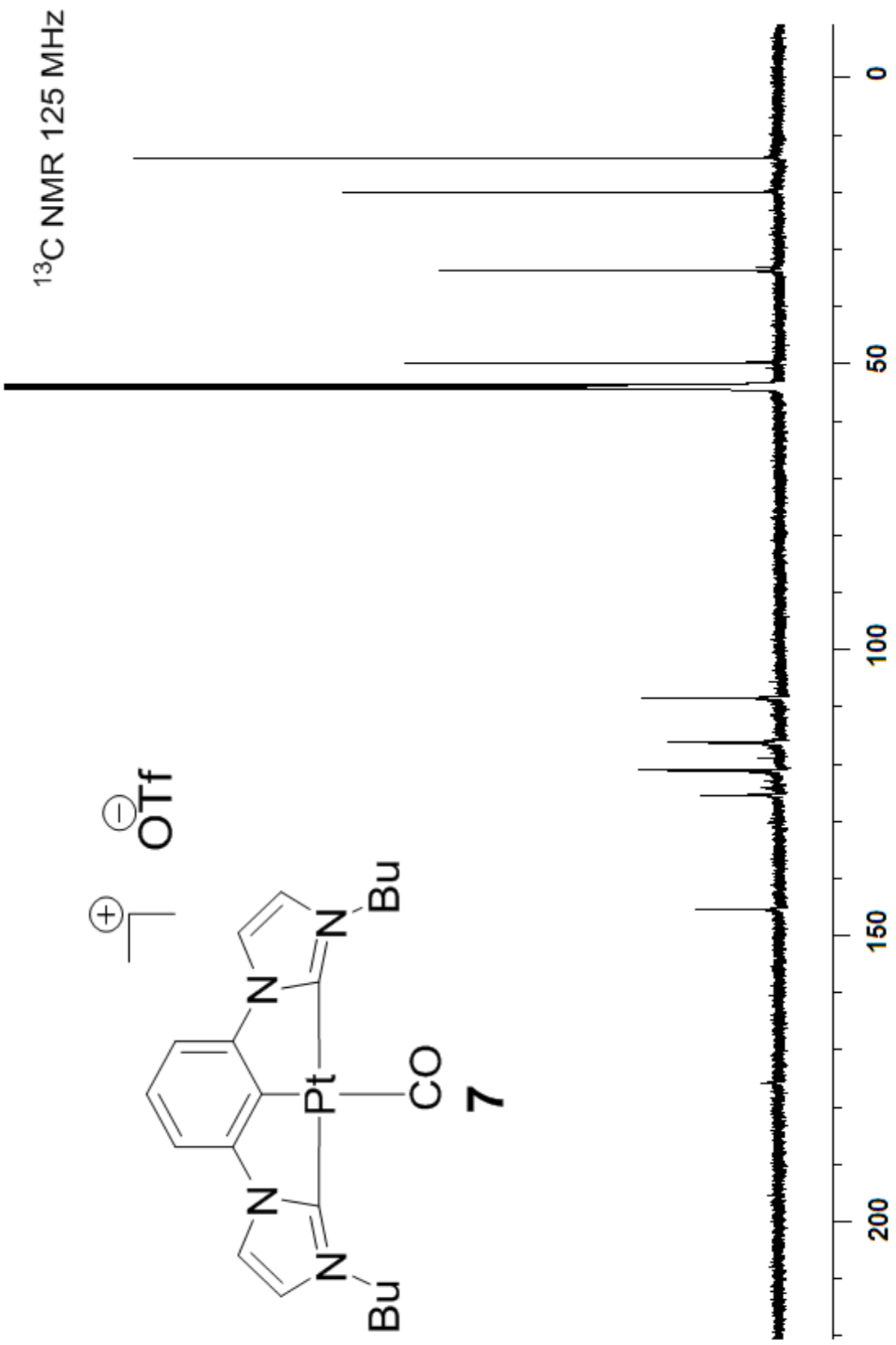
^{13}C NMR 125 MHz
0
50
100
150
200
Bu
N
N
Pt
CO
N
N
Bu
OTf
7

VITA

- 2005 Wuhan University B.S. in Applied Chemistry
- 2007 Wuhan University M.S. in Electrochemistry
- 2008 Mississippi College Laboratory Assistant
- 2010 Graduate Achievement Award in University of Mississippi (limited up to 18 nominees annually)
- 2012 ACS Graduate Student Research Award 1st place

The author, Xiaofei Zhang, was born in the city of Wuhan, Hubei, China, in 1982. His chemistry career started in 2001 when he entered Wuhan University as an undergraduate. Upon graduation he was admitted to graduate school and joined an electrochemistry laboratory at the same institution. After obtaining his M.S degree in 2007, he worked for a car battery factory shortly and then decided to continue his further education oversea. At the University of Mississippi, he began to explore the organic/organometallic field and chose it as his new research area.